

**DEPARTMENT OF ENERGY**  
Environmental Management Los Alamos Field Office (EM-LA)  
Los Alamos, New Mexico 87544

Mr. John E. Kieling  
Bureau Chief  
Hazardous Waste Bureau  
New Mexico Environment Department  
2905 Rodeo Park Drive East, Building 1  
Santa Fe, NM 87505-6303



APR 25 2019

Dear Mr. Kieling:

Subject: Submittal of the 2018 Sandia Wetland Performance Report

Enclosed please find two hard copies with electronic files of the "2018 Sandia Wetland Performance Report." The U.S. Department of Energy (DOE) Environmental Management Los Alamos Field Office (EM-LA) and Newport News Nuclear BWXT-Los Alamos, LLC (N3B) have prepared this report in response to requirements set forth in the "Work Plan and Final Design for Stabilization of the Sandia Canyon Wetland." The requirement to design a Sandia wetland monitoring program was previously set forth in the New Mexico Environment Department's (NMED's) "Approval with Modification, Interim Measures Work Plan for Stabilization of the Sandia Canyon Wetland," in response to the previously submitted "Interim Measures Work Plan for Stabilization of the Sandia Canyon Wetland." The "2017 Sandia Wetland Performance Report" was approved by NMED on June 5, 2018. The 2018 report satisfies Appendix B, Milestones and Targets, Milestone 5, of the 2016 Compliance Order on Consent (Consent Order).

Pursuant to Section XXIII.C of the Consent Order, a pre-submission review meeting was held with the EM-LA, N3B, and NMED on February 6, 2019, to discuss changes in monitoring requirements for 2019.

If you have any questions, please contact Amanda White at (505) 309-1366 (amanda.white@em-la.doe.gov) or Cheryl Rodriguez at (505) 665-5330 (cheryl.rodriguez@em.doe.gov).

Sincerely,

Arturo Q. Duran  
Compliance and Permitting Manager  
Environmental Management  
Los Alamos Field Office

Enclosures:

1. Two hard copies with electronic files – 2018 Sandia Wetland Performance Report (EM2019-0091)

cc (letter with hard-copy enclosure[s]):

S. Veenis, N3B

C. Rodriguez, EM-LA

cc (letter with CD/DVD enclosure[s]):

L. King, EPA Region 6, Dallas, TX

R. Martinez, San Ildefonso Pueblo, NM

D. Chavarria, Santa Clara Pueblo, NM

S. Yanicak, NMED

A. Chan, N3B

B. Dail, N3B

E. Day, N3B

L. Huntoon, N3B

F. Lockhart, N3B

B. Robinson, N3B

J. von Rohr, N3B

A. White, N3B

emla.docs@em.doe.gov

N3B Records

Public Reading Room (EPRR)

PRS Website

cc (date-stamped letter emailed):

E. Evered, N3B

J. Legare, N3B

G. Morgan, N3B

A. Duran, EM-LA

D. Nickless, EM-LA

D. Rhodes, EM-LA

EM-LA-40AD-00428

April 2019  
EM2019-0091

# 2018 Sandia Wetland Performance Report




Newport News Nuclear BWXT-Los Alamos, LLC (N3B), under the U.S. Department of Energy Office of Environmental Management Contract No. 89303318CEM000007 (the Los Alamos Legacy Cleanup Contract), has prepared this document pursuant to the Compliance Order on Consent, signed June 24, 2016. The Compliance Order on Consent contains requirements for the investigation and cleanup, including corrective action, of contamination at Los Alamos National Laboratory. The U.S. government has rights to use, reproduce, and distribute this document. The public may copy and use this document without charge, provided that this notice and any statement of authorship are reproduced on all copies.



# 2018 Sandia Wetland Performance Report

April 2019


Responsible project director:

Bruce Robinson		Project Director	Water Program	4/16/2019
Printed Name	Signature	Title	Organization	Date

Responsible N3B representative:

Erich Evered		Program Manager	N3B Environmental Remediation Program	4/17/2019
Printed Name	Signature	Title	Organization	Date

Responsible DOE EM-LA representative:

Arturo Q. Duran		Compliance and Permitting Manager	Office of Quality and Regulatory Compliance	4/25/19
Printed Name	Signature	Title	Organization	Date



## EXECUTIVE SUMMARY

The 2018 Sandia wetland performance report is the fifth annual performance report following the 2012 to 2014 baseline that assessed the overall condition of the wetland at the head of Sandia Canyon. Canyon wetland monitoring was performed in the context of the wetland's ability to mitigate migration of contaminants of concern (i.e., chromium, polychlorinated biphenyls [PCBs], and polycyclic aromatic hydrocarbons) detected in wetland sediments as a result of historical releases at Los Alamos National Laboratory (LANL or the Laboratory). The geochemistry and physical stability of wetland sediments, along with the extent of wetland vegetation, are the key indicators of wetland conditions. The condition of the wetland is assessed to evaluate the effectiveness of the grade-control structure (GCS) completed in 2013 at the terminus of the wetland, and to monitor changes to the Laboratory's operational practices that have affected outfall volumes discharging to the wetland. This report presents the results of monitoring conducted for surface water, alluvial groundwater, vegetation, and geomorphology between January and December 2018, and in the context of findings from 2014 through 2017. The data are assessed relative to baseline conditions presented in the "Sandia Wetland Performance Report, Baseline Conditions 2012–2014," the data presented in the "Sandia Performance Report, Performance Period April 2014–December 2014," and the 2015, 2016, and 2017 Sandia wetland performance reports to identify any physical and geochemical changes that occurred during the 2018 monitoring period. Monitoring data include physical field parameters (i.e., water level, temperature, dissolved oxygen, turbidity, pH) and water chemistry from 12 alluvial wells that monitor the alluvial groundwater in the wetland. Additionally, effluent and storm water discharge and chemical data are obtained from 2 gaging stations located upstream of the wetland and 1 gaging station located downstream of the wetland. Interannual changes to wetland and stream channel structure are determined through vegetation monitoring, geomorphic change detection data from bank and thalweg surveys, repeat photos, and general field observations.

The monitoring conducted during the performance period indicates the Sandia wetland remains stable following the installation of the GCS, even with generally lower, but variable, effluent volumes entering the wetland. The GCS continues to be effective in arresting headcutting at the terminus of the wetland. Log check dams were installed in September 2017 to reduce sediment entering the wetland from a southern tributary; however, indications that storm flows are undercutting the dams were noted in a walkdown with New Mexico Environment Department personnel in the fall of 2018, and there are plans to remedy the situation in 2019. Groundwater within the shallow alluvium remains in a reducing condition, with no obvious detrimental temporal trends in chemistry observed. Sampling of hexavalent chromium indicates concentrations at or below the method detection limit within the wetland. Water levels in the wetland remained similar over the last 5 yr, with temporary drops in the easternmost transect during the summers. These decreases in water levels are possibly a result of enhanced evapotranspiration associated with meteorological conditions and robust growth of additional wetland vegetation planted as part of the GCS restoration effort. Despite the observed decreases, water levels remained sufficiently high to sustain and allow some expansion of obligate wetland vegetation, and analytical results indicate alluvial groundwater remained in strongly reducing conditions in the eastern portion of the wetland immediately upgradient of the GCS. Storm water data indicate that the GCS has had a positive effect in reducing contaminant mobility, and this trend continued through 2018. Suspended sediment, PCBs, and chromium concentrations have decreased significantly compared with pre- and post-GCS data immediately downgradient of the wetland at gaging station E123, presumably from eliminating headcutting at the terminus of the wetland and from sediment trapping efficiency because of the dense vegetation within the wetland.

Geomorphic change detection studies indicate the wetland is stable, with no significant geomorphic change experienced by the wetland between post-2017 to post-2018 monsoon bank and thalweg surveys. Overall, the banks and thalweg were stable between 2017 and 2018, with minor lateral changes in thalweg position. The minor thalweg nick point has remained stable since 2015 with no indication of upstream erosion. Likewise, the plunge pool at the head of the reach has remained relatively stable from 2017 to 2018, with small changes to the shape and areal extent of the pool. In addition, based on erosion pin monitoring, the alluvial fan deposits from the Los Alamos County landfill have remained stable.

Vegetation perimeter mapping, cross-section transects, and photographic comparison suggest that the wetland is stable. Between 2017 and 2018, wetland vegetation area has decreased slightly (-4%) over the whole study area, with some areas of expansion occurring at the upstream end of the reach as new cattails and willows expanded along the stream channel.

Surface water and alluvial groundwater analytical data collected in 2018 were compared with New Mexico surface water-quality criteria (20.6.4 New Mexico Administrative Code [NMAC]) and groundwater standards (20.6.2 NMAC), respectively. Exceedances of water-quality criteria are presented in this report and are determined to be associated with historical Laboratory releases, runoff from developed areas in the upper watershed, naturally occurring chemicals, and/or with the natural reducing conditions of the wetland within the alluvial system.

Five yr of alluvial well data indicate that spatial and temporal stability exists in the wetland and, therefore, redundancy exists in the current monitoring plan. Reduced sampling frequency and maintaining a subset of wells that capture edge effects (wetland-upland) and water table fluctuations is supported by existing long-term data. Additionally, speciation of some metals and other indicators of reducing conditions are redundant; thus, conservative measures of wetland reducing conditions will remain in the monitoring plan.

## CONTENTS

<b>1.0</b>	<b>INTRODUCTION .....</b>	<b>1</b>
1.1	Project Goals .....	2
1.2	Design and Function of the GCS .....	3
1.3	Sandia Canyon Outfalls and SERF .....	4
1.4	Monitoring Planned during the Performance Period .....	5
1.5	Conceptual Model for Assessing Wetland Performance .....	7
1.5.1	Hydrologic Status .....	7
1.5.2	Contamination in Wetland Sediment .....	8
1.5.3	Cr(III) Stability in the Sandia Wetland .....	8
1.5.4	Current State of the Sandia Wetland .....	9
<b>2.0</b>	<b>MONITORING PERFORMED DURING THE 2018 MONITORING PERIOD .....</b>	<b>9</b>
2.1	Monitoring of Surface Water .....	9
2.2	Monitoring of Alluvial System .....	10
2.3	Water-Level Monitoring .....	10
2.4	Geomorphic Monitoring .....	11
2.5	Vegetation Monitoring .....	11
2.6	Monitoring of the GCS .....	11
<b>3.0</b>	<b>SUMMARY OF RESULTS FROM WETLAND PERFORMANCE METRICS .....</b>	<b>11</b>
3.1	Key Monitoring Locations and Performance Metrics .....	11
3.2	Spatial and Temporal Geochemical Patterns .....	12
3.2.1	Surface Water and Alluvial Groundwater Exceedances .....	13
3.3	Temporal and Spatial Trends in Water-Level .....	13
3.4	Geomorphic Trends in the Wetland .....	14
3.5	Spatial and Temporal Trends in Vegetation .....	14
3.6	Performance of GCS .....	14
3.7	2019 Monitoring Plan .....	15
3.8	Proposed Changes to Monitoring Plan from 2018 .....	16
<b>4.0</b>	<b>CONCLUSIONS .....</b>	<b>17</b>
<b>5.0</b>	<b>REFERENCES AND MAP DATA SOURCES .....</b>	<b>17</b>
5.1	References .....	17
5.2	Map Data Sources .....	19

### Figures

Figure 1.0-1	Locations of the Sandia GCS, NPDES outfalls, precipitation gage E121.9, alluvial wells, surface and storm water gaging stations, former Los Alamos County landfill, surrounding TAs, and reaches S-1N, S-1S, and S-2 (reaches S-1N and S-1S are upstream of the wetland, S-2 essentially encompasses the wetland). .....	21
Figure 1.3-1	Daily, monthly average, and yearly average effluent release volumes (expressed as Kgal./day) for Outfall 001 from 2006 to December 2018. ....	23
Figure 1.3-2	Updated process schematic for the power plant, SWWS, and SERF connections to Outfall 001 (current configuration) .....	24

## Tables

Table 1.4-1	Completion Data for Alluvial Piezometers and Collocated Alluvial Wells .....	25
Table 1.4-2	Schema Crosswalk: Past Piezometers and Current Alluvial Wells .....	26
Table 1.4-3	Alluvial Groundwater Sampling and Analysis Plan for 2018 Sandia Wetland Stabilization Monitoring .....	26
Table 1.4-4	ISCO Bottle Configurations and Analytical Suites 2018 Storm Water Sampling Plan for E121, E122, and E123.....	27
Table 2.1-1	Field Data for Alluvial Locations and Surface Water Stations 2018 Sampling Events .....	28
Table 2.1-2	Precipitation, Storm Water Peak Discharge, and Samples Collected at Gaging Stations E121, E122, and E123 for Each Sample-Triggering Storm Event in 2018.....	29
Table 3.7-1	Significant Geomorphic Changes and Associated Peak Discharges .....	30
Table 3.7-2	Proposed 2019 Sampling and Preservation Requirements for Sandia Wetland .....	31

## Appendixes

Appendix A	Acronyms and Abbreviations, Metric Conversion Table, and Data Qualifier Definitions
Appendix B	2018 Geomorphic Changes in Sandia Canyon Reach S-2
Appendix C	2018 Wetland Vegetation Monitoring in Sandia Canyon Reach S-2
Appendix D	Geochemical and Hydrologic Monitoring in Sandia Canyon
Appendix E	2018 Watershed Mitigations Inspections
Appendix F	Analytical Data and 5-Min Stage, Discharge, and Precipitation Data (on CD included with this document)

## 1.0 INTRODUCTION

In response to liquid effluent released by the Los Alamos National Laboratory (LANL or the Laboratory), the Sandia wetland, located at the head of Sandia Canyon, has expanded from a relatively small footprint in the early 1950s to its current size. The wetland area, indicated by obligate wetland plant species, is 14,764 m<sup>2</sup> as of 2018 (calculated to include the total coverage of overlapping vegetation zones; see Appendix C). Overall, there has been a 22% increase in the total wetland vegetation area from 2014 to 2018. Throughout the course of Laboratory operations, the wetland has been perpetuated by sustained effluent releases to the canyon. Contamination is present in wetland sediments because of historical releases from Laboratory operations (LANL 2009, 107453).

Newport News Nuclear BWXT-Los Alamos, LLC (N3B) has prepared this “2018 Sandia Wetland Performance Report” in response to requirements set forth in the “Work Plan and Final Design for Stabilization of the Sandia Canyon Wetland” (LANL 2011, 207053). In that plan, the Laboratory proposed reporting of Sandia wetland monitoring data to the New Mexico Environment Department (NMED) by April 30 of each year. The requirement for designing a Sandia wetland monitoring program was previously set forth in NMED’s “Approval with Modification, Interim Measures Work Plan for Stabilization of the Sandia Canyon Wetland” (NMED 2011, 203806) in response to the Laboratory’s “Interim Measures Work Plan for Stabilization of the Sandia Canyon Wetland” (LANL 2011, 203454). The monitoring plan was provided in the work plan (LANL 2011, 207053) and is summarized in section 1.5 of this report. The monitoring plan is designed to identify physical or chemical changes in the Sandia wetland related to (1) the installation of a grade-control structure (GCS) at the terminus of the wetland (LANL 2013, 251743) and (2) changes in outfall chemistry and discharge volumes related to the Sanitary Effluent Reclamation Facility (SERF) expansion (DOE 2010, 206433).

This report assesses the overall condition and stability of the wetland in the context of the GCS at the terminus of the wetland, and changes to the volume and chemistry of effluent released into Sandia Canyon resulting from changes in the Laboratory’s water-management practices associated with SERF and National Pollutant Discharge Elimination System (NPDES) Outfall 001 (Figure 1.0-1). The results of monitoring conducted in 2018 for surface water, alluvial groundwater, vegetation, and geomorphology are presented herein. Data are assessed relative to baseline conditions presented in the “Sandia Wetland Performance Report, Baseline Conditions 2012–2014” (LANL 2014, 257590). In turn, considered with previous data presented in the “Sandia Performance Report, Performance Period April 2014–December 2014” (LANL 2015, 600399), the “2015 Sandia Wetland Performance Report” (LANL 2016, 601432), the “2016 Sandia Wetland Performance Report” (LANL 2017, 602341), and the “2017 Sandia Wetland Performance Report” (LANL 2018, 603022) to identify any physical and geochemical changes during the monitoring period. Monitoring data include the following:

- Water levels and water chemistry from 12 alluvial wells that monitor the alluvial groundwater in the wetland,
- Surface water and storm water data from 2 gaging stations located upstream of the wetland and 1 gaging station located downstream,
- Vegetation monitoring, and
- Geomorphic change detection data from ground survey points and field observations.

Hexavalent chromium [Cr(VI)] was historically released into liquid effluent from the Technical Area 03 (TA-03) power plant at the head of Sandia Canyon from 1956 to 1972. Some of the Cr(VI) made its way to the regional aquifer beneath Sandia and Mortandad Canyons, and Cr(VI) concentrations in the regional aquifer presently exceed NMED groundwater standards and U.S. Environmental Protection Agency (EPA)

maximum contaminant levels (MCLs). Historical releases of polychlorinated biphenyls (PCBs) from a one-time transformer storage area and polycyclic aromatic hydrocarbons (PAHs) from an asphalt batch plant also discharged to the wetland, which still contains an inventory of these contaminants. Sandia Canyon wetland performance monitoring is related to the overall chromium remediation project because a large portion of the original chromium inventory and other contaminants (i.e., PCBs and PAHs, discussed in section 1.1 below) are currently sequestered in the wetland sediment. The results of characterization work conducted to date in Sandia Canyon are described in the “Investigation Report for Sandia Canyon” (hereafter, the Phase I IR) (LANL 2009, 107453) and in the “Phase II Investigation Report for Sandia Canyon” (hereafter, the Phase II IR) (LANL 2012, 228624).

New Mexico Water Quality Control Commission groundwater standards (20.6.2 New Mexico Administrative Code [NMAC]), EPA MCLs, NMED screening levels for tap water, and EPA regional screening levels for tap water were used to establish a set of screening values for evaluating monitoring data (see Appendix D, section D-3.3). Base-flow and storm water analytical results were screened against the appropriate surface water-quality standards in 20.6.4 NMAC (see Appendix D, section D-2.1).

Information on radioactive materials and radionuclides, including the results of sampling and analysis of radioactive constituents, is voluntarily provided to NMED in accordance with U.S. Department of Energy policy.

## 1.1 Project Goals

The overall objective of this project is to monitor the physical and chemical stability of the Sandia wetland in the context of its inventory of contaminants of concern. Monitoring was initiated to evaluate the influence of the GCS (which was installed to reduce erosion at the terminus of the wetland) and anticipated decreases in discharge volume associated with the expansion of SERF on the discharge of contaminants.

Geochemical reducing conditions within the Sandia wetland converted some of the Cr(VI) released from 1956 to 1972 to stable, relatively insoluble trivalent chromium [Cr(III)]. A significant inventory of chromium as Cr(III), possibly around 15,000 kg, remains in wetland sediment (LANL 2009, 107453). Studies presented in the Phase I IR have shown the trivalent form of chromium is unlikely to oxidize and convert to mobile Cr(VI) whether sequestered in the saturated reducing conditions of the wetland alluvium or exposed to oxygen upon dewatering of wetland sediments (LANL 2009, 107453). Maintaining the saturated reducing condition, however, is a prudent measure to ensure stability of the chromium inventory as Cr(III) within the wetland sediment and alluvial groundwater. Cr(III) is, in most forms, sparingly soluble and non-toxic, whereas Cr(VI) is highly soluble and very toxic. Cr(VI) compounds are stable under aerobic conditions, but are reduced to chromium (III) compounds under anaerobic conditions, which limits both mobility and toxicity.

The wetland also contains an inventory of PCBs and PAHs from historical Laboratory releases that have adsorbed to sediment within the wetland. This inventory will remain in place as long as the sediment remains physically stable. Abundant vegetation stabilizes sediments through root binding and also enhances deposition of suspended solids from storm water. PCBs in wetland sediment are primarily attributed to releases of PCBs from a transformer storage area, Solid Waste Management Unit 03-056(c). The PCB inventory in the wetland sediments is estimated to be 5.5 kg, 3.3 kg, 31.1 kg, and 24.4 kg for Aroclor-1242, Aroclor-1248, Aroclor-1254, and Aroclor-1260, respectively (LANL 2009, 107453). Maintenance of reducing and anaerobic conditions in the wetland potentially reduces the PCB inventory as anaerobic bacterial dehalogenation is a necessary first step in PCB degradation. Four PAHs (benzo[a]anthracene, benzo[a]pyrene, benzo[b]fluoranthene, and indeno[1,2,3-cd]pyrene) were identified in the Phase I IR as being the most important for evaluating human health risk. PAHs are primarily attributed to releases from a former asphalt batch plant located upgradient of the wetland. The highest



concentrations of benzo[a]anthracene and benzo[a]pyrene in sediment were found in investigation reaches S-1N and S-1S above the wetland (Figure 1.0-1). Much smaller concentrations, typically less than 1 mg/kg, have been measured in reach S-2, which includes the Sandia wetland (Figure 1.0-1).

The monitoring presented in this report is intended, in part, to assess the stabilizing impacts of the GCS on the eastern terminus of the wetland. Before the GCS was constructed, the terminus of the wetland had an active headcut (up to 3 m high). Installation of the GCS at the former active headcut has arrested it, thereby stabilizing the grade (Figure 1.0-1). Stabilization of vegetation, hydrology, and geochemistry at the easternmost end of the wetland indicates the efficacy of the GCS, backing up groundwater because of its impervious subgrade face (section 1.2) (LANL 2015, 600399) and stabilizing the grade at the terminus of the wetland. Maintenance of physical and chemical stability will, in turn, help prevent potential physical mobilization of adsorbed contaminants associated with sediment and chemical mobilization of precipitated or reduced contaminants under changing geochemical conditions in groundwater (LANL 2011, 203454; LANL 2011, 207053).

The Sandia wetland has experienced generally decreased liquid outfall effluent volumes (both daily and annually) from NPDES-permitted Outfalls 001 and 03A027 as part of the SERF expansion project. As part of the SERF expansion, a portion of the effluent previously released to Sandia Canyon is now being rerouted to cooling towers at various facilities, including the Strategic Computing Complex (SCC) and the Trinity supercomputer. Though effluent releases to Sandia Canyon may be reduced further, discharge will need to be maintained at a minimum of 30,000 gallons per day (gpd) during months when evapotranspiration is highest. This discharge level is believed to be sufficient to maintain the ecologic, hydrologic, and geochemical functioning of the wetland—as described in the “100% Design Memorandum for Sandia Wetlands Stabilization Project” (LANL 2012, 240016). If future changes to effluent volume or chemistry are shown to adversely impact the wetland, or wetland evapotranspiration is appreciably increased, adaptive management will be used to ensure wetland stability (e.g., engineered controls to manage sediment and water distribution to increase the area of wetland saturation).

More detailed background on the SERF-related outfall chemistry and discharge volume changes is provided in section 1.3. The monitoring plan and associated rationale designed to identify physical and chemical changes in the wetland are presented in section 1.4. A conceptual model for wetland performance is presented in section 1.5. Monitoring performed during the 2018 performance period is discussed in section 2. Detailed monitoring results are presented in Appendix D. Section 3 summarizes monitoring results in the context of wetland performance metrics and suggests proposed changes to the monitoring plan.

## 1.2 Design and Function of the GCS

The location of the GCS is shown in Figure 1.0-1. The overall objectives of the GCS were to arrest the headcut in the lower portion of the wetland and to maintain favorable hydrologic and geochemical conditions to minimize contaminant migration (LANL 2011, 203454, Figure 2.4-2). The GCS was designed to meet the following objectives:

- Minimize erosion during large flow events,
- Provide an even grade to allow wetland expansion and further stabilization,
- Be sufficiently impervious to prevent the draining of alluvial soils and promote a high water table,
- Facilitate nonchannelized flow, and
- Support wetland function under potentially reduced effluent conditions.

The GCS transitions the grade approximately 11 vertical ft from the elevation of the wetland just upgradient of the former headcut location to the natural streambed just upstream of gage E123. To maintain grade and to reduce the overall fill and size of a single structure, a set of three steel sheet pile walls was installed with decreasing elevation drops. Downstream of the third sheet pile wall, a cascade pool was constructed of boulders and cobbles to transition to the final grade. The transition from the wetland above the GCS to the stream channel below is gradual, smooth, and stepped to prevent erosive flows that could scour and destabilize the stream reach below the structure (LANL 2013, 251743). The design of the GCS should allow for a reduction of outfall effluent discharge into the wetland without compromising the physical and geochemical function of the wetland, particularly of the eastern terminus where the GCS controls wetland water levels. The area behind the GCS was backfilled and wetland vegetation was planted to allow expansion of the wetland area. These measures physically stabilize the wetland by reducing sediment and associated contaminant transport into the lower sections of the canyon and should also maintain reducing conditions within the sediment near the terminus of the wetland, thus contributing to the goal of reducing potential contaminant transport (LANL 2013, 251743). A set of as-built diagrams for the GCS is presented in Appendix C of the completion report for the construction of the GCS (LANL 2013, 251743).

### 1.3 Sandia Canyon Outfalls and SERF

Outfalls have released liquid effluent to Sandia Canyon since the development of TA-03 in the early 1950s. There are currently three NPDES outfalls permitted to release to upper Sandia Canyon upstream of the wetland: Outfalls 001, 03A027, and 03A199 (EPA 2007, 099009, Figure 1.0-1). Effluent releases at these outfall discharge points are monitored in compliance with the Laboratory's industrial NPDES permit (Permit No. NM0028355, EPA 2014, 600257). Operational changes that affect these outfalls have occurred since mid-2012. Figure 1.3-1 shows daily, monthly, and yearly average effluent volumes from 2006 through 2018 for Outfall 001, which releases the greatest volume of effluent to Sandia Canyon. Figure 1.3-1 also shows daily releases from August 2007 to January 2010 and from November 2012 to December 2018 for the two smaller outfalls, Outfalls 03A027 and 03A199. (The record for these two outfalls is incomplete.) The "2015 Sandia Wetland Performance Report" discusses liquid effluent releases to Sandia Canyon from 2006, when the Laboratory's chromium investigation began, to 2015 (LANL 2016, 601432). Late 2015 to 2017 releases and operations are discussed below:

*September 18, 2015, to March 7, 2016:* Operational changes at the SERF plant resulted in increased discharge at Outfalls 001 and 03A027 in late 2015 and early 2016. During this time, incoming flows from the Sanitary Waste Water System (SWWS) plant increased, resulting in a corresponding increase in discharge at Outfall 001. In addition, the SERF plant discharged more effluent to Outfall 001 and sent less SERF-blended water for reuse in the SCC cooling towers. This combination of increases resulted in an additional 95,000 gpd (58%) of effluent at Outfall 001 compared with the same period from September 2014 to March 2015. Total daily discharges ranged from ~170 to 375 gpd for this period. Makeup water for the SCC cooling towers was largely potable water (70%) rather than SERF-blended makeup water during this period (Figure 1.3-2). As a result, effluent volumes have increased by approximately 11,500 gpd at Outfall 03A027 because fewer cycles could be run using the silica-rich potable water. These changes represented a significant increase in the water input to the wetland but did not negatively affect wetland stability. Changes in water chemistry entering the wetland are discussed in Appendix D. The SERF product water has continued to be blended at a 4:1 ratio with SWWS effluent. However, a second blending point available near Outfall 001 was employed during this time period to mix SERF product water with SWWS effluent water; the blending of SERF to SWWS water (from the reuse and fire protection tank). Beyond this blending point, water mixture is not maintained at a constant ratio and likely has a higher ratio of SWWS water than usual when more water comes in from the SWWS plant.

*March 8, 2016, to December 31, 2017:* The operational changes at the SERF plant described above were temporary, and a return to reuse of SERF-blended water in the SCC cooling towers occurred on March 8, 2016. During this period, more than 99% of the water used by the SCC cooling towers was SERF-blended water. As a result, discharges at Outfall 001 decreased to an average of 152,000 gpd from March to December 2016. Another operational change is also noted. Since then, including through the end of 2017, the SCC blowdown effluent volumes are accounted for in the Outfall 001 discharge volumes and releases to Outfall 03A027 have been zero. This change is illustrated in Figure 1.3-1, which shows discharges at Outfall 03A027 dropping to zero, and in Figure 1.3-2, which shows the “combined Outfalls 001 and 03A027” data (turquoise line) converging with the Outfall 001 data (dashed light-green line). This change in discharge location and in accounting for the SCC cooling tower blowdown volume is expected to be permanent; Outfall 03A027 will be used only during maintenance or in the event of an emergency.

The Trinity supercomputer was brought online for early access trial use late in 2016, and transitioned to full-scale use in July 2017. The long-term plan is that this computing facility will also use SERF-blended water for cooling. Cooling tower effluent from this new facility is discharged to Outfall 001, and discharge volumes from this source are accounted for in Outfall 001 data (i.e., the Outfall 001 effluent volumes shown in Figure 1.3-1 include these inputs). During the trial phase before July, operations at Trinity were not continuous and potable makeup water was used for cooling. SERF-blended water was used for most of June to August 2017, and again for most of December 2017; otherwise, potable water was used. While the SERF-blended water was used, the effluent volumes at Outfall 001 were on the order of 30,000 gpd less than when potable water was used.

Once the Trinity facility transitions to full-time use of SERF-blended makeup water, this change will result in a further decrease in discharge to Outfall 001 and therefore less surface water entering the wetland. The variability in effluent volumes and water chemistry that may be released to the wetland will depend on return flow from facilities to outfalls that release to the wetland.

#### **1.4 Monitoring Planned during the Performance Period**

The original monitoring plan for the Sandia wetland is described in section 6.0 of the “Work Plan and Final Design for Stabilization of the Sandia Canyon Wetland” (LANL 2011, 207053). Proposed revisions to the monitoring plan were presented in the “Sandia Wetland Performance Report, Baseline Conditions 2012-2014” (LANL 2014, 257590); in the “Sandia Wetland Performance Report, Performance Period April 2014–December 2014” (LANL 2015, 600399); in the “2015 Sandia Wetland Performance Report” (LANL 2016, 601432); in the “2016 Sandia Wetland Performance Report” (LANL 2017, 602341), and in the “2017 Sandia Wetland Performance Report” (LANL 2018, 603022).

The initial work plan (LANL 2011, 207053) called for a multi-phased approach to monitoring to evaluate hydrologic and geochemical changes associated with the GCS and/or with the SERF expansion and subsequent effluent reduction. This approach includes the following:

- Evaluate changes in hydrology and key geochemical indicators to monitor the health of the wetland at 12 alluvial groundwater sampling locations,
- Evaluate transport of metals and organic chemicals through the wetland by monitoring surface-water base flows and storm flows at 3 gaging stations,
- Monitor vegetation every 2 yr via photographic survey, and
- Conduct periodic geomorphic surveys to evaluate erosion and aggradation of sediments within the wetland.

Monitoring of alluvial groundwater chemistry until February 2016 had been accomplished through a series of 13 drive-point 1-in.-inside diameter wells (henceforth denoted as “piezometers” because of their small well-casing diameter and method of installation) arranged in 4 transects in the wetland that were sampled quarterly. In the pilot sampling method comparison performed in 2015 and discussed in Appendix E of the “2015 Sandia Wetland Performance Report” (LANL 2016, 601432), alluvial wells were deemed the best method to obtain ample amounts of water and provide representative samples and field parameters. By October 2016, all the piezometers (prefix: SCPZ) were removed and replaced with 12 alluvial wells (prefix: SWA) placed in undisturbed locations adjacent to the piezometers with approximately the same screening depth (Table 1.4-1). These alluvial wells are constructed of a 2-in.- inside diameter polyvinyl chloride (PVC) casing and a 2-in. slotted PVC casing to act as a screen surrounded by a filter pack consisting of 1/20 silica sand. As the piezometers were gradually replaced with alluvial wells in 2016, water from the piezometers was sampled until the alluvial wells were installed. In 2017 and 2018, only water from the alluvial wells was sampled. The alluvial well name will be used to refer to the approximate location shared by the former piezometers and the current alluvial wells (the piezometers and wells are cross-walked in Table 1.4-2) through the rest of this report.

The alluvial well (piezometer) transects are:

- Alluvial wells SWA-1-1 (SCPZ-1), SWA-1-2 (SCPZ-2/SWA-1), and SWA-1-3 (SCPZ-3) are located on a sand-and-gravel terrace near the active channel (c1 geomorphic unit) towards the western end of the wetland, which has experienced channel incision and dewatering relative to historical conditions. These alluvial systems are located on the c3 geomorphic unit (see Figure D-4.0-1 and Appendix D for maps and definitions of geomorphic surfaces from the “2015 Sandia Wetland Performance Report” (LANL 2016, 601432)), away from the active channel and associated inset terrace (c2a geomorphic unit), which are locations of recent cattail expansion. Well SWA-1-1 is screened towards the base of alluvial fill, while the tops of the screens in wells SWA-1-2 and SWA-1-3 are approximately 6 ft and 3 ft below ground surface (bgs), respectively (Table 1.4-1).
- Wells SWA-2-4 (SCPZ-4), SWA-2-5 (SCPZ-5), and SWA-2-6 (SCPZ-6/SWA-2) form a transect in the widest portion of the wetland. The tops of the well screens are 2–3 ft bgs because the wetland water level is at or very near the ground surface at this transect. It is at these shallowest depths that deleterious changes in water level and sediment oxidation state, were they to occur, would be expected to manifest as a result of reduced effluent discharge. Similarly, the lateral margins of the wetland may dewater before the longitudinal axis of the wetland as a result of reduced effluent volumes. This effect could be most pronounced where the wetland is widest and water flux is most spread out. It is also at such locations that preferential flow paths within the alluvium may form.
- Wells SWA-3-7 (SCPZ-7), SWA-3-8 (SCPZ-8/SWA-3), and SWA-3-9 (SCPZ-9) are located in a narrow part of the wetland closer to its distal (eastern) end. This transect includes two shallow wells, SWA-3-7 and SWA-3-9, with the tops of the screens at 0.6 and 2.2 ft bgs, respectively, and the SWA-3-8 with the top of the screen at 4.8 ft bgs (Table 1.4-1). The wetland water level is at or just below the ground surface at this transect. These alluvial locations provide indications of changes near the surface of the wetland and at depth in a narrow portion of the wetland where preferential flow paths are less likely to develop.
- The final transect of wells SWA-4-10 (SCPZ-10), SWA-4-11 (SCPZ-11B), and SWA-4-12 (SCPZ-12/SWA-4) have responded most to the rewatering that has occurred at the eastern terminus of the wetland because of the effect of the GCS. The wetland water level is at or near the surface at this transect. Water was routed around this area during the period of construction of the GCS.

The 2018 sampling and analysis plan for the alluvial wells is provided in Table 1.4-3. Most of the analyses were designed as indicators of redox changes associated with potential dewatering of the wetland. Alluvial locations were instrumented with sondes for continuous monitoring of water levels, specific conductance, and temperature.

Samples from base flow were collected quarterly with the alluvial wells. The same analytical suites, with the addition of unfiltered metals, PCB congeners, PAHs, and suspended sediment concentration (SSC), were monitored in base flow at surface water gaging stations E121, E122, and E123 (Figure 1.0-1).

Flow rates into and out of the wetland are measured at gaging stations E121, E122, and E123 during sample-triggering storm events, as well as during base flow conditions. Analyses of storm water samples collected in 2018 were planned as presented in Table 1.4-4. Analytical results with data plots are discussed in Appendix D and analytical data is available on CD (Appendix F).

Since 2016, aerial light detection and ranging (LiDAR) surveys are performed every 3 yr, or if large storm events result in significant geomorphic changes in a year when a survey is not scheduled. The next survey was scheduled for 2019; however, a baseline LiDAR survey was performed in 2018 because of quality issues with the 2016 LiDAR survey. Ground-based global positioning system (GPS) surveying along geomorphic features of concern and monitoring of erosion pins was performed. Vegetation zone perimeters of the Sandia wetland and photographs from established locations were monitored from year to year and define the extent of obligate wetland species that depend upon saturated wetland conditions. Details of the monitoring scheme and the results from this vegetation monitoring are presented in Appendix C. This monitoring effort replaces and supersedes that originally proposed in the “Work Plan and Final Design for Stabilization of the Sandia Canyon Wetland” (LANL 2011, 207053).

The GCS is inspected twice a year and following rain events with discharges greater than 50 cubic feet per second (cfs) (LANL 2014, 600083). If erosion or any indications of instability are observed, appropriate actions will be taken to ensure continued stability and functionality of the GCS. The new controls installed upstream of the GCS where sediment was running into the wetland from a southern drainage were installed in September 2017, but damages were found during the December 2017 inspection. New controls were completed in January 2018 to protect from scouring in the southern drainage. The GCS inspections, with inspections and photographs of these drainage controls, are presented in Appendix E.

## **1.5 Conceptual Model for Assessing Wetland Performance**

### **1.5.1 Hydrologic Status**

The Sandia wetland is an effluent-supported cattail wetland. Surface water is generally present in a discrete channel (though in some areas surface water spreads from bank to bank) and passes through the wetland with a short residence time relative to alluvial groundwater (LANL 2009, 107453; LANL 2014, 257590). Wetland sediments are underlain by Bandelier Tuff upon which alluvial groundwater is perched. A water-balance analysis conducted in 2007 and 2008 showed little surface water loss (approximately 2% of both effluent and runoff) occurs through the wetland (LANL 2009, 107453). A direct-current (DC) electrical-resistivity–based geophysical survey found that large continuous areas of the wetland are underlain by highly resistive welded tuffs (Qbt 2 of the Tshirege Member of the Bandelier Tuff) that represent a significant barrier to the infiltration of alluvial groundwater into the subsurface (LANL 2012, 228624). In several areas, the survey also identified subvertical conductive zones that penetrate the upper bedrock units and, in some cases, appear to correlate with mapped fault and/or fracture zones. These conductive zones may represent present-day or historical infiltration pathways. However, the DC resistivity data do not differentiate between conductive zones that contain higher water content (possibly representing active infiltration) and wetted clay-rich fracture fill that may hinder infiltration.

Installation of the GCS has led to cessation of headcutting at the terminus of the wetland and has created an impermeable barrier to subsurface flow such that alluvial groundwater must resurface before exiting the wetland. Given the impermeable nature of this barrier and the largely impermeable tuff underlying the wetland, the system can conceptually be thought of as a bathtub that effectively holds water with excess water spilling over the GCS at the wetland terminus. Annual evaluation of base-flow rates confirms this “bathtub” assumption as rates entering and exiting the wetland are similar, although this assumption breaks down during storm events because of additional flow from subtributaries such as the former Los Alamos County landfill (Figure 1.0-1). However, as long as water inputs from the outfalls exceed wetland evapotranspiration, even significantly reduced outfall discharge may sustain water levels and sufficient saturation within wetland sediments. Extreme decreases in effluent input volumes into the wetland, however, could potentially result in wetland dewatering. The wetland sediment is typically saturated at the eastern end of the wetland; these conditions extend westward, but near-surface sediment is unsaturated at the margins and at the western end of the wetland. Over the last 3 yr, there appears to be recovery of cattails in the west end of the wetland, which had been largely dewatered when the outfall that discharged directly into the wetland was relocated further upstream to the current location of Outfall 001. Channel meandering and sediment redistribution, however, are resulting in the reestablishment and expansion of cattails in this area (LANL 2016, 601432). Recent decreases in effluent volume to the wetland have not resulted in a lowering of the water table (dewatering) or decreased wetland vegetation cover (LANL 2016, 601432). The wetland vegetation community is important in mitigating storm water–related mobilization of contaminants through root binding and physical trapping of suspended sediments.

### **1.5.2 Contamination in Wetland Sediment**

Detailed sediment mapping was performed during the Phase I IR (LANL 2009, 107453). Canyon reach S-2, which contains the Sandia wetland, contains high concentrations and proportions of the originally released contaminant inventory. Reasons include (1) proximity to contaminant sources; (2) the large volume of sediment deposited during the period of active contaminant releases; (3) the presence of high concentrations of organic matter in the wetland; and (4) the presence of large amounts of silt and clay (Figure 1.0-1). Contaminants commonly adsorb to, or can be precipitated with, sediment particles or organic matter.

Chromium is the major inorganic contaminant of concern in the wetland that could be affected by both redox changes in the wetland and physical destabilization. Sections 1.0 and 1.1 present the background for chromium contamination in wetland sediments, and the desirable conditions that mitigate chromium form and mobility. Arsenic may also be released from wetland sediments upon dewatering (LANL 2009, 107453). Two groups of organic contaminants of concern, PCBs and PAHs, are primarily subject to physical transport in floods because of low solubility and a strong affinity for organic material and sediment particles. Important source areas for these contaminants are the former outfall for the power plant cooling towers in upper Sandia Canyon (chromium), a former transformer storage area along the south fork of Sandia Canyon (PCBs), and the former asphalt batch along the north fork of Sandia Canyon (PAHs) (LANL 2009, 107453).

### **1.5.3 Cr(III) Stability in the Sandia Wetland**

The inventory of chromium contamination within the Sandia wetland exists primarily in the form of Cr(III) because of reducing conditions. Alluvial saturation, along with significant amounts of solid organic matter produced from wetland vegetation, results in reducing alluvial aquifer conditions as indicated by detectable concentrations of ammonia and sulfide, high dissolved iron and manganese concentrations, and low nitrate and sulfate in alluvial groundwater (LANL 2014, 257590; LANL 2015, 600399; LANL 2016,

601432; LANL 2017, 602341). Oxidation by manganese oxides under aqueous conditions is the primary mechanism responsible for oxidation of Cr(III) to Cr(VI) (Rai et al. 1989, 249300). Complete oxidation of Cr(III) to Cr(VI) is likely to occur if the molar concentrations of manganese dioxide [Mn(IV)] exceed those of ferrous oxide [Fe(II)], Cr(III), and organic carbon. This situation, however, is unlikely within the active Sandia wetland because concentrations of total iron, consisting mainly of Fe(II), and solid organic matter are present at much higher weight-percent concentrations than Mn(IV), which is usually present in the parts per million range (discussed in more detail in Appendix J of the Phase I IR (LANL 2009, 107453). In addition, drying and leaching experiments conducted on Sandia wetland sediments to quantify the potential release of Cr(VI) during drying of the wetland material showed that Cr(III) appears to remain stable, suggesting insufficient Mn(IV) is produced to oxidize appreciable amounts of Cr(III) to Cr(VI) (LANL 2009, 107453). Total “dissolved” chromium in leachates was primarily in the form of Cr(III), indicating most chromium measured in a filtered wetland performance monitoring sample occurs as colloids. This explanation is supported by analyses of Cr(VI), which is generally below the method detection limit (LANL 2016, 601432).

#### **1.5.4 Current State of the Sandia Wetland**

Data from geochemical studies presented in the Phase I IR (LANL 2009, 107453) and the “2017 Sandia Wetland Performance Report” (LANL 2018, 603022) indicate chromium in wetland sediments is predominantly geochemically stable as Cr(III) and is not likely to become a future source of chromium contamination in groundwater, especially if saturated conditions are maintained within the wetland. The frequent nondetects of Cr(VI) in the wetland water confirms that most if not all the chromium exists as Cr(III) (see results in Appendix D). Results from baseline monitoring of the wetland (LANL 2014, 257590) and from monitoring in 2014 (LANL 2015, 600399), 2015 (LANL 2016, 601432), 2016 (LANL 2017, 602341), and 2017 (LANL 2018, 603022) show that the Sandia wetland system is chemically and physically stable, with stable to increasing wetland vegetation cover in different parts of the system. Most importantly, results of storm-water monitoring from gage station E123 have shown a reduction of PCBs and chromium post-GCS installation.

## **2.0 MONITORING PERFORMED DURING THE 2018 MONITORING PERIOD**

Quarterly sampling of Sandia wetland surface water and alluvial groundwater is coordinated with the chromium investigation monitoring group sampling conducted under the Interim Facility-Wide Groundwater Monitoring Plan (LANL 2017, 602406). In 2018, performance sampling was conducted at 12 alluvial wells within the wetland (collocated to the piezometers where water was collected through 2016 [Table 1.4-2]), as well as at surface water gaging stations E121 and E122 [above the wetland] and E123 [below the wetland] (Figure 1.0-1).

### **2.1 Monitoring of Surface Water**

Surface water gaging stations E121 and E122 are located in the upgradient western end of the Sandia Canyon watershed. Surface water gaging station E123 is located to the east immediately below the terminus of the wetland. Figure 1.0-1 shows the location of the gaging stations, outfalls, and the extent of the Sandia wetland. In 2018, gaging station E121 measured discharge from Outfall 001, Outfall 03A027, and storm water runoff from approximately 50 acres from TA-03. With changes at SERF in September 2016, discharge from SCC cooling towers is primarily directed to Outfall 001, with Outfall 03A027 used only for maintenance and emergency discharge (see section 1.4). Gaging station E122 measures discharge from Outfall 03A199 and storm water runoff from approximately 50 acres from TA-03.

Gaging station E123 measures surface water flow below the wetland, including discharge from all outfalls and storm water runoff from approximately 185 acres, 100 acres of which are from E121 and E122.

Tables 2.1-1 and 2.1-2 detail surface water base-flow sampling and field parameters, respectively, for samples collected in calendar year 2018 (see section 1.5).

In 2018, ISCO 3700 automated samplers attempted to collect storm water samples when discharge was greater than 10 cfs above the base flow at gaging stations E121 and E123. At gaging station E122, the automated samplers attempted to collect storm water samples when discharge was greater than 2.0 cfs. This sample threshold at E122 was set lower than 10 cfs because of the lack of significant storm runoff at gaging station E122. Base-flow and storm-flow samples in 2018 were analyzed based on the suites presented in Table 1.4-3 and Table 1.4-4, respectively. Samplers at E121, E122, and E123 were activated in June 2018, before the monsoon season, and turned off for the winter in November 2018. Stations E121 and E123 are equipped with a Sutron 9210 data logger, an MDS 4710 radio transceiver, and a Sutron Accubar bubbler. Station E122 is equipped with a Sutron 9210 data logger, an MDS 4710 radio transceiver, and a VEGAPULS 61 radar sensor. Stage is recorded every 5 min and transmitted to a base station where it is archived in a database. All three gaging stations are equipped with two automated ISCO samplers: one with a 24-bottle base for SSC analyses throughout the storm event, and one with a 12-bottle base for collection of chemistry samples (Table 1.4-4).

For each sample-triggering storm event in 2018, Table 2.1-2 shows precipitation at rain gage RG121.9, storm water peak discharge, and whether a sample was collected at E121, E122, and E123 (Figure 1.0-1). Storm water discharge at E121 equaled or exceeded the trip level (10 cfs above the base flow) seven times in 2018 and samples were collected from six of those events. Discharge at E122 equaled or exceeded the lowered trip level ~2.5 cfs) four times in 2018 and samples were collected from four of those events. Discharge at E123 exceeded the trip level (10 cfs above the base flow) five times in 2018 and samples were collected from five of those events.

## **2.2 Monitoring of Alluvial System**

Full suites were collected at all locations in each quarter, except where otherwise noted. All analyses were performed off-site after the May round with the exception of sulfide, which has a holding time of 24 hr and was analyzed on-site. Though often the sulfide holding time is exceeded, these data are still useful for interpreting redox conditions in the wetland. Actual sulfide concentrations are expected to be higher than those measured outside the holding time, so measured sulfide concentrations are conservative in terms of assessing redox conditions. Cr(VI) was measured at all alluvial wells and surface water locations (base flow) quarterly. Arsenite [As(III)] and Fe(II) were measured quarterly in only the alluvial wells. The field parameter data from the surface water and alluvial wells are provided in Table 2.1-1.

## **2.3 Water-Level Monitoring**

Water-level and temperature data collected by sondes are discussed in section D-4.0 in Appendix D. Sondes at alluvial well locations along transects 1 and 2 were sent in for routine calibration in mid-February 2017 and reinstalled at the beginning or April. Sondes in alluvial well locations along transects 3 and 4 were sent in for routine calibration in mid-March 2017 and reinstalled by the end of April. The sondes were left in the wells over the winter. The water level results for 2018 were consistent with those of previous years. All transects showed attenuated water level change because of reduced annual discharge and precipitation events in 2018. Temperatures were consistent, showing temporal changes with seasons and with less variation in wells located in the channel (SWA-2-5) and wells at a depth greater than 10 ft (SWA-1-1)



## **2.4 Geomorphic Monitoring**

A full description of the approach and results for geomorphic surveys is presented in Appendix B.

## **2.5 Vegetation Monitoring**

A full description of the approach and results for vegetation surveys is presented in Appendix C.

## **2.6 Monitoring of the GCS**

Inspection results from monitoring of the GCS are presented in Appendix E.

## **3.0 SUMMARY OF RESULTS FROM WETLAND PERFORMANCE METRICS**

Detailed results of performance metrics are presented in Appendix D and are summarized here.

### **3.1 Key Monitoring Locations and Performance Metrics**

It is important to note that deleterious changes in any one metric do not necessarily represent a detriment to the overall function of the wetland and will not necessarily lead to contaminant release from wetland sediments. The wetland should be evaluated in terms of total system performance over time with multiple lines of evidence used to determine if the system is stable.

Gaging station E121 is a good location to monitor the integrated impacts of changing input chemistry and decreasing effluent volumes from Outfalls 001 and 03A027 in base flow. Gaging station E123 is the key integrating location of total wetland performance in mitigating discharges of contaminants of concern. Monitoring of storm water at E123 will reveal if anomalously high levels of sediment and contaminants (e.g., chromium, PCBs, PAHs) are mobilized during floods because of a reduction in chemical and/or physical stability in the wetland. Monitoring during base flow conditions will indicate changes in outfall chemistry and changes associated with wetland biogeochemistry and function. The metric for identifying deleterious impacts monitored at this location would be increases in base flow or storm water contaminant concentrations that occur year after year since the installation of the GCS.

The alluvial well array provides valuable water-level and alluvial groundwater chemistry data (Appendix D). These locations monitor potential changes associated with outfall volumes, evolving geomorphology, redistribution of reducing zones, and changes in chemistry of the outfall (in the case of more conservative constituents). The metrics for identifying deleterious impacts as monitored in the wells would be: (1) persistent increases in contaminant concentrations [e.g., Cr(VI)] and/or increases in oxidizing conditions as indicated by redox-sensitive species (e.g., dissolved iron) and (2) persistent decreases in water levels that have deleterious effects on obligate wetland vegetation.

Geomorphic change detection using ground-based surveys of the thalweg and the established erosion pins has been performed during the 5-yr of post-GCS monitoring (Appendix B). In the future, aerial-based surveying of the thalweg and plunge-pool, and ground-based monitoring of the established erosion pins, will be performed.

The quantitative vegetation cross-sections and perimeter mapping over the year (Appendix C) are used to monitor both the physical stability and the saturation state of the wetland, as indicated by changes in obligate and facultative wetland vegetation. Increases in upland vegetation within the current extent of the wetland would indicate deleterious impacts on wetland function. In the future, aerial-based surveying of the vegetation will be performed.

As of December 2018, 5 yr of post-GCS monitoring has been conducted. Section 3.9 outlines the plan for 2019 monitoring. This monitoring plan will continue to be refined and improved in an effort to fully identify, and monitor for, key criteria that are reliable proxies for wetland stability (e.g., vegetation, spatial contaminant trends, geomorphic stability, and key redox indicators).

### **3.2 Spatial and Temporal Geochemical Patterns**

PCB and total chromium concentrations in both base flow and storm flow at E123 continue to be reduced post-GCS construction, and less variable under base flow conditions (Appendix D, Figure D-2.0-7). While PCB concentrations in base flow and storm flow were generally higher downgradient of the wetland (relative to upgradient locations E121 and E122) before the GCS was built, the concentrations are closer in magnitude upgradient and downgradient of the wetland since the GCS was constructed. The trend in PCBs and total chromium concentrations at all of the gaging stations, both in base flow and storm flow, indicate a general decrease over the past 7 yr or so, with a slight increase in storm flow in 2017, but comparable to most post-GCS data. The trends in PCBs and total chromium at E123 may be a result of continued growth of wetland vegetation, corresponding to stabilization of the sediment (Appendixes B and C); however, the decreasing trend at the upgradient locations may be a result of less intense precipitation and erosive runoff during the years following construction of the GCS. While it is difficult to absolutely attribute causes for PCB mobilization, the intense 2017 storm event on July 26 had high PCB and total chromium concentrations in storm flow, likely driving increased mean concentrations between 2016 and 2017. The 2018 stormflow PCB concentrations were higher at E123 than the previous year, yet still within the range of concentrations for most years post-GCS (Appendix D, Figure D-2.0-7).

PAHs were not analyzed in base flow or storm flow before the GCS was built. In base flow, total PAH results were mostly nondetections, with the exception of one sample collected at E123 in 2016 and one sample collected at E121 in 2017. In 2018, PAH detects in base flow were determined to be outliers (Appendix D, Figure D-2.0-7). Therefore, base flow total PAH concentrations were significantly lower than in storm flow where detections were more common. In storm flow, total PAH concentrations were highly variable and thus were indistinguishable upgradient and downgradient of the wetland. Overall, higher concentrations of PAHs were detected at E122 than at E121 and E123, which is consistent with expected spatial influence of the former asphalt batch plant near the northern fork of upper Sandia Canyon. This source is the most likely genesis of PAHs at the downstream gaging station because the low concentrations elsewhere indicate confined source material.

Base flow water quality indicators illustrate the impact of recent improvements in water quality because of the SERF upgrade (Appendix D-2.0). Persistent redox indicators (i.e., reducing conditions) show evidence of biogeochemical reduction as surface water flows through the wetland, generating reduced iron and manganese in alluvial wells). The sum of base flow Cr(VI) concentrations at E121 and E122 have been generally higher than at E123, indicating chromium reduction and immobilization in the wetland (Appendix D, Figure D-2.0-5). Dissolved chromium at E123 (baseflow conditions) for 2018 is higher than 2015 and 2016, yet similar to 2017.

Low sulfate concentrations in alluvial groundwater relative to base flow, along with frequent detects of sulfide, emphasize the strong reducing nature of the wetland sediments. Exceptions include the SWA-3-7 and SWA-4-10 wells wherein sulfate is variable through time indicating redox hotspots in the wetland. As sulfate reduction occurs at much lower redox potentials than the reduction of chromate, nitrate, and iron, the wetland environment is highly favorable in terms of chemical stability of chromium as Cr(III). Several analytes clearly reflect reducing conditions in all alluvial locations throughout the wetland (sulfate, arsenic, iron, manganese, and sulfide), and these findings are supported by the qualitative organoleptic signatures of reducing conditions frequently recorded by field team members. Sulfide and ammonium are present at all locations as opposed to more oxidized forms of these elements. Consistent with the sulfide/sulfate

alluvial well data for SWA-4-10, iron and manganese are highly variable and likely indicate well known reductions and co-precipitations that occur with these elements as the vadose zone in this area dries and re-wets. While no preferential flow paths were identified in the alluvium, there do appear to be distinct geochemical domains in terms of redox conditions.

Slight temporal increases in iron and manganese concentrations over the period of sampling may be the result of ongoing inputs of organic matter, leading to organic acids that continue to promote strong reducing conditions in the wetland, and biogeochemical weathering of parent material (section D-3). No temporal trends were observed in chromium concentrations.

### 3.2.1 Surface Water and Alluvial Groundwater Exceedances

Base-flow and storm water analytical results from gaging stations E121, E122, and E123 in 2017 were screened against the appropriate surface water–quality criteria (SWQC) (see section D-2.1). The two main sources of surface water that enter the wetland are discharges from outfalls and storm water runoff from the developed landscape within TA-03. This run-on sourced water influences the results from E121 and E122. Flow at E123 is composed of a mix of waters from E121, E122, runoff through the Sandia wetland, and urban runoff from the Laboratory and Los Alamos County. The exceedances detected in storm water in 2018 include aluminum, cadmium, copper, gross-alpha, lead, total PCBs, selenium, and zinc; the exceedances detected in base flow in 2018 include only copper and total PCBs. Most of the exceedances occurred in storm water (98), a lesser number occurred in perennial base flow (12).

A comparison of the average and maximum results from E121 and E122 to E123 shows that, with exception of PCBs, the Sandia wetland is not a source of industrial site-related pollutants that exceed New Mexico SWQC. Aluminum, copper, gross-alpha, lead, and zinc exceedances are attributed to urban runoff and naturally occurring sediments routed to the wetlands from LANL (TA-03) and Los Alamos County. Lead and copper continued to exhibit no discernable trend in attenuation during 2018.

The alluvial system data from 2018 were screened to groundwater standards (Appendix D, section D-3.3 and Table D-3.3-1). Exceedances in alluvial groundwater included arsenic, chromium, iron, and manganese. Arsenic exceedances were observed at SWA-2-5 once and consistently at SWA-2-6 for all four monitoring rounds. Previous speciated arsenic data indicate that most of the aqueous arsenic in the alluvial system is As(III), the reduced form. Iron and manganese exceedances were the most commonly observed elements and are expected because of the reducing wetland conditions, bringing these likely geology-derived metals into solution. Dissolved manganese is more persistent than iron because of manganese oxidation kinetics; and, it has been observed in surface water at E123 in past surveys. Most of the total chromium concentration in alluvial groundwater in the wetland is colloidal Cr(III), leading to exceedances; the measured Cr(VI) at the locations of the exceedances is at or below the minimum detection limit.

### 3.3 Temporal and Spatial Trends in Water-Level

Water level monitoring continues as a means to determine how operational effluent releases affect the overall wetland hydrology. Comparisons between the 2017 and 2018 water levels, shown in Appendix D, Figure D-4.0-2, indicate they have been relatively stable, even with changes in outfall volumes. Seasonal decreases in water levels are observed in a few wells in the easternmost transect, presumably as a result of high rates of evapotranspiration associated with warm temperatures and lower-magnitude precipitation events in the summers compared with those in the previous year (section D-2.0). The water levels in the alluvial system tend to stay stable because the relatively impermeable Bandelier Tuff bedrock base of the wetland, and an impermeable downgradient end (the GCS) keeps the water contained in the wetland. As such, as long as water inputs exceed wetland evapotranspiration, even significantly reduced outfall

discharge may sustain water levels and sufficient saturation within wetland sediments. Decreased outfall discharge may manifest more in the surface water balance of the wetland than in alluvial groundwater levels.

### **3.4 Geomorphic Trends in the Wetland**

Repeat GPS surveys in conjunction with field observations indicated that no significant geomorphic changes occurred in the wetland during the 2018 monsoon season. Similar geomorphic change detection studies indicate only minor geomorphic change has occurred between 2014 and 2018 (Appendix B). The thalweg and bank tops persist as stable features, with minor lateral changes in thalweg position from 2014 to 2018 correlating to the development of riparian vegetation throughout the wetland area. Additionally, the thalweg nick point has remained stable since 2015 with no indication of upstream erosion. Between 2017 and 2018, changes to the plunge pool were observed at the eastern end of the pool where rapid sedimentation occurs at the channel outlets. Since 2014, minor changes in areal extent of the plunge pool have occurred as a result of episodic sedimentation events and vegetation development. A side channel located at the toe of the southern alluvial fan that developed in 2015 continued to redistribute sediment in the area, but no significant loss of cattail vegetation was observed in 2018. Furthermore, three alluvial fans entering the wetland from the north (drainage from the former Los Alamos County landfill) did not show signs of continued deposition.

### **3.5 Spatial and Temporal Trends in Vegetation**

In 2018, notable expansion was observed in the GCS wetland and the western-end of the wetland, especially occurring in the satellite cattail populations by the plunge pool and in the fields north and south of the channel in the western cattail zone. The delineation of a new willow zone adjacent to the central mixed cattail/willow zone, where a previously gradational conversion into cattails existed, has become more distinct (Appendix C, Figure C-1.0-2). The western mixed cattail/willow zone and the central cattail zone remain generally stable and do not appear to be affected by gravel bars or the reworking of sediment from the southern drainage. Between 2014 and 2018, the wetland vegetation area has expanded by about 22% over the whole study area (Appendix C, Figure C-1.0-3). Repeat photos and perimeter mapping suggest that increased coverage of wetland vegetation has occurred since 2014 and that the wetland has remained stable between 2017 and 2018 (see Attachment C-1).

Vegetation monitoring documented in this report does not constitute a formal, U.S. Army Corps of Engineers-approved wetland delineation. For example, the occurrence of hydric soils has not been determined. The combined approach of monitoring the saturation status of the wetland through water-level measurements and redox chemistry, along with spatial and temporal patterns in obligate wetland vegetation, however, is sufficiently robust to evaluate the performance of the wetland. For example, should the wetland begin to dewater as a result of operational changes associated with the SERF, these changes would be noted immediately in water-level data and subsequently in alluvial groundwater chemistry and obligate wetland vegetation patterns.

### **3.6 Performance of GCS**

Inspection results from monitoring of the GCS, presented in Appendix E, indicate that the GCS is stable and does not require corrective or mitigative actions. Appendix E describes repairs performed in January 2018 to log check dams installed in 2017 to capture sediment running off from a southern drainage into the wetland. However, on a fall 2018 walkdown with NMED, it was noted that these controls were operating suboptimal, a condition that will be revisited/repared in 2019 (no photos of the damage are available at this time as the area was snow covered during the walkdown).

### 3.7 2019 Monitoring Plan

The monitoring plan for 2019 includes the following:

- Annual post-monsoon walkdowns with NMED;
- Biannual and greater than 50 cfs inspections of the GCS and the log check dams on the southern tributary to the wetland;
- Aerial-based geomorphologic and vegetation surveys every third year, except in the case of a large disturbance event; and
- Determine a path forward with SERF to maintain sufficient flow into the wetlands (progress updates and copies of any agreement between N3B and Triad National Security, LLC, will be sent to NMED).

A large disturbance event has been defined based on historical knowledge. Storm events where significant erosion or channel alterations occurred were examined, along with the associated discharge at the downstream gaging station, E123 (Table 3.7-1). Based on this analysis, the discharge magnitude that has the potential to cause significant erosion was determined to be approximately 100 cfs. If discharge at gaging station E123 reaches this discharge value, N3B will consider this a large storm event that might warrant an aerial-based geomorphic and vegetation survey before the routine third year survey. After a field visit is performed, if significant erosion or vegetation disturbance is observed, aerial surveys will be performed after/during the monsoon season (after for geomorphic surveys and during for vegetation surveys). A baseline LiDAR aerial survey was performed in 2018 during which points were measured at a density at least equivalent to the 2016 LiDAR data set (18–24 points per m<sup>2</sup>). The LiDAR surveys will provide a detailed digital elevation model (DEM) of the entire active channel within the wetland area so a comparison with the previous survey's DEM can show areas of geomorphic change. If noteworthy features are identified in the LiDAR comparison, the features will be field-checked and additional ground-based survey methods may be implemented.

Aerial vegetation monitoring has not been performed in the past; however, a baseline vegetation survey will be performed in 2019 and will continue every third year. The next aerial-based vegetation survey will be conducted in 2022. A hyperspectral sensor will be deployed via plane or unmanned aerial vehicle, and will be used to classify vegetation species and determine vegetation density, stand height, and spatial extent. In addition, the normalized difference vegetation index (NDVI), which is an indicator of photosynthetic activity using the red and near-infrared bands, will be computed as a measure of the health of the wetlands.

For the alluvial wells, the following will be performed for 3 yr (2019, 2020, and 2021), after which the monitoring plan will be reevaluated:

- Annual sampling post-monsoon in October;
- Analyze dissolved Cr(VI) and target analyte list (TAL) metals and collect field parameters during sampling;
- Monitor transects 1 (SWA-1-1, SWA-1-2, and SWA-1-3), transect 4 (SWA-4-10, SWA-4-11, and SWA-4-12), and wells SWA-2-6 and SWA-2-4, for a total of eight wells; and
- Continue monitoring water levels at these eight wells.

Annual alluvial well sampling is proposed in the post-monsoon, post-growing season period (October) in order to optimize for several functional indicators monitored in the sampling plan. Monsoonal storms have the potential to generate a flush of turbid, well-aerated water to the alluvial system and this presents a

“worst-case scenario” for reducing conditions, and thus the wetland’s function as a retainer of constituents of concern. Additionally, reducing conditions driven by the production of organic acids will have slowed appreciably because of declining air temperature, which is the main driver of water temperature, hence declining organic decomposition. In total, the proposed October alluvial sampling is designed to capture several seasonal events that challenge beneficial ecosystem functions in the wetland, when the system is most challenged to provide conditions amenable to immobilization of chromium and breakdown of PCBs.

Redundancy in alluvial well water reducing conditions will be maintained, but measurement of some analytes and speciated analytes will be reduced. Dissolved iron, for instance, is a good indicator of the presence of Fe(II) as ferric oxide [Fe(III)] is sparingly soluble at standard temperature, pressure, and pH. Thus, determination of Fe(II) by direct means is unnecessarily redundant.

For base flow (quarterly) and storm flow (four samples) at gaging stations E121, E122, and E123, the following will be analyzed:

- Dissolved Cr(VI) in base flow and total and dissolved chromium for storm flow
- PCBs
- PAHs
- Semivolatile organic compounds (SVOCs)—Note: Both SVOC and PAH methods are needed to obtain the lowest method detection limits for PAHs.
- Total and dissolved TAL metals
- SSC

In 2019, the automated samplers for collecting storm water will be set up as presented in Table 1.4-4 (except 10-µm filtered aluminum will be added to the list of TAL metals). Four storm water runoff events will be sampled at gaging stations E121, E122, and E123 during the monitoring year. In addition, streamflow discharge will be monitored at gaging stations E121, E122, and E123.

In summary, alluvial wells, surface water base flow, and surface water storm flow requirements for the Sandia wetland performance monitoring are proposed in Table 3.7-2. Note that other analytes are being sampled in storm flow in 2019 (Table 1.4-4 plus 10-µm filtered aluminum) for purposes other than the monitoring of wetland performance (i.e., total organic carbon [TOC], dissolved organic carbon [DOC], chloride, sulfate, alkalinity, pH, gross alpha, and 10-µm filtered aluminum). Only analytes required for the monitoring of wetland performance are presented in Table 3.7-2.

### **3.8 Proposed Changes to Monitoring Plan from 2018**

Changes for 2019 include the following:

- Sampling and water level monitoring at alluvial wells SWA-2-5, SWA-3-7, SWA-3-8, and SWA-3-9 will be discontinued;
- Sampling frequency of alluvial wells will be reduced from quarterly to annually in October;
- Sampling suite in alluvial wells will be reduced to only dissolved Cr(VI) and dissolved TAL metals, and discontinuing As(III), Fe(II), and Fe(III) speciation, anions, ammonium, nitrate-nitrite, phosphorus, alkalinity/pH, DOC, and sulfide; and
- Geomorphological and vegetation monitoring will be aerial-based (vs. ground-based) and will be performed every third year (vs. annually for the geomorphological monitoring and biannually for the vegetation monitoring) or after a large disturbance event.

The basis for these changes is that 5 yr of alluvial well data indicate that spatial and temporal stability exists in the wetland and, therefore, redundancy exists in the current monitoring plan. Reduced sampling frequency and maintaining a subset of wells that capture edge effects (wetland-upland) and water table fluctuations is supported by existing long-term data. Additionally, speciation of some metals and other indicators of reducing conditions are significantly redundant and conservative measures of wetland reducing conditions will be kept in the monitoring plan.

## **4.0 CONCLUSIONS**

This performance period covers the fifth year following baseline monitoring. The monitoring performed during the performance period indicates that the Sandia wetland is stable and generally expanding following installation of the GCS. Yearly comparisons of analytical results indicate that the wetland is discharging lower concentrations of contaminants of concern in storm water since construction of the GCS. Even with periods of lower effluent volumes entering the wetland and periods of evapotranspiration, the alluvial system remains stable and wetland sediments remain highly reducing, with no concerning temporal trends in chemistry noted.

Despite overall reduced effluent discharge volumes, water levels remain sufficiently high to sustain and promote the expansion of the obligate wetland vegetation. Continuing vegetation monitoring in future years will be valuable in assessing wetland performance, with abundant wetland vegetation promoting sediment stability and preserving reducing conditions. No large-scale, systematic erosion has been noted in the wetland, and the system seems to be highly stable from a physical perspective. The GCS has arrested headcutting at the terminus of the wetland. Planted wetland vegetation has rapidly established around the GCS, and wetland vegetation is expanding in the upper portion of the system. Storm water data indicate that the GCS has had a positive impact on mitigation of contaminant transport. Suspended sediment, PCBs, and chromium concentrations have decreased at E123 post-GCS, presumably because of cessation of headcutting at the terminus of the wetland, and conditions that promote immobilization.

Ongoing monitoring will continue to allow assessment of changes within the Sandia wetland related to the GCS, changes in effluent chemistry, and decreases in effluent volumes and discharge rates. An adaptive management strategy will be employed should adverse changes be noted.

## **5.0 REFERENCES AND MAP DATA SOURCES**

### **5.1 References**

*The following reference list includes documents cited in this report. Parenthetical information following each reference provides the author(s), publication date, and ERID, ESHID, or EMID. This information is also included in text citations. ERIDs were assigned by the Laboratory's Associate Directorate for Environmental Management (IDs through 599999); ESHIDs were assigned by the Laboratory's Associate Directorate for Environment, Safety, and Health (IDs 600000 through 699999); and EMIDs are assigned by N3B (IDs 700000 and above). IDs are used to locate documents in N3B's Records Management System and in the Master Reference Set. The NMED Hazardous Waste Bureau and N3B maintain copies of the Master Reference Set. The set ensures that NMED has the references to review documents. The set is updated when new references are cited in documents.*

- DOE (U.S. Department of Energy), August 24, 2010. "Final Environmental Assessment for the Expansion of the Sanitary Effluent Reclamation Facility and Environmental Restoration of Reach S-2 of Sandia Canyon at Los Alamos National Laboratory, Los Alamos, New Mexico," U.S. Department of Energy document DOE/EA-1736, Los Alamos Site Office, Los Alamos, New Mexico. (DOE 2010, 206433)
- EPA (U.S. Environmental Protection Agency), June 8, 2007. "Authorization to Discharge under the National Pollutant Discharge Elimination System, NPDES Permit No. NM 0028355," Region 6, Dallas, Texas. (EPA 2007, 099009)
- EPA (U.S. Environmental Protection Agency), August 12, 2014. "NPDES Permit No. NM0028355 Final Permit Decision," U.S. Environmental Protection Agency Region 6, Dallas, Texas. (EPA 2014, 600257)
- LANL (Los Alamos National Laboratory), October 2009. "Investigation Report for Sandia Canyon," Los Alamos National Laboratory document LA-UR-09-6450, Los Alamos, New Mexico. (LANL 2009, 107453)
- LANL (Los Alamos National Laboratory), May 2011. "Interim Measures Work Plan for Stabilization of the Sandia Canyon Wetland," Los Alamos National Laboratory document LA-UR-11-2186, Los Alamos, New Mexico. (LANL 2011, 203454)
- LANL (Los Alamos National Laboratory), September 2011. "Work Plan and Final Design for Stabilization of the Sandia Canyon Wetland," Los Alamos National Laboratory document LA-UR-11-5337, Los Alamos, New Mexico. (LANL 2011, 207053)
- LANL (Los Alamos National Laboratory), March 2012. "100% Design Memorandum for Sandia Wetlands Stabilization Project," Los Alamos National Laboratory, Los Alamos, New Mexico. (LANL 2012, 240016)
- LANL (Los Alamos National Laboratory), September 2012. "Phase II Investigation Report for Sandia Canyon," Los Alamos National Laboratory document LA-UR-12-24593, Los Alamos, New Mexico. (LANL 2012, 228624)
- LANL (Los Alamos National Laboratory), December 2013. "Completion Report for Sandia Canyon Grade-Control Structure," Los Alamos National Laboratory document LA-UR-13-29285, Los Alamos, New Mexico. (LANL 2013, 251743)
- LANL (Los Alamos National Laboratory), June 2014. "Sandia Wetland Performance Report, Baseline Conditions 2012–2014," Los Alamos National Laboratory document LA-UR-14-24271, Los Alamos, New Mexico. (LANL 2014, 257590)
- LANL (Los Alamos National Laboratory), December 15, 2014. "2014 Annual Monitoring Report for Sandia Canyon Wetland Grade-Control Structure (SPA-2012-00050-ABQ)," Los Alamos National Laboratory letter and attachments (ENV-DO-14-0378) to K.E. Allen (USACE) from A.R. Grieggs (LANL), Los Alamos, New Mexico. (LANL 2014, 600083)
- LANL (Los Alamos National Laboratory), April 2015. "Sandia Wetland Performance Report, Performance Period April 2014–December 2014," Los Alamos National Laboratory document LA-UR-15-22463, Los Alamos, New Mexico. (LANL 2015, 600399)



LANL (Los Alamos National Laboratory), April 2016. "2015 Sandia Wetland Performance Report," Los Alamos National Laboratory document LA-UR-16-22618, Los Alamos, New Mexico. (LANL 2016, 601432)

LANL (Los Alamos National Laboratory), April 2017. "2016 Sandia Wetland Performance Report," Los Alamos National Laboratory document LA-UR-17-23076, Los Alamos, New Mexico. (LANL 2017, 602341)

LANL (Los Alamos National Laboratory), May 2017. "Interim Facility-Wide Groundwater Monitoring Plan for the 2018 Monitoring Year, October 2017–September 2018," Los Alamos National Laboratory document LA-UR-16-24070, Los Alamos, New Mexico. (LANL 2017, 602406)

LANL (Los Alamos National Laboratory), April 2018. "2017 Sandia Wetland Performance Report," Los Alamos National Laboratory document LA-UR-18-23194, Los Alamos, New Mexico. (LANL 2018, 603022)

NMED (New Mexico Environment Department), June 9, 2011. "Approval with Modification, Interim Measures Work Plan for Stabilization of the Sandia Canyon Wetland," New Mexico Environment Department letter to G.J. Rael (DOE-LASO) and M.J. Graham (LANL) from J.E. Kielling (NMED-HWB), Santa Fe, New Mexico. (NMED 2011, 203806)

Rai, D., L.E. Eary, and J.M. Zachara, October 1989. "Environmental Chemistry of Chromium," *Science of the Total Environment*, Vol. 86, No. 1–2, pp. 15–23. (Rai et al. 1989, 249300)

## 5.2 Map Data Sources

Rain Gages; Los Alamos National Laboratory; ER-ES Surface Hydrology Group; 2017.

WQH NPDES Outfalls; Los Alamos National Laboratory, ENV Water Quality and Hydrology Group; Edition 2002.01; 01 September 2003.

Alluvial Well Locations; Los Alamos National Laboratory, Waste and Environmental Services Division; Locus EIM database pull; 2017.

Paved Road Arcs; Los Alamos National Laboratory, FWO Site Support Services, Planning, Locating and Mapping Section; 06 January 2004; as published 29 November 2010.

Grade Control Structure and Cascade Pool; Los Alamos National Laboratory; ER-ES Engineering Services; as published, project 14-0015; 2017.

Structures; Los Alamos National Laboratory, FWO Site Support Services, Planning, Locating and Mapping Section; 06 January 2004; as published 29 November 2010.

Former Los Alamos County Landfill; Los Alamos National Laboratory; ER-ES Engineering Services; as published, project 14-0015; 2017.

Canyon Reaches; Los Alamos National Laboratory, ENV Environmental Remediation and Surveillance Program, ER2002-0592; 1:24,000 Scale Data; Unknown publication date.

Technical Area Boundaries; Los Alamos National Laboratory, Site Planning & Project Initiation Group, Infrastructure Planning Office; September 2007; as published 13 August 2010.

Orthophotography, Los Alamos National Laboratory Site, 2014; Los Alamos National Laboratory, Site Planning and Project Initiation Group, Space and Site Management Office; 2014.

Contours, 20 and 5-ft intervals; as generated from 2014 LiDAR elevation data; Los Alamos National Laboratory, ER-ES; as published, project 14-0015; 2017.



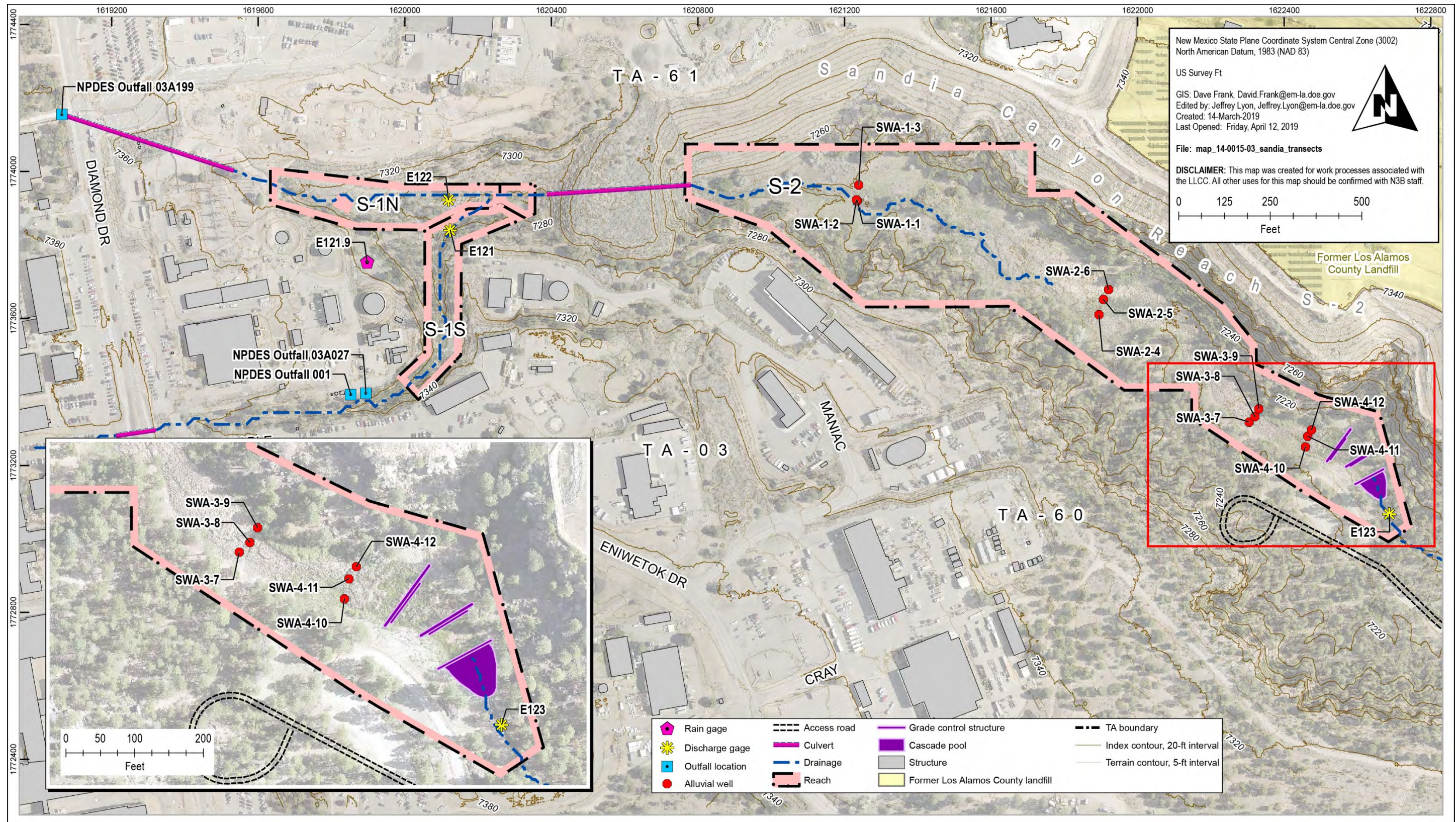


**Figure 1.0-1** Locations of the Sandia GCS, NPDES outfalls, precipitation gage E121.9, alluvial wells, surface and storm water gaging stations, former Los Alamos County landfill, surrounding TAs, and reaches S-1N, S-1S, and S-2 (reaches S-1N and S-1S are upstream of the wetland, S-2 essentially encompasses the wetland).





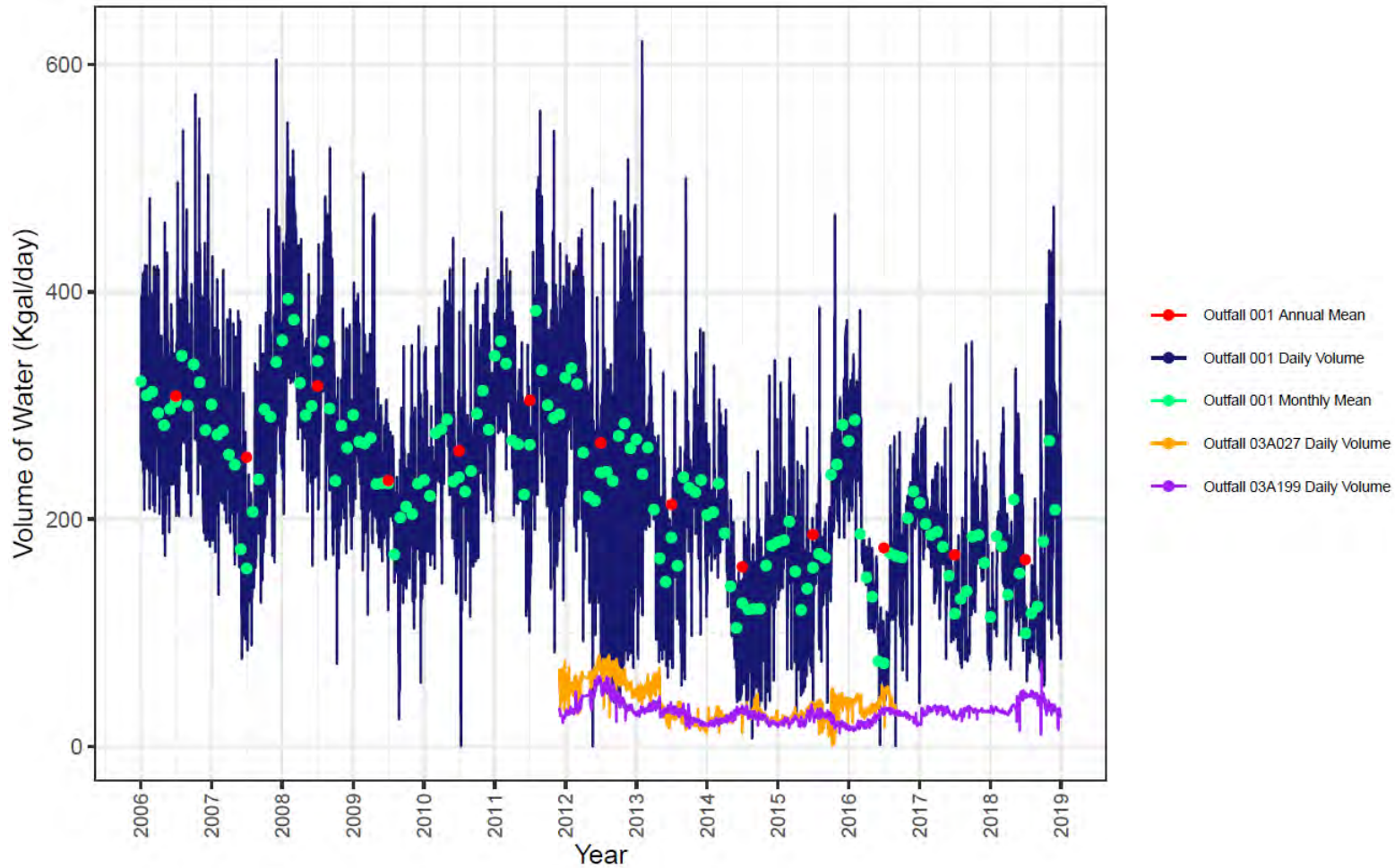


**Figure 1.3-1** Daily, monthly average, and yearly average effluent release volumes (expressed as Kgal./day) for Outfall 001 from 2006 to December 2018. Daily effluent releases for Outfall 03A027 is from November 2011 to September 2016. Outfall releases from 03A199 are plotted from August 2007 to January 2010 and from November 2012 to December 2018. No discharges to Outfall 03A027 have occurred since September 2016

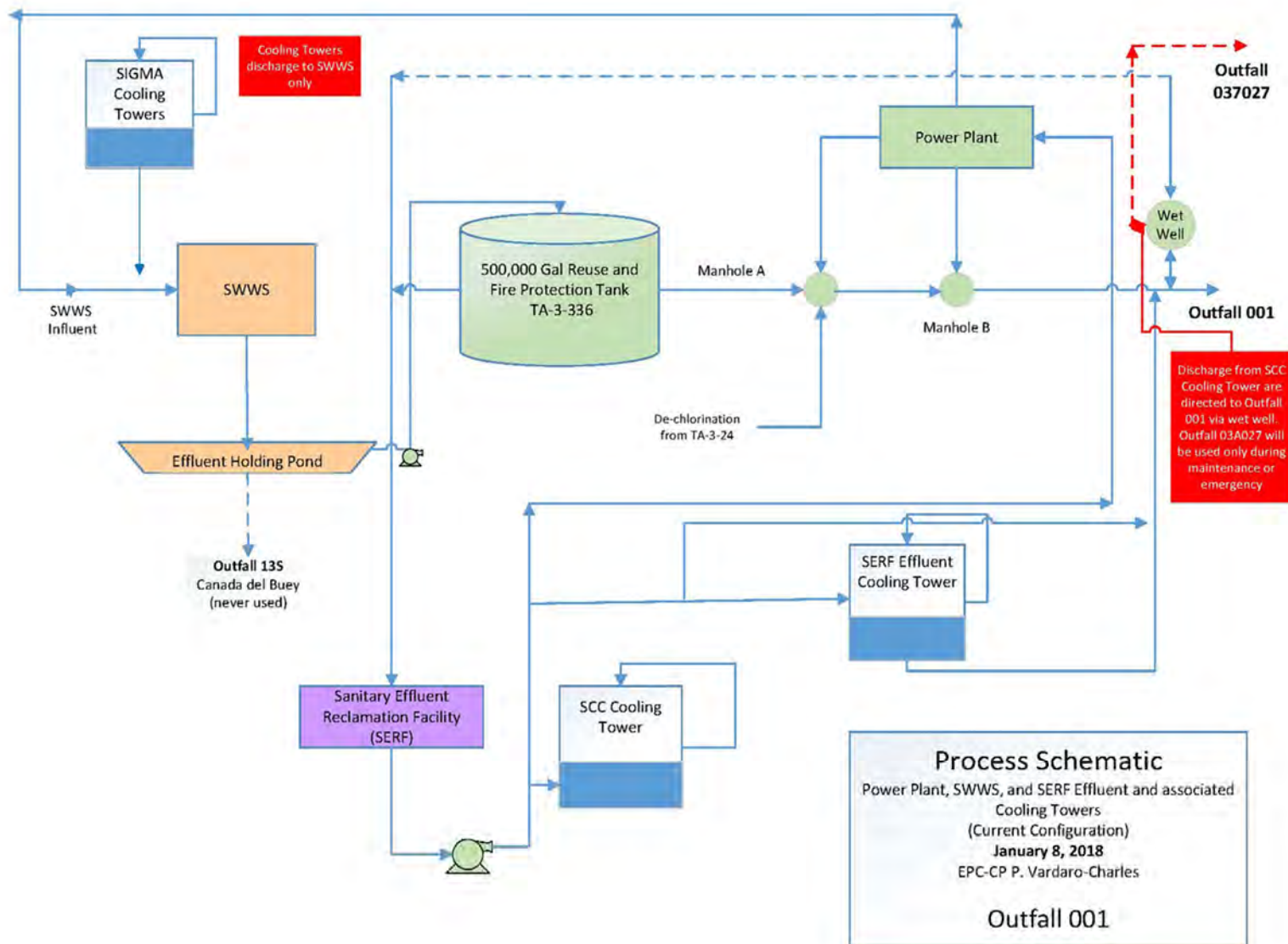


Figure 1.3-2 Updated process schematic for the power plant, SWWS, and SERF connections to Outfall 001 (current configuration)

**Table 1.4-1**  
**Completion Data for Alluvial Piezometers and Collocated Alluvial Wells**

Piezometers													
	SCPZ-1	SCPZ-2	SCPZ-3	SCPZ-4	SCPZ-5	SCPZ-6	SCPZ-7	SCPZ-8	SCPZ-9	SCPZ-10	SCPZ-11(A)	SCPZ-11(B)	SCPZ-12
Total length (ft)	20.5	11.4	8.3	8.3	8.3	8.3	8.3	11.4	8.3	8.3	8.3	8.3	8.3
Stick up (ft)	4.36	3.26	3.19	3.16	2.64	3.18	4.32	4.78	3.35	4.01	3.8	4.48	3.77
Top of screen (ft bgs)	13.8	6.0	3	3	3	3	1.6	5.3	3	3	3	1	3
Total depth (ft bgs)	16.2	8.3	5.4	5.4	5.4	5.4	4.0	7.6	5.4	5.4	5.4	5.4	5.4
Alluvial Wells													
	SWA-1-1	SWA-1-2	SWA-1-3	SWA-2-4	SWA-2-5	SWA-2-6	SWA-3-7	SWA-3-8	SWA-3-9	SWA-4-10		SWA-4-11	SWA-4-12
Ground elevation (ft amsl*)	7239.9	7240.0	7239.2	7223.3	7223.0	7222.9	7212.7	7213.1	7212.9	7209.6		7210.8	7210.5
Total length (ft)	18.33	13.17	9.37	9.00	8.96	8.22	6.84	10.68	8.22	8.44		7.93	8.19
Stick up (ft)	2.33	4.14	3.02	3.00	2.96	2.1	3.24	2.88	3.02	3.94		1.93	2.2
Top of screen (ft bgs)	13.0	6.03	3.0	3.0	3.0	3.12	0.6	4.8	2.2	2.5		3	2.99
Bottom of screen (ft bgs)	15.5	8.53	5.5	5.5	5.5	5.62	3.1	7.3	4.7	5		5.5	5.49
Total depth (ft bgs)	16.0	9.03	6.0	6.0	6.0	6.12	3.6	7.8	5.2	5.5		6	5.99

Note: Alluvial wells shown below collocated piezometer.

\*amsl = Above mean sea level.

**Table 1.4-2**  
**Schema Crosswalk: Past Piezometers and Current Alluvial Wells**

Piezometer	To	Alluvial Well	Date of Alluvial Well Installation
SCPZ-1	→	SWA-1-1	8/19/2016
SCPZ-2	→	SWA-1 / SWA-1-2*	12/18/2014
SCPZ-3	→	SWA-1-3	7/21/2016
SCPZ-4	→	SWA-2-4	7/20/2016
SCPZ-5	→	SWA-2-5	7/20/2016
SCPZ-6	→	SWA-2 / SWA-2-6*	12/16/2014
SCPZ-7	→	SWA-3-7	4/27/2016
SCPZ-8	→	SWA-3 / SWA-3-8*	12/16/2014
SCPZ-9	→	SWA-3-9	4/28/2016
SCPZ-10	→	SWA-4-10	4/27/2016
SCPZ-11B	→	SWA-4-11	7/19/2016
SCPZ-12	→	SWA-4 / SWA-4-12*	12/15/2014

\* SWA-1, SWA-2, SWA-3, and SWA-4 were pilot wells installed in December 2016; SWA-1-2, SWA-2-6, SWA-3-8, SWA-4-12 are the same wells relabeled in 2015.

**Table 1.4-3**  
**Alluvial Groundwater Sampling and Analysis Plan**  
**for 2018 Sandia Wetland Stabilization Monitoring**

Suite	Frequency	Comment
Metals <sup>a</sup> (filtered)	Quarterly	Includes redox-sensitive metals Fe, Mn, Cr, and As
Anions <sup>b</sup> (filtered)	Quarterly	Includes redox-sensitive anions, sulfate, and nitrate; nitrate is a wetland vegetation nutrient
Sulfide (unfiltered)	Quarterly	Redox indicator (reduction of sulfate)
Alkalinity/pH (unfiltered)	Quarterly	Organic matter degradation
Ammonia (unfiltered)	Quarterly	Indicator of organic matter degradation; wetland vegetation nutrient
DOC (filtered)	Annually	Organic matter degradation (collected in July 2018)
Fe(II) <sup>c</sup> (filtered)	Quarterly	Indicator of Fe(III) reducing to Fe(II)
As(III) <sup>c</sup> (filtered)	Quarterly	Indicator of As(V) reducing to As(III)
Cr(VI) (unfiltered)	Quarterly	Indicator of Cr(III) oxidizing to Cr(VI)

<sup>a</sup> Metals consists of the following suite: Ag, Al, As, B, Ba, Be, Cd, Co, Cr, Cs, Cu, Fe, K, Li, Mg, Mn, Na, Ni, Pb, Rb, Se, Si, Sr, Ti, Tl, U, V, Zn, Hg, Mo, Sb, Sn, and Th.

<sup>b</sup> Anions consists of the following suite: Br, F, Cl, NO<sub>2</sub>, NO<sub>3</sub>, PO<sub>4</sub>, SO<sub>4</sub>, and C<sub>2</sub>O<sub>4</sub>H<sub>2</sub> (oxalic acid).

<sup>c</sup> The Laboratory/N3B, per agreement with NMED, analyzed the phase and oxidation state of arsenic (As) and iron (Fe) for a four-quarter finite term.



**Table 1.4-4**  
**ISCO Bottle Configurations and Analytical Suites**  
**2018 Storm Water Sampling Plan for E121, E122, and E123**

Sample Bottle (1 L)	Start Time (min) 12-Bottle ISCO	Analytical Suites 12-Bottle ISCO	Start Time (min) 24-Bottle ISCO	Analytical Suites 24-Bottle ISCO
1	Peak+10	SSC; particle size	Trigger	SSC
2	Peak+12	PCBs (UF <sup>a</sup> ) Part 1 <sup>b</sup>	Trigger+2	SSC
3	Peak+14	TOC (UF), DOC (F <sup>c</sup> ) + chloride (F) + sulfate (F) + alkalinity (UF) + pH (UF)	Trigger+4	SSC
4	Peak+16	PCBs (UF) Part 2	Trigger+6	SSC
5	Peak+18	TAL metals <sup>d</sup> + B + U + hardness (F/UF)	Trigger+8	SSC
6	Peak+20	PAH (UF)	Trigger+10	SSC
7	Peak+22	SVOC (UF)	Trigger+12	SSC
8	Peak+24	Gross alpha (UF)	Trigger+14	SSC
9	Peak+26	SSC	Trigger+16	SSC
10	Peak+28	Extra bottle	Trigger+18	SSC
11	Peak+30	Extra bottle	Trigger+20	SSC
12	Peak+32	Extra bottle	Trigger+22	SSC
13	n/a <sup>e</sup>	n/a	Trigger+24	SSC
14	n/a	n/a	Trigger+26	SSC
15	n/a	n/a	Trigger+28	SSC
16	n/a	n/a	Trigger+30	SSC
17	n/a	n/a	Trigger+50	SSC
18	n/a	n/a	Trigger+70	SSC
19	n/a	n/a	Trigger+90	SSC
20	n/a	n/a	Trigger+110	SSC
21	n/a	n/a	Trigger+130	SSC
21	n/a	n/a	Trigger+150	SSC
23	n/a	n/a	Trigger+170	SSC
24	n/a	n/a	Trigger+190	SSC

Notes: E121 = Sandia right fork at power plant, E122 = Sandia left fork at asphalt plant or South fork of Sandia at E122, and E123 = Sandia below Wetlands. The 12-bottle ISCO begins collection 10 min after the peak discharge (i.e., "Peak+10") and the 24-bottle ISCO begins collection as soon as water is detected by the liquid level actuator (i.e., "Trigger").

<sup>a</sup> UF = Unfiltered.

<sup>b</sup> Bottles 2 and 4 are to be sent to the laboratory together for one PCB analysis.

<sup>c</sup> F = Filtered through a 0.45-µm membrane.

<sup>d</sup> TAL metals are Ag, Al, As, Ba, Be, Ca, Cd, Co, Cr, Cu, Fe, Hg, K, Mg, Mn, Na, Ni, Pb, Sb, Se, Ti, V, and Zn; hardness is calculated from calcium and magnesium, components of the TAL list.

<sup>e</sup> n/a = Not applicable.

**Table 2.1-1**  
**Field Data for Alluvial Locations and Surface Water Stations 2018 Sampling Events**

Location Name	Date	Dissolved Oxygen (mg/L)	Oxidation-Reduction Potential (mV)	pH	Specific Conductance (μS/cm)	Temperature (°C)	Turbidity (NTU <sup>a</sup> )
<b>Surface Water Stations</b>							
E121	2/27/2018	8.39	ND <sup>b</sup>	8.01	403.5	ND	0.6
E121	7/24/2018	6.85	ND	8.01	333.6	ND	1.1
E123	2/27/2018	10.23	ND	7.79	615	ND	4.3
E123	7/24/2018	6.50	ND	7.43	379.5	ND	5.1
E123	11/26/2018	10.55	ND	8.46	443.5	ND	2.3
<b>Piezometers and Alluvial Wells</b>							
SWA-1-1	2/28/2018	0.59	-140.5	7.21	529	10.8	5.3
SWA-1-1	5/30/2018	0.93	-144.0	7.22	568	11.6	2.94
SWA-1-1	7/24/2018	0.41	-144.0	7.06	531	12.5	1.81
SWA-1-1	11/27/2018	0.70	-137.9	7.25	508	13.7	6.8
SWA-1-2	2/28/2018	0.73	-103.2	7.33	408.5	5.3	8.0
SWA-1-2	5/30/2018	0.62	-109.3	7.33	453.6	12.3	6.2
SWA-1-2	7/24/2018	0.75	-116.6	4.22	407.0	16.6	1.9
SWA-1-2	11/27/2018	1.10	-93.1	7.29	457.5	10.5	4.6
SWA-1-3	2/28/2018	0.35	-88.5	6.98	119.6	4.4	5.5
SWA-1-3	5/30/2018	0.64	-109.9	7.11	441.5	14.6	5.3
SWA-1-3	7/24/2018	0.37	-97.3	6.84	434.7	17.7	1.8
SWA-1-3	11/27/2018	0.65	-85.5	7.16	490.4	8.0	6.4
SWA-2-4	2/28/2018	0.35	-89.5	6.89	664	5.2	0.5
SWA-2-4	5/30/2018	0.64	-72	7.05	448.9	12.5	0.6
SWA-2-4	7/24/2018	0.37	-86.5	6.88	433.8	14.6	0.6
SWA-2-4	11/27/2018	0.65	109	6.86	466.9	6.9	0.6
SWA-2-5	2/28/2018	0.56	-161.5	7.24	522	9.7	5.0
SWA-2-5	5/30/2018	ND	ND	ND	ND	ND	ND
SWA-2-5	7/26/2018	0.33	-169.3	7.29	546	10.6	1.5
SWA-2-5	11/27/2018	0.58	-77.6	7.24	514	10.4	5.7
SWA-2-6	2/28/2018	0.27	-162.3	7.14	528	7.2	7.7
SWA-2-6	5/30/2018	0.66	-139.2	7.15	515	10.7	6.3
SWA-2-6	7/26/2018	0.34	-171.2	7.24	543	11.0	0.9
SWA-2-6	11/27/2018	0.63	-92.9	6.97	516	8.1	9.6
SWA-3-7	3/1/2018	0.39	-15.1	6.24	764	2.1	7.7
SWA-3-7	5/31/2018	0.474	-37.9	6.30	675	10.5	2.7
SWA-3-7	7/25/2018	0.52	-79.9	6.39	562	15.1	2.0
SWA-3-7	11/28/2018	0.58	91.5	6.24	697	5.4	3.5

**Table 2.1-1 (continued)**

Location Name	Date	Dissolved Oxygen (mg/L)	Oxidation-Reduction Potential (mV)	pH	Specific Conductance (μS/cm)	Temperature (°C)	Turbidity (NTU <sup>a</sup> )
<b>Piezometers and Alluvial Wells (continued)</b>							
SWA-3-8	3/1/2018	0.62	-97.7	6.81	567	4.9	2.3
SWA-3-8	5/31/2018	0.59	-75.6	6.79	561	8.7	2.2
SWA-3-8	7/25/2018	0.60	-113.6	6.85	558	11.6	0.57
SWA-3-8	11/28/2018	0.58	95	6.76	549	7.2	4
SWA-3-9	3/1/2018	0.83	-106.0	6.75	519	4.3	4.4
SWA-3-9	5/31/2018	0.96	-67.1	6.64	584	936	1.0
SWA-3-9	7/25/2018	0.35	-118.9	6.72	556	11.8	1.64
SWA-3-9	11/28/2018	0.58	34.5	6.66	519	6.4	4
SWA-4-10	5/31/2018	0.73	-90.0	6.47	584	9.3	15.0
SWA-4-10	7/25/2018	0.60	-53.5	6.32	569	14.0	5.5
SWA-4-10	ND	ND	ND	ND	ND	ND	ND
SWA-4-10	ND	ND	ND	ND	ND	ND	ND
SWA-4-11	5/31/2018	0.84	-97.2	6.83	382.3	13.6	6.2
SWA-4-11	7/25/2018	0.60	-77.2	6.62	431.1	16.6	7.2
SWA-4-11	ND	ND	ND	ND	ND	ND	ND
SWA-4-11	11/28/2018	1.01	-59.7	6.80	448.1	3.6	5.6
SWA-4-12	3/1/2018	0.42	-58.7	6.57	650	2.9	0.7
SWA-4-12	5/31/2018	0.50	-82.7	6.71	431.1	11.3	1.0
SWA-4-12	7/25/2018	0.44	-67.8	6.59	435.0	15.5	5.3
SWA-4-12	11/28/2018	0.90	-42.0	6.52	545.0	6.1	3.4

<sup>a</sup> NTU = Nephelometric turbidity unit.<sup>b</sup> ND = No data.

**Table 2.1-2**  
**Precipitation, Storm Water Peak Discharge, and Samples Collected at**  
**Gaging Stations E121, E122, and E123 for Each Sample-Triggering Storm Event in 2018**

Storm Event Date	RG121.9 Total Precipitation (in.)	E121 Peak Discharge (ft <sup>3</sup> /s)	E122 Peak Discharge (ft <sup>3</sup> /s)	E123 Peak Discharge (ft <sup>3</sup> /s)
7/15/18	0.17	14 S <sup>a</sup>	3.3 S	11 BT
7/17/18	0.71	29 S	5.0 S	31 S
8/07/18	0.37	18 S	3.3 BT <sup>b</sup>	14 BT
8/09/18	0.31	21 S	3.8 S	19 S
8/15/18	0.56	42 S	3.4 BT	19 S
9/03/18	0.46	17 NS <sup>c</sup>	2.9 BT	21 S
9/04/18	0.79	38 S	4.3 S	35 S

<sup>a</sup> S = Sample was collected. These discharge levels are shaded in green to emphasize those events for which discharge exceeded the trip level and samples were collected.<sup>b</sup> BT = Below trip level.<sup>c</sup> NS = No sample was collected because of equipment malfunction. The sampler tubing came loose during sample event.

**Table 3.7-1**  
**Significant Geomorphic Changes and Associated Peak Discharges**

Date*	Station	Peak Discharge (cfs)	Noted Erosion in Geomorphic Surveying
9/13/2013	E123	108	Extensive repairs were required, including the design and construction of best management practice run-on control structures, replacement of boulders and repair of the cascade pool liner, removal of deposited sediments, and replanting of the lost vegetation in the GCS (Section 3.4.2 of "Completion Report for Sandia Grade-Control Structure," [LANL 2013, 251743]).
7/7/2014	E123	80	Overall, erosion within the system seems to be associated with scouring in small side channels outside the wetland proper or to channel rearrangement within the wetland proper. There is evidence of increased channelization in the lower part of the wetland and a new nick point, located upgradient of the most upstream sheet pile.
7/8/2014	E123	76	Overall, erosion within the system seems to be associated with scouring in small side channels outside the wetland proper or to channel rearrangement within the wetland proper. There is evidence of increased channelization in the lower part of the wetland and a new nick point, located upgradient of the most upstream sheet pile.
7/31/2014	E123	109	Overall, erosion within the system seems to be associated with scouring in small side channels outside the wetland proper or to channel rearrangement within the wetland proper. There is evidence of increased channelization in the lower part of the wetland and a new nick point, located upgradient of the most upstream sheet pile.
7/26/2017	E121	87	Repeat GPS surveys in conjunction with field observations indicated that no significant geomorphic changes occurred in the wetland after the 2017 monsoon season. A small amount of deposition was detected in the plunge pool from storm runoff but has not affected the plunge pool area.
7/26/2017	E123	78	Repeat GPS surveys in conjunction with field observations indicated that no significant geomorphic changes occurred in the wetland after the 2017 monsoon season. A small amount of deposition was detected in the plunge pool from storm runoff but has not affected the plunge pool area.

\* There were no large storm events in 2015, 2016, or 2018.

**Table 3.7-2**  
**Proposed 2019 Sampling and Preservation Requirements for Sandia Wetland**

Analytical Suite	Analytical Method	Sample Type <sup>a</sup>	Frequency	Filtered <sup>b</sup>	Preservation	Field Storage	Holding Time	Ideal Volume	Minimum Volume	Comment
<b>Alluvial Wells<sup>c</sup></b>										
Cr(VI) Speciation	IC-ICPMS:Metals	W	Annually	F	NH <sub>4</sub> OH / (NH <sub>4</sub> ) <sub>2</sub> SO <sub>4</sub> (liquid) buffer (1 mL to 100 mL of sample) to pH >9.0–9.5; zero headspace; ice	<4°C	28 days	125 mL	125 mL	— <sup>d</sup>
TAL Metals	SW-846:6010C and SW-846:6020 EPA:245.2 (Hg)	W	Annually	F	Nitric acid; ice	<4°C	6 mo 28 days for Hg	1 L	300 mL	—
<b>Surface Water Base Flow at Gages E121, E122, and E123</b>										
PAH Congeners	EPA:625_SIM	WS	Qtrly	UF	Na <sub>2</sub> O <sub>3</sub> S <sub>2</sub> if residual Cl is present; ice	<4°C	7 days	3 L	1 L	Amber glass with Teflon lid
PCB Congeners	EPA:1668C	WS	Qtrly	UF	Ice	<4°C	1 yr	3 L	1L	Amber glass with Teflon lid
SVOC	SW-846:8270D	WS	Qtrly	UF	Ice	<4°C	7 days	3 L	1 L	Amber glass with Teflon lid
TAL Metals	SW-846:6010C and SW-846:6020 EPA:245.2 (Hg)	WS	Qtrly	F and UF	Nitric acid; ice	<4°C	6 mo 28 days for Hg	1 L	300 mL	—
Cr(VI) Speciation	IC-ICPMS:Metals	WS	Qtrly	F	NH <sub>4</sub> OH / (NH <sub>4</sub> ) <sub>2</sub> SO <sub>4</sub> (liquid) buffer (1 mL to 100 mL of sample) to pH >9.0–9.5; zero headspace; ice	<4°C	14 days	100 mL	100 mL	—
SSC	ASTM:D3977-97	WS	Qtrly	UF	Ice	no requirement	n/a <sup>e</sup>	1 L	1 L	—
<b>Surface Water Storm Flow at Gages E121, E122, and E123</b>										
PAH Congeners	EPA:625_SIM	WT	>10 cfs <sup>f</sup>	UF	Na <sub>2</sub> O <sub>3</sub> S <sub>2</sub> if residual Cl is present; Ice	<4°C	7 days	3 L	1 L	Amber glass with Teflon lid
PCB Congeners	EPA:1668C	WT	>10 cfs	UF	Ice	<4°C	1 yr	3 L	1L	Amber glass with Teflon lid
SVOC	SW-846:8270D	WT	>10 cfs	UF	Ice	<4°C	7 days	3 L	1 L	Amber glass with Teflon lid
TAL Metals + Total recoverable aluminum <sup>g</sup>	SW-846:6010C and SW-846:6020 EPA:245.2 (Hg)	WT	>10 cfs	F and UF	Nitric acid; ice	<4°C	6 mo 28 days for Hg	1 L	300 mL	—
SSC	ASTM:D3977-97	WT	>10 cfs	UF	Ice	no requirement	n/a	1 L	1 L	—

<sup>a</sup> W = Alluvial groundwater samples; WS = base flow water samples; WT = storm flow water samples.

<sup>b</sup> F = Filtered; UF = unfiltered.

<sup>c</sup> Alluvial wells will be reduced to transect 1 (SWA-1-1, SWA-1-2, SWA-1-3), transect 4 (SWA-4-10, SWA-4-11, SWA-4-12), and wells SWA-2-4 and SWA-2-6.

<sup>d</sup> — = None.

<sup>e</sup> n/a = not applicable.

<sup>f</sup> Greater than 10 cfs, up to four samples.

<sup>g</sup> Filtered using a 10-µm filter.



# Appendix A

---

*Acronyms and Abbreviations,  
Metric Conversion Table, and Data Qualifier Definitions*





**A-1.0 ACRONYMS AND ABBREVIATIONS**

As(III)	arsenite
amsl	above mean sea level
bgs	below ground surface
cfs	cubic foot per second
Cr(III)	trivalent chromium
Cr(VI)	hexavalent chromium
DC	direct current
DEM	digital elevation model
DOC	dissolved organic carbon
EPA	Environmental Protection Agency (U.S.)
F	filtered
Fe(III)	ferric oxide
Fe(II)	ferrous oxide
GCS	grade-control structure
gpd	gallons per day
gpm	gallons per minute
GPS	global positioning system
HH-OO	human health-organism only
IR	investigation report
LANL	Los Alamos National Laboratory
LiDAR	light detection and ranging
MCL	maximum contaminant level
MDL	method detection limit
Mn(IV)	manganese dioxide
MY	monitoring year
N3B	Newport News Nuclear BWXT-Los Alamos, LLC
NMAC	New Mexico Administrative Code
NMED	New Mexico Environment Department
NMWQCC	New Mexico Water Quality Control Commission
NPDES	National Pollutant Discharge Elimination System
NTU	nephelometric turbidity unit
PAH	polycyclic aromatic hydrocarbon

PCB	polychlorinated biphenyl
PVC	polyvinyl chloride
RTK	real-time kinematic
SCC	Strategic Computing Complex
SERF	Sanitary Effluent Reclamation Facility
SSC	suspended sediment concentration
SVOC	semivolatile organic compound
SWMU	solid waste management unit
SWQC	surface water–quality criteria
SWWS	Sanitary Waste Water System
TA	technical area
TAL	target analyte list
TOC	total organic compound
TSS	total suspended sediment
UF	unfiltered
VE	vertical exaggeration

**A-2.0 METRIC CONVERSION TABLE**

Multiply SI (Metric) Unit	by	To Obtain U.S. Customary Unit
kilometers (km)	0.622	miles (mi)
kilometers (km)	3281	feet (ft)
meters (m)	3.281	feet (ft)
meters (m)	39.37	inches (in.)
centimeters (cm)	0.03281	feet (ft)
centimeters (cm)	0.394	inches (in.)
millimeters (mm)	0.0394	inches (in.)
micrometers or microns ( $\mu\text{m}$ )	0.0000394	inches (in.)
square kilometers ( $\text{km}^2$ )	0.3861	square miles ( $\text{mi}^2$ )
hectares (ha)	2.5	acres
square meters ( $\text{m}^2$ )	10.764	square feet ( $\text{ft}^2$ )
cubic meters ( $\text{m}^3$ )	35.31	cubic feet ( $\text{ft}^3$ )
kilograms (kg)	2.2046	pounds (lb)
grams (g)	0.0353	ounces (oz)
grams per cubic centimeter ( $\text{g/cm}^3$ )	62.422	pounds per cubic foot ( $\text{lb/ft}^3$ )
milligrams per kilogram ( $\text{mg/kg}$ )	1	parts per million (ppm)
micrograms per gram ( $\mu\text{g/g}$ )	1	parts per million (ppm)
liters (L)	0.26	gallons (gal.)
milligrams per liter ( $\text{mg/L}$ )	1	parts per million (ppm)
degrees Celsius ( $^{\circ}\text{C}$ )	$9/5 + 32$	degrees Fahrenheit ( $^{\circ}\text{F}$ )

**A-3.0 DATA QUALIFIER DEFINITIONS**

Data Qualifier	Definition
U	The analyte was analyzed for but not detected.
J	The analyte was positively identified, and the associated numerical value is estimated to be more uncertain than would normally be expected for that analysis.
J+	The analyte was positively identified, and the result is likely to be biased high.
J-	The analyte was positively identified, and the result is likely to be biased low.
UJ	The analyte was not positively identified in the sample, and the associated value is an estimate of the sample-specific detection or quantitation limit.
R	The data are rejected as a result of major problems with quality assurance/quality control (QA/QC) parameters.



## **Appendix B**

---

*2018 Geomorphic Changes in Sandia Canyon Reach S-2*



## CONTENTS

<b>B-1.0 INTRODUCTION .....</b>	<b>B-1</b>
<b>B-2.0 HYDROLOGIC EVENTS DURING THE 2018 MONSOON SEASON.....</b>	<b>B-1</b>
<b>B-3.0 GROUND-BASED SURVEY METHODS OF THE SANDIA WETLAND .....</b>	<b>B-1</b>
<b>B-4.0 RESULTS AND DISCUSSION .....</b>	<b>B-2</b>
B-4.1 Thalweg Characterization .....	B-2
B-4.2 Plunge Pool Characterization .....	B-3
B-4.3 Channel Bank Characterization .....	B-3
B-4.4 Alluvial Fan Characterization .....	B-3
<b>B-5.0 CONCLUSIONS AND RECOMMENDATIONS .....</b>	<b>B-3</b>
<b>B-6.0 REFERENCES AND MAP DATA SOURCES .....</b>	<b>B-4</b>
B-6.1 References .....	B-4
B-6.2 Map Data Sources .....	B-5

### Figures

Figure B-1.0-1 Sandia Canyon reach S-2 orthophoto with gaging station E123, alluvial wells, and survey locations, including channel banks, thalweg, alluvial fans, and the plunge pool .....	B-7
Figure B-4.0-1 5-yr comparison of thalweg and bank top surveys in reach S-2 .....	B-8
Figure B-4.1-1 1-yr thalweg profile comparison .....	B-9
Figure B-4.1-2 5-yr thalweg profile comparison .....	B-10
Figure B-4.2-1 1-yr plan view of plunge pool in Sandia Canyon reach S-2 .....	B-11
Figure B-4.2-2 5-yr plan view of plunge pool in Sandia Canyon reach S-2 .....	B-11

### Table

Table B-4.2-1 Plunge Pool Area and Growth Assessment.....	B-13
---	------

### Attachment

Attachment B-1 2018 Geomorphic Changes in Sandia Canyon Reach S-2 Survey Data (on CD included with this document)	
---	--





## **B-1.0 INTRODUCTION**

This report evaluates geomorphic changes that occurred from October 2017 to November 2018 as well as well as a 5-yr comparison to evaluate the stability of several geomorphic features in reach S-2, above the Sandia Canyon grade-control structure (GCS) within the Los Alamos National Laboratory (LANL or the Laboratory). Geomorphic change was evaluated using post-monsoon ground-based surveys of the thalweg, channel banks, plunge pool, and alluvial fans. Results from those surveys are presented in this appendix, representing change in the 2018 monsoon season and over the past 5 yr. Figure B-1.0-1 shows site locations discussed in this appendix.

## **B-2.0 HYDROLOGIC EVENTS DURING THE 2018 MONSOON SEASON**

Discharge in 2018 was similar to discharge in 2017 at all gaging stations, near or well below the mean for the 10-yr period of record. Storm water discharge at E121 equaled or exceeded the trip level (10 cubic feet per second [cfs] above the base flow) seven times in 2018. Discharge at E122 equaled or exceeded the lowered trip level (2 cfs above the base flow) four times in 2018. Discharge at E123 exceeded the trip level (10 cfs above the base flow) five times in 2018. Peak discharge at E121, E122, and E123 occurred on August 15, July 17, and September 4, respectively, in response to varied spatial and precipitation intensities on those dates (see section 2.1 and Table 2.1-2 in the main text for more details).

## **B-3.0 GROUND-BASED SURVEY METHODS OF THE SANDIA WETLAND**

The 2018 post-monsoon channel thalweg, channel banks, and plunge pool were surveyed using ground-based methods to document change. These features were surveyed using real-time kinematic differentially corrected GPS surveying equipment. The alluvial fans on the northern and southern edges of the wetland were also monitored via visual inspection and erosion pins during the 2018 monsoon season.

The 2018 longitudinal channel thalweg profile was surveyed for the entire study reach. However, since the thalweg location is not well defined in the central section of reach S-2 because of diffuse flow and channel branching, a continuous line was not surveyed but split in two distinct sections from gaging station E123 up to the GCS, and in the western section of wetland vegetation up to the plunge pool. For each thalweg survey point, the distance along the thalweg was calculated as the straight-line distance between the plunge pool and that point. This distance is referred to as the “canyon distance.” Data tables of thalweg survey points and distances and ArcGIS shape files are included in Attachment B-1. This report presents the 2018 thalweg gradient and map-view location in comparison with data from 2014–2017 for all sections of reach S-2 where data were available.

Channel banks were initially surveyed in 2015 to document baseline conditions. Channel bank surveys have been repeated every year since then including 2018 at the western end of reach S-2 as well as the eastern end that drains the wetland area. In the central portion of the reach, where flow is diffused and there is standing water, there are no prominent channel banks. Data tables of channel survey points and ArcGIS shape files are included in Attachment B-1.

The plunge pool perimeter was surveyed at the lateral extent of the ponded area. The 2018 results are compared with the survey results from 2014–2017 of the same area. Data tables of plunge pool survey points and ArcGIS shape files are also included in Attachment B-1.

Three alluvial fan deposits on the north side and one on the south side of reach S-2 were visually inspected and monitored using erosion pins during the 2018 monsoon season. Flow generally occurs on the fans within 2–4-in.-wide and 2–3-in.-deep channels. Erosion pins are placed near or on these

channels to track the places most likely to experience geomorphic changes. Erosion pins record episodic erosion and deposition. Since the pins are monitored on a quarterly basis, all changes are inferred to be the result of the cumulative effect of the rainfall events during a given quarter. Erosion pins are installed on a given feature and then the height from the top of the pin to the ground is measured. A washer is placed on the pin and the height is then measured from the washer to the pin top. During a monitoring period, the washer cannot physically move upwards; therefore, it serves as the overall estimation of erosion or deposition at that location. An increase in the height of the washer from the pin top since the last measurement is interpreted as erosion occurring at that location. If it is observed that the washer is covered, the distance from the ground to the pin top has decreased and the distance between the ground and the pin top is interpreted as the amount of deposition that has occurred at that location.

## **B-4.0 RESULTS AND DISCUSSION**

The monsoon season of 2018, being generally below average in rainfall intensity, has resulted in minor annual changes to morphology of monitored features but caused no significant geomorphic changes within reach S-2. While minor geomorphologic changes occurred during the 2018 monsoon season, repeat GPS surveys and erosion pin data support the conclusion that features within the reach have stabilized over the past 5-yr monitoring period (Figure B-4.0-1).

### **B-4.1 Thalweg Characterization**

In 2018, the channel thalweg profile was surveyed in two sections from gaging station E123 up to the GCS and from western section of wetland vegetation up to the plunge pool breaking in the central region of the wetland because of diffuse flow and channel branching.

No major departures occurred between 2017 and 2018, but small lateral shifts correlate with continued development of riparian vegetation, causing flow throughout the central region of the study area to become more diffuse and thus making the thalweg more difficult to distinguish. Overall, the thalweg survey from 2018 closely matches those between 2015–2017 where data are comparable. The largest lateral departures in the thalweg path occurred between 2014 and 2016 (Figure B-4.0-1). In these cases, the expansion of vegetation likely attributed to southward shifts of the thalweg in two areas of the western region of the reach as well as in a small section of the eastern region (LANL 2016, 601432). Over time, the preferred pathway of the thalweg has been heavily influenced by wetland vegetation as these riparian species tends to prevent the down-cutting or straight line cutting of channels. For example, changes in the western end of reach S-2 between 2014 and 2016 were a result of the expansion of cattails in the area. In 2017, the continued expansion of cattails caused further movement of the thalweg to the north. A shift at the eastern end of the reach between 2015 and 2016 also coincided with the expansion of cattails and willows in the GCS area, pushing the thalweg south.

The channel thalweg profile (Figure B-4.1-1) compares 2017 and 2018 post-monsoon survey data displayed with a vertical exaggeration (VE) of 17 times. Between 2017 and 2018, minor changes occurred in the elevation of the thalweg over the entirety of reach S-2. These changes are most likely because of differential settling of the survey staff into the wetland substrate, rather than real topographic changes. Similarly, elevation differences observed in the thalweg profile between 2014 and 2018 (VE 16) are also a product of inherent sampling error, or in some cases because of a shift in the pathway, resulting in the surveying of a different channel thalweg for small portions of the reach (Figure B-4.1-2). Repeat surveys of the small nick point upstream of alluvial wells 4-10, 4-11, and 4-12 have demonstrated stability of that feature since 2015 (Figure B-1.0-1; LANL 2016, 601432).

#### **B-4.2 Plunge Pool Characterization**

The 2018 monsoon season perimeter survey of the plunge pool shows slight variations compared with 2017, with small changes to the shape and areal extent of the pool (Table B-4.2-1 and Figure B-4.2-1). In part, these differences are because of the continuous input of sandy alluvium runoff immediately south of the culvert into the plunge pool, which has allowed a small population of cattails to flourish. Since its initial establishment in 2016, this cattail population has continued to expand, increasing in size from 1.7 m<sup>2</sup> in 2016 to 16 m<sup>2</sup> in 2018 (Appendix C, Figure C-3.1-1). Between 2014 and 2018, the most dynamic changes have occurred at the eastern edge of the pool where it is mostly likely to undergo episodic change as a result of rapid sedimentation and/or erosion at the channel outlets (Figure B-4.2-2). While small changes in the shape and area of the pool occur year to year as a result of sedimentation and vegetation development, repeat surveying suggests that this area will remain stable under the conditions experienced since 2014.

#### **B-4.3 Channel Bank Characterization**

Stream banks below the plunge pool area and between the GCS and gaging station E123 show minimal changes between surveys conducted from 2015 to 2018 (Figure B-4.0-1). Slight differences between the bank surveys are attributed to different interpretations of what constituted the most important breaks in slope between surveys and do not reflect significant bank erosion or deposition.

#### **B-4.4 Alluvial Fan Characterization**

Continued monitoring of the extent and nature of sedimentation/erosional processes on alluvial fans within reach S-2 suggests that the features had no detectable change during calendar year 2018. Erosion pins placed on the alluvial fans are in biased positions to illustrate when changes have occurred (Figure B-1.0-1). Such changes include: changes to alluvial fan extent, incision of the fan surface either at the head or toe, or input of sediment since the previous monitoring event.

Trends from erosion pin monitoring data suggest that during a monitoring period, incision may occur in one event that is later negated by redeposition of sediments in a subsequent event or possibly the same event. This results in the primary channels on the fan changing position on the fan surface during a monitoring year. For example, in 2018, the alluvial fan on the south side of the canyon continued to redistribute sandy gravel at its toe and along a side channel adjacent to the wetland but did not impact vegetation growth of the wetland. Overall, rain events during the 2018 monitoring season have caused minor incision on fan surfaces (generally near the head of the fan) as well as the deposition of sediments (at both the head and toe) with the largest changes occurring later in the season. Between 2016 and 2018, results from erosion pin monitoring have shown that all locations experience fluctuations back and forth from incising to aggrading, but with very small magnitudes. Erosion pin analyses suggest that to affect the extent of these alluvial fans on large scales, the runoff from rain events must be of greater magnitude than that which has occurred during the last 3 yr of monitoring.

#### **B-5.0 CONCLUSIONS AND RECOMMENDATIONS**

Repeat GPS surveys in conjunction with field observations indicate that between 2017 and 2018 no major detectable geomorphic change occurred in reach S-2. The survey conducted in 2018 is largely comparable to surveys conducted between 2014 and 2016, indicating the continued stabilization of the surveyed features over time.

Repeat surveys of the channel thalweg indicate few, minor lateral changes between the 2017 and 2018 surveys that coincide with the expansion of cattails in the wetland area. Lateral changes occurring between 2014 and 2018 correlate with the expansion and development of wetland vegetation, suggesting that wetland vegetation is influencing the thalweg feature in an expected manner. Channel bank surveys conducted on the western end, below the plunge pool, and eastern end, below gaging station E123, of the study area (the only areas in reach S-2 with prominent channel banks) also show minimal change between the last two monitoring years, and have been stable since their baseline survey in 2015. Since 2017, small changes to the area of the plunge pool have occurred at the channel outlets near the northeast side because of episodic sedimentation/erosion events during the 2018 monsoon season. These episodic events are likely to occur every monsoon season and have likely resulted in small changes to the area of the plunge pool since 2014. Other influences, such as a population of cattails that continues to expand on the south side, have also affected the area of the plunge pool since 2014. Based on 2018 erosion pin monitoring, the downslope extent of alluvial fan deposits on the northern side of the reach below the former Los Alamos County landfill has remained stable. On the south side of the canyon, side channels entering reach S-2 have continued to redistribute sandy gravel within the alluvial fan and along a side channel adjacent the wetland. However, the continued redistribution of the alluvial sediments in 2018 has not resulted in any significant vegetation (e.g., cattail) loss.

In 2019, if storm water peak discharge at gaging station E123 is greater than 100 cfs, a visual inspection of the wetland will occur to document qualitative geomorphic changes. If the visual observations indicate significant geomorphic changes that are not consistent with last year's observations, a LiDAR aerial survey will be planned for the fall of 2019. The processed LiDAR data will be field-verified to ensure that geomorphic changes shown in a digital elevation model comparison represent actual geomorphic changes. If no large storm events occur, creating significant geomorphic change, aerial LiDAR surveys will be performed every 3 yr, with the next survey scheduled for 2021. Ground-based monitoring of erosion pins will be performed annually.

## **B-6.0 REFERENCES AND MAP DATA SOURCES**

### **B-6.1 References**

*The following reference list includes documents cited in this report. Parenthetical information following each reference provides the author(s), publication date, and ERID, ESHID, or EMID. This information is also included in text citations. ERIDs were assigned by the Laboratory's Associate Directorate for Environmental Management (IDs through 599999); ESHIDs were assigned by the Laboratory's Associate Directorate for Environment, Safety, and Health (IDs 600000 through 699999); and EMIDs are assigned by Newport News Nuclear BWXT-Los Alamos, LLC (N3B) (IDs 700000 and above). IDs are used to locate documents in N3B's Records Management System and in the Master Reference Set. The New Mexico Environment Department (NMED) Hazardous Waste Bureau and N3B maintain copies of the Master Reference Set. The set ensures that NMED has the references to review documents. The set is updated when new references are cited in documents.*

LANL (Los Alamos National Laboratory), April 2016. "2015 Sandia Wetland Performance Report," Los Alamos National Laboratory document LA-UR-16-22618, Los Alamos, New Mexico. (LANL 2016, 601432)

## **B-6.2 Map Data Sources**

*The following list provides data sources for maps included in this appendix.*

Gaging stations; Los Alamos National Laboratory, Waste and Environmental Services Division; 1:2,500; March 19, 2011.

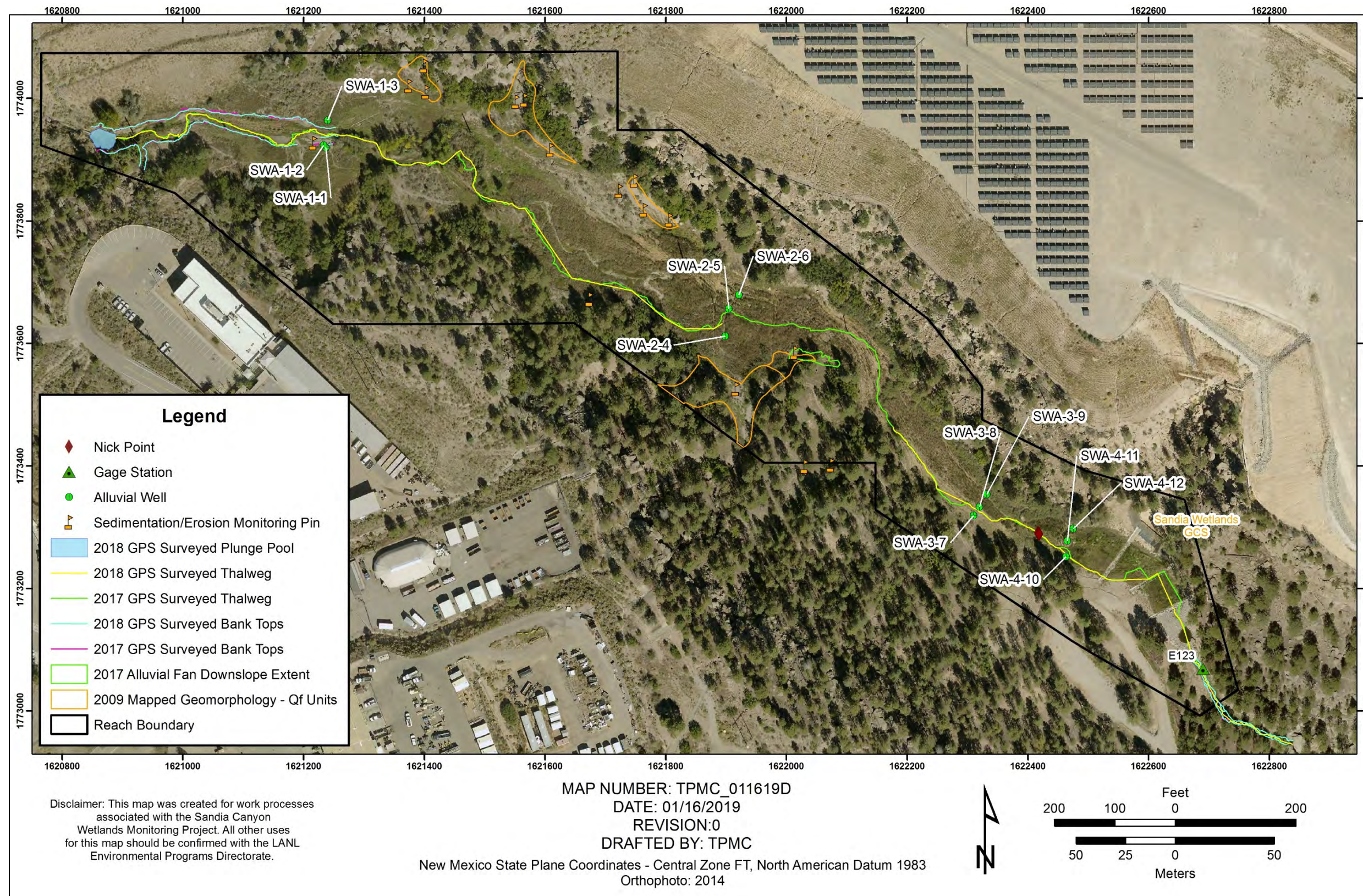
LANL area orthophoto; Los Alamos National Laboratory, 2014.

Geomorphic Reach Boundary, Los Alamos National Laboratory, Earth and Environmental Science, GISLab, 2009.

Geomorphology Units; Los Alamos National Laboratory, Earth and Environmental Sciences, GISLab, 2009.







Note: Qf (alluvial fan) consists of relatively young sands, gravel, and cobbles made up of Bandelier Tuff and pumice fragments and quartzite gravels.

**Figure B-1.0-1 Sandia Canyon reach S-2 orthophoto with gaging station E123, alluvial wells, and survey locations, including channel banks, thalweg, alluvial fans, and the plunge pool**



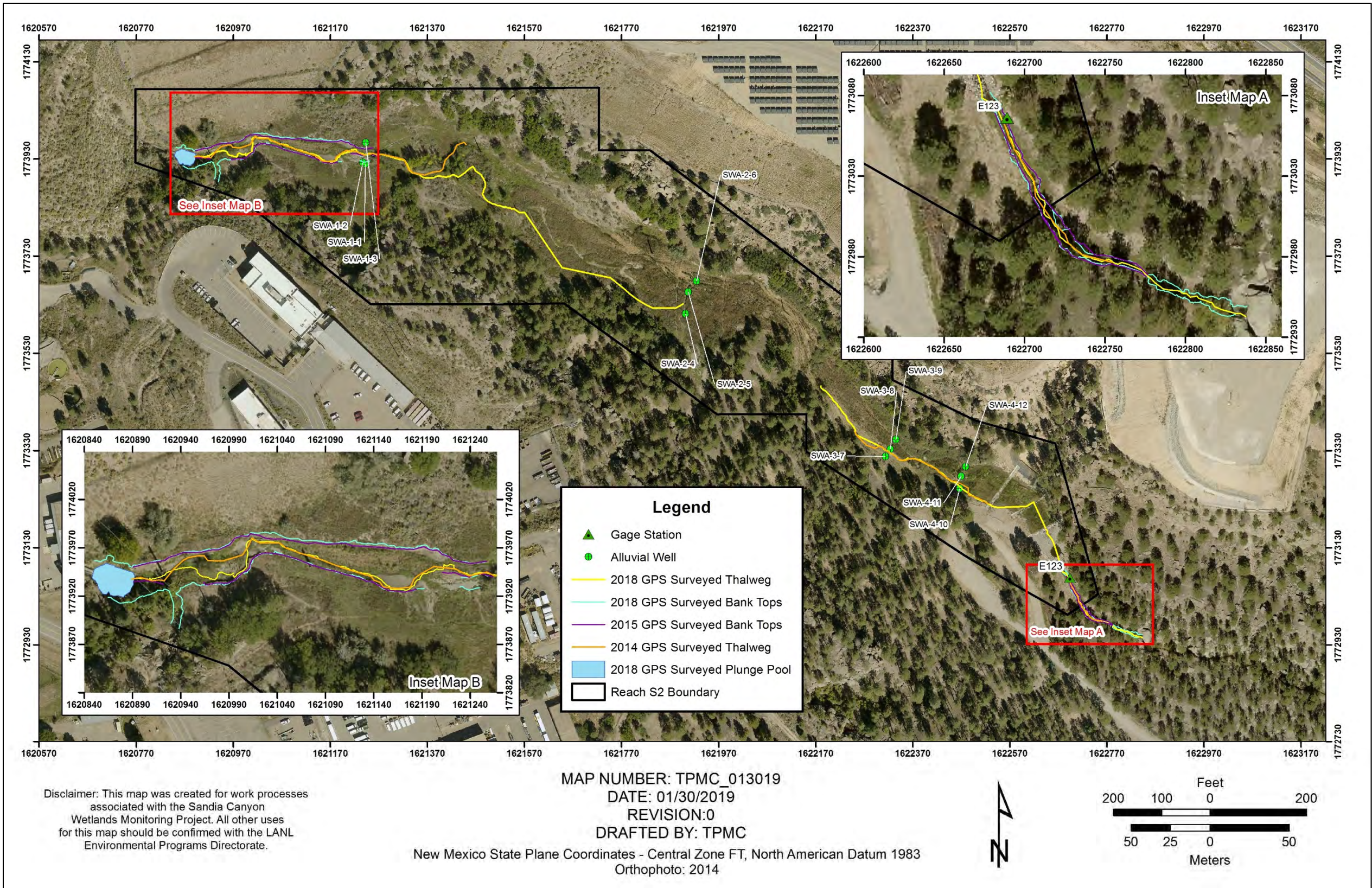


Figure B-4.0-1 5-yr comparison of thalweg and bank top surveys in reach S-2



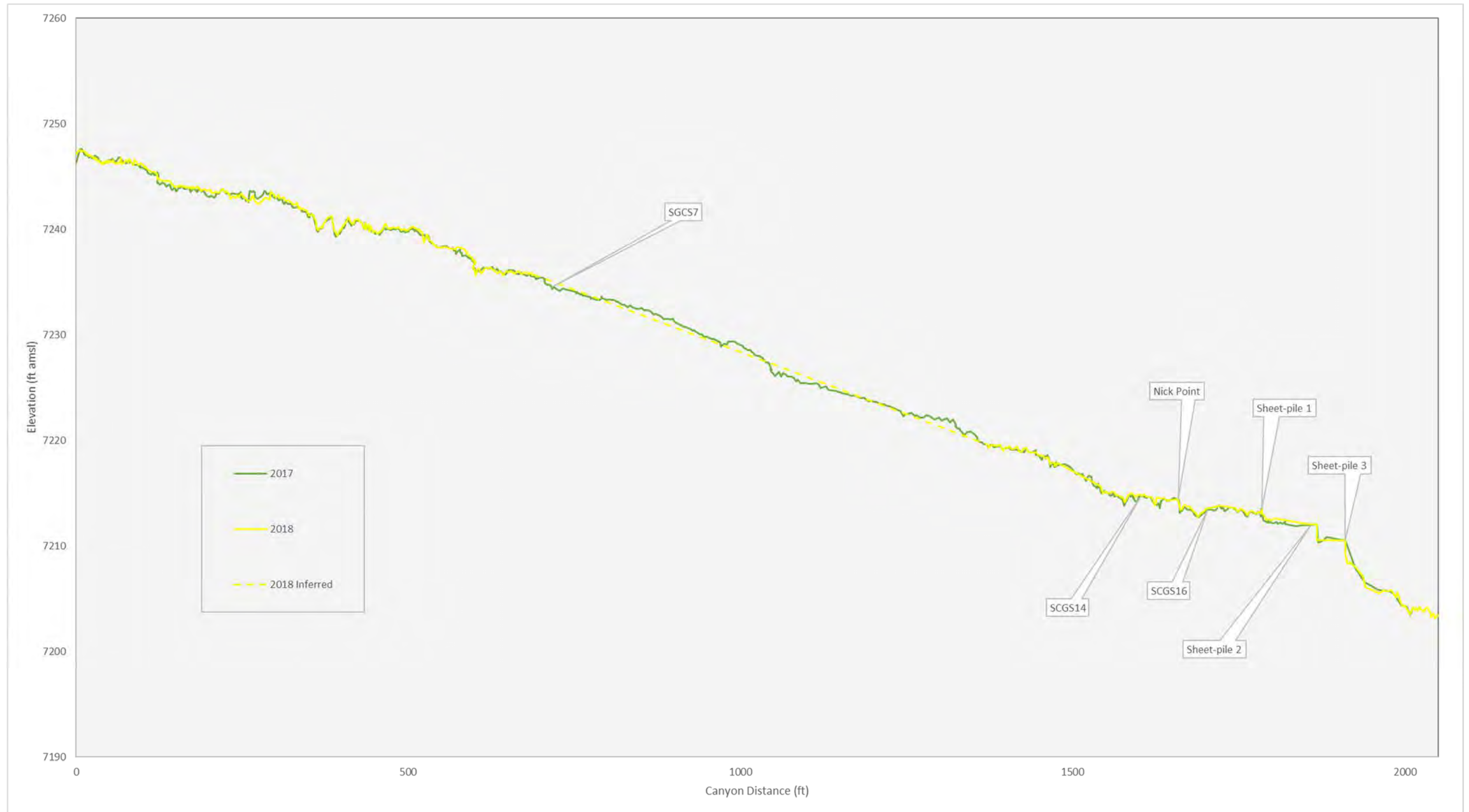


Figure B-4.1-1 1-yr thalweg profile comparison

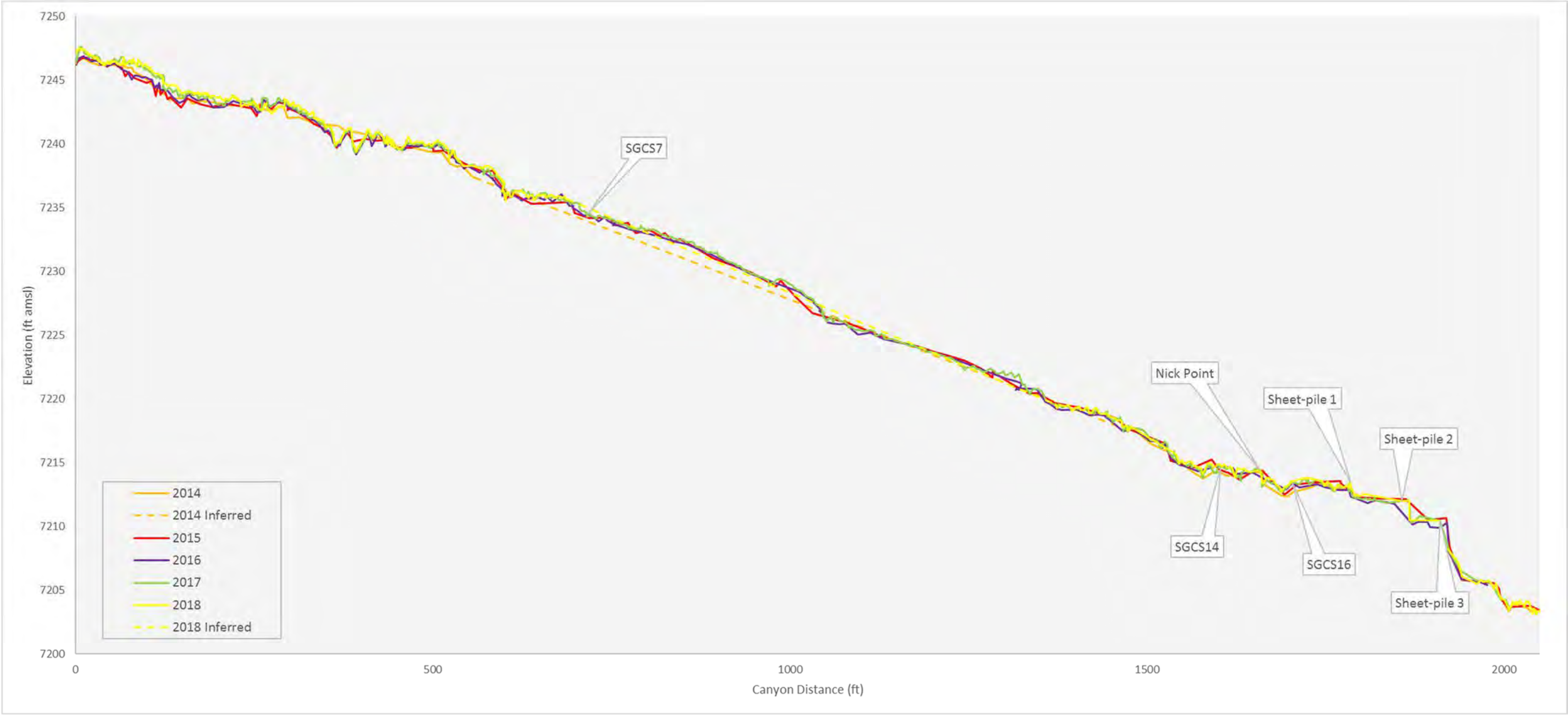


Figure B-4.1-2 5-yr thalweg profile comparison

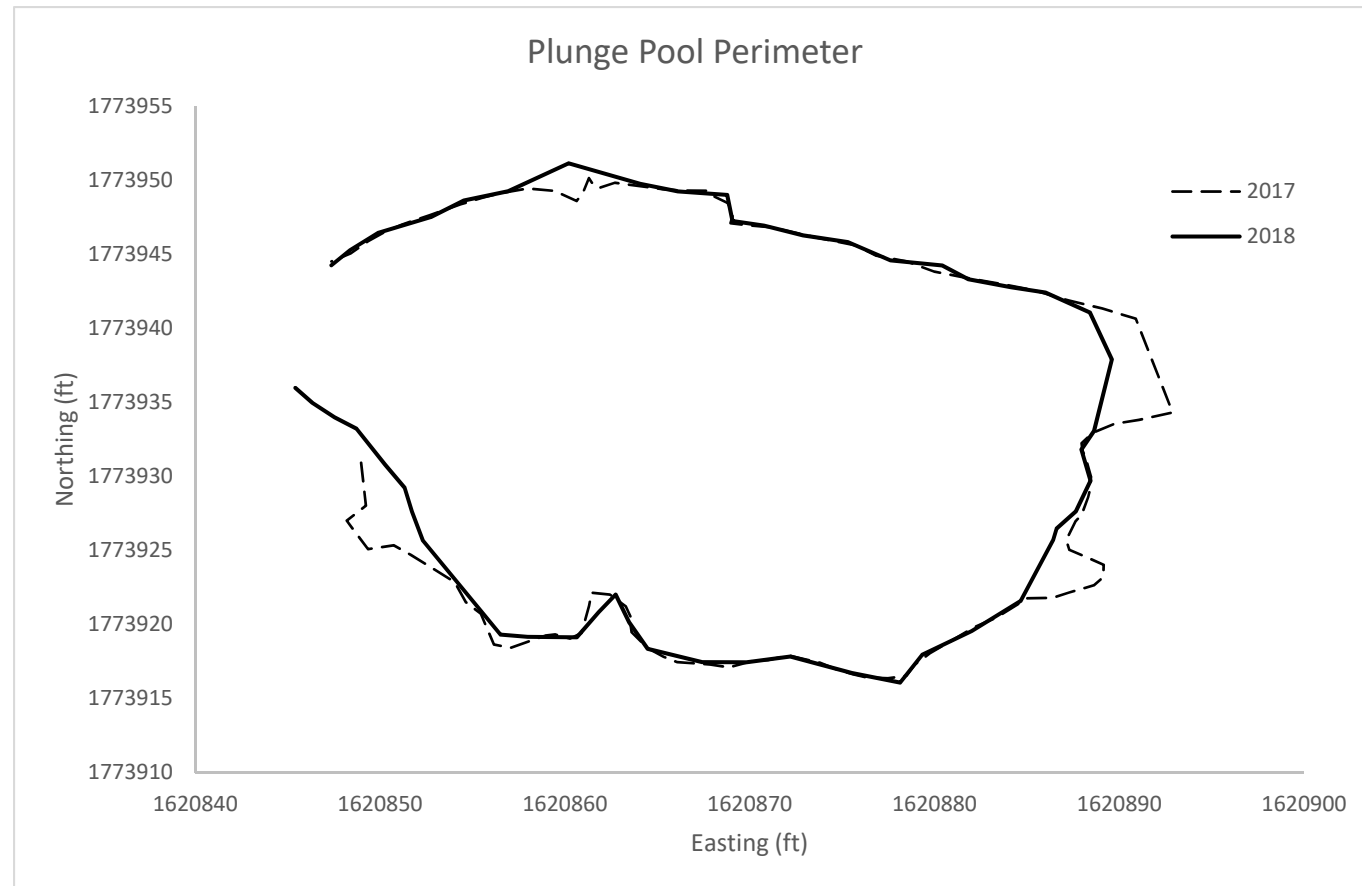


Figure B-4.2-1 1-yr plan view of plunge pool in Sandia Canyon reach S-2

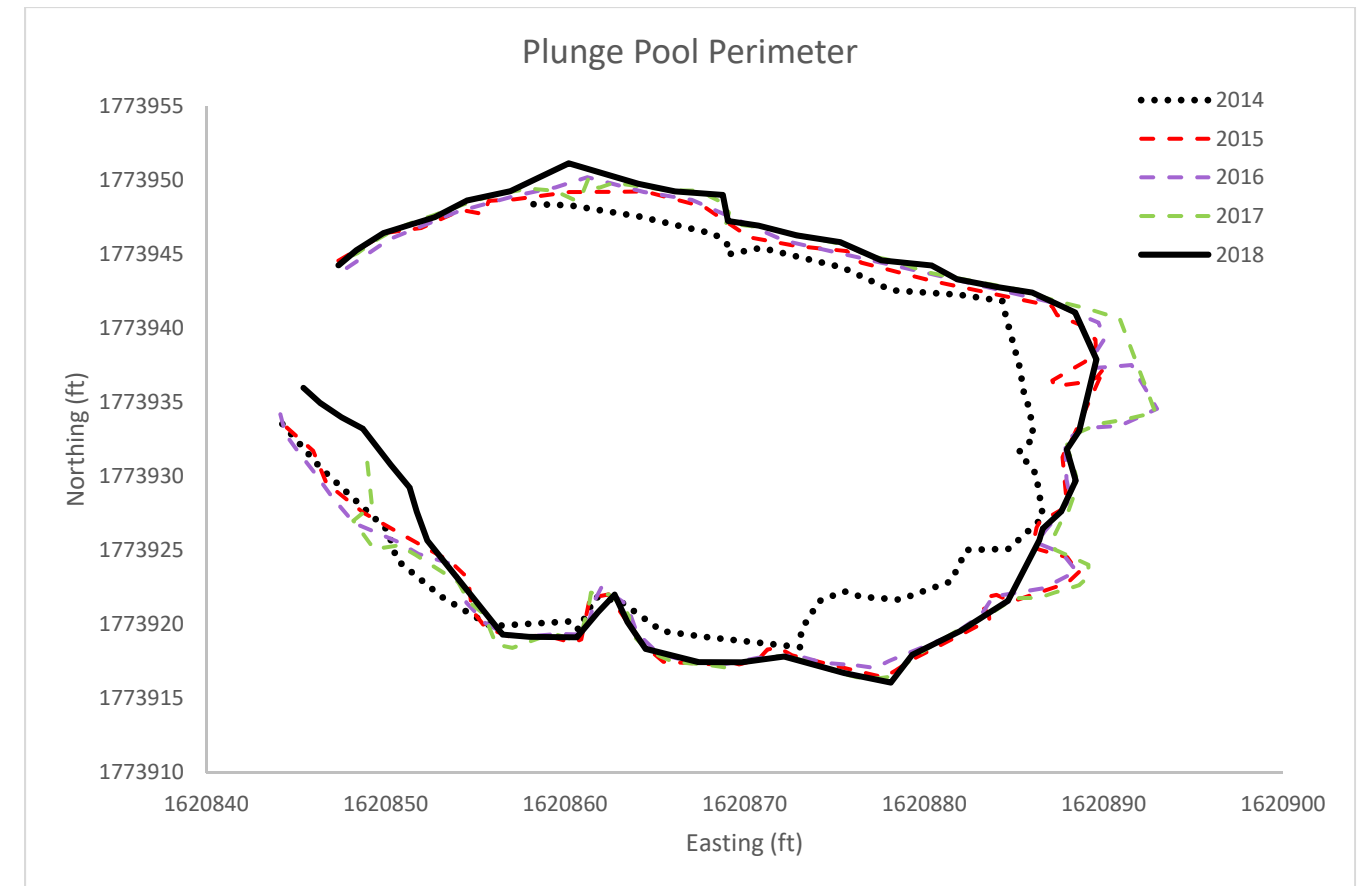


Figure B-4.2-2 5-yr plan view of plunge pool in Sandia Canyon reach S-2



**Table B-4.2-1**  
**Plunge Pool Area and Growth Assessment**

Year	Area (ft <sup>2</sup> )	Area (m <sup>2</sup> )	% Change in Area From Previous Year	Rate of Change (ft <sup>2</sup> /yr)
2018	1067.7	99.2	5.03	-56.50
2017	1124.2	104.4	1.9	20.81
2016	1103.4	102.5	2.4	25.58
2015	1077.9	100.1	3.4	35.35
2014	1042.5	96.9	18.5	162.98
2013 <sup>a</sup>	879.5	81.7	na <sup>b</sup>	na

<sup>a</sup> 2013 is baseline survey year for plunge pool perimeter mapping.

<sup>b</sup> na = Not available.



## **Attachment B-1**

---

*2018 Geomorphic Changes in  
Sandia Canyon Reach S-2 Survey Data  
(on CD included with this document)*





## **Appendix C**

---

*2018 Wetland Vegetation Monitoring  
in Sandia Canyon Reach S-2*



## CONTENTS

<b>C-1.0 INTRODUCTION .....</b>	<b>C-1</b>
<b>C-2.0 VEGETATION MONITORING METHODS .....</b>	<b>C-1</b>
<b>C-3.0 MONITORING RESULTS .....</b>	<b>C-2</b>
C-3.1 Wetland Vegetation Area .....	C-2
C-3.2 Wetland Vegetation Photograph Comparisons .....	C-3
<b>C-4.0 CONCLUSIONS AND RECOMMENDATIONS .....</b>	<b>C-4</b>
<b>C-5.0 REFERENCES AND MAP DATA SOURCES .....</b>	<b>C-5</b>
C-5.1 References .....	C-5
C-5.2 Map Data Sources .....	C-5

### Figures

Figure C-1.0-1	Locations of transect lines, piezometers, sheet piles, and 2018 thalweg and plunge pool profile in Sandia Canyon reach S-2.....	C-7
Figure C-1.0-2	2017 and 2018 vegetation perimeter mapping comparison results at Sandia Canyon reach S-2.....	C-8
Figure C-1.0-3	2014 and 2018 vegetation perimeter mapping comparison results at Sandia Canyon reach S-2.....	C-9
Figure C-3.1-1	Upper wetland area highlighting cattail populations.....	C-10

### Tables

Table C-3.1-1	1-yr Wetland Vegetation Area Totals .....	C-11
Table C-3.1-2	5-yr Wetland Vegetation Area Totals .....	C-11

### Attachments

Attachment C-1	Comparison Photographs of Sandia Wetland Vegetation Monitoring
Attachment C-2	2018 Vegetation Survey Data (on CD included with this document)



## **C-1.0 INTRODUCTION**

This appendix evaluates vegetation changes that occurred in Sandia Canyon reach S-2 within Los Alamos National Laboratory (LANL or the Laboratory). The vegetation survey perimeter map and qualitative photographic comparisons for 2018 document vegetation conditions in reach S-2 satisfy annual vegetation monitoring requirements (LANL 2018, 603022). This appendix compares the 2017 vegetation perimeter map and photographs with those prepared in fall 2018, as well as a 5-yr comparison to evaluate the overall stability of the wetland area.

Vegetation surveys are performed because the vitality of wetland species is a good indicator of redox and saturation conditions over a spatial distribution that cannot be easily measured by other point data techniques such as alluvial well/piezometer monitoring. Specifically, the presence of obligate wetland vegetation implies persistent saturation. Persistent saturation and contribution of organic matter from wetland vegetation are highly favorable to producing and maintaining reducing conditions. Perimeter mapping of wetland vegetation is also performed and is supplemented with annual photographic comparisons to help evaluate the extent of obligate wetland vegetation and the establishment of overbank vegetation and their ability to compete for any remaining bare ground. Figure C-1.0-1 shows the geographic locations of transects where annual photographs are taken. Figures C-1.0-2 and C-1.0-3 show 1-yr and 5-yr comparisons of the perimeter extent of mapped wetland species, respectively. Attachment C-1 presents photographs from 2014 to 2018 that compare vegetation conditions in Sandia Canyon reach S-2 to help assess the overall condition, extent, and stability of Sandia wetland vegetation. For a comprehensive species list, refer to Appendix C, Table C-3.1-1 of the "2017 Wetland Performance Report" (LANL 2018, 603022).

## **C-2.0 VEGETATION MONITORING METHODS**

Vegetation perimeter mapping was used to document the spatial distribution and areal extent of targeted wetland species. Through the comparison of annual perimeter maps, success of wetland zones can be quantified based on the areal extent of specific wetland obligate zones. Vegetation perimeter mapping documents targeted cattails, coyote willows, and grade-control structure (GCS) wetland species. These targeted areas are defined by wetland obligate species or species expected to occur almost always (estimated probability of >99%) in wetland systems. While these targeted species represent the majority of vegetation in their designated zone, many other species (both wetland obligate and nonobligate) coexist within the same zones. In some instances (western end of reach S-2), targeted species were intermixed with other plant species and/or are discontinuous. When a gap in the targeted species was encountered along the length of the reach, the survey perimeter (i.e., polygon) was closed. While most of these targeted species were of sufficient concentration to be easily identified as a mappable unit, no spatial density interpretations of the interior of the mapped perimeters are implied. Surveys were conducted using real-time kinematic (RTK) differentially corrected GPS surveying equipment. Raw survey data (x and y coordinates using the New Mexico State Plane coordinate system and elevations of all survey points) for surveyed perimeters are included electronically as Attachment C-2 (on CD included with this document).

Photograph points that were established at both the north and south ends of each vegetation transect (see Attachment C-1 for photos) were used to qualitatively compare annual changes in vegetation. Vegetation growth (height) and species diversity can be analyzed qualitatively from these comparison photographs documenting changes from 2017 to 2018 and over the period of record 2014 and 2018.

### **C-3.0 MONITORING RESULTS**

Overall, this analysis indicates an expansion of vegetation and a corresponding increase in wetland obligate species competition among vegetative groups in the Sandia wetland since 2014. However, the slight decreased area of wetland species and changing spatial distribution in the Sandia wetland between 2017 and 2018 signify a complex vegetative environment that continues to change on an annual basis (Figure C-1.0-2). A representative photo of each transect as they appeared in calendar years 2017 and 2018 is presented in Attachment C-1, Photographs C1-1 through C1-13. Representative photos from each transect as they were first documented are also include in Attachment C-1, Photographs C1-14 through C1-27.

#### **C-3.1 Wetland Vegetation Area**

The perimeter of wetland vegetation was surveyed using four vegetation communities with RTK GPS equipment. Mapping of these communities results in seven distinct areas or “zones” labelled in Figures C-1.0-2 and C-1.0-3. The zones are as follows: a western cattail zone, which includes the cattail populations in the northern and southern meadows of redtop grass as well as the population bordering the western edge of the plunge pool; central and western mixed cattail/willow zones; a central cattail zone; central and northeast willow zones; and a GCS wetland vegetation zone. Areas and percent change of these zones are provided in Table C-3.1-1 and Table C-3.1-2.

The western cattail zone is a narrow strip of cattails with no willows that parallels the open channel at the head of the study area and encompasses an area of 802 m<sup>2</sup>, a 6% between 2017 and 2018 (Table C-3.1-1). While the main body of this zone remained the same from 2017, an increase in areal coverage was observed at several satellite cattail populations. Since these satellite populations were first identified during the 2016 vegetation perimeter surveying near the plunge pool and in the field of giant redtop grass south of the western cattail zone, they have expanded to cover approximately 100 m<sup>2</sup> (including a newly identified population on the north side of the western cattail zone) (Figure C-3.1-1). During the 5-yr monitoring period, the western cattail zone has grown 129% as areal coverage has expanded upstream towards the plunge pool and in satellite cattail populations of the meadows directly adjacent (Table C-3.1-2).

The willow zones are located along the northern extent of the central cattail zone and adjacent to the central cattail/willow mixed zone. Together, the zones encompass 1488 m<sup>2</sup>, a decrease of 6% from 2017 (Table C-3.1-1). A new, willow-only area was delineated in 2018 on the southeast edge of the central mixed cattail/willow zone, constituting 126 m<sup>2</sup> of the total area. Although the southernmost extent of this willow population was previously included in the central mixed cattail/willow zone, this delineation was made as the willow population continues to expand while cattails have remained relatively stable. A baseline survey of the northern willow zone was first conducted in 2015 and has expanded 387% since 2014. This increase is a result of the growth of willows into upland areas previously absent of wetland species and competitive advancement of the species into the established central cattail zone.

There are two mixed cattail/willow zones: One (central mixed cattail/willow zone) located on the south-central edge and the second (western mixed cattail/willow zone) located on the northwestern extent of the central cattail zone that together encompass 1842 m<sup>2</sup> in 2018 (Table C-3.1-1 and Figure C-1.0-2). These zones are primarily dominated by coyote willows with stands of cattails along the stream channel and vegetative boundaries as well as several lanceleaf cottonwood trees occurring at the western mixed cattail/willow zone.

In 2018, two changes were made to the mapping of both mixed zones. First, the perimeter of the western mixed cattail/willow zone near SGCS-4 and SGCS-3B was mapped using cattails or coyote willow as the primary species defining the extent of the zone instead of following the farthest extent of the common three-square sedge as occurred in 2017, making comparison of areal changes between the two years incalculable. Second, a willow-only zone was delineated along the southeast edge of the central mixed cattail/willow zone where a previously gradational contact into strictly cattails has become more distinct. Visual inspection and repeat photos confirm that both mixed stands are stable and healthy (Attachment 1, Photos C1-2, C1-3, and C1-7). Ultimately, the mixed cattail/willow zone has grown by 92% since 2014 (Table C-3.1-2), further indicating the continued stabilization of these communities over time.

The central cattail zone encompasses 10,052 m<sup>2</sup> in 2018, a decrease of 1% since 2017, and is the dominant vegetation feature of the study area (Table C-3.1-1). Despite the minor decrease in area, the central cattail zone continued to thrive as a stable vegetative unit in 2018 (Figure C-1.0-1). Between 2014 and 2018, the central cattail zone increased in area by 3%, the smallest of any monitored zone (Table 3.-1.2). This increase is most likely because it has been a relatively large and stable vegetative community since 2014. Expansion could also be because of an alluvial fan and a side channel off the toe on the south side of the central cattail zone that deposited a small amount of sandy gravel into the wetland, burying a small patch of cattails in 2015 (LANL 2016, 601432). Monitoring of this feature from 2016 to 2018 has demonstrated that storm runoff has continued to redistribute sandy gravel within the alluvial fan and along the side channel adjacent to the wetland but has not resulted in any significant vegetation (cattail) loss (Appendix B, section 4; LANL 2017, 602341; LANL, 2018, 603022). However, it is possible that the continuation of storm deposits may affect the ability of cattails to effectively populate this area in the future.

Gravel bars devoid of wetland vegetation in the middle of the central cattail zone began to form in 2014 and were first surveyed in 2015 (Figure C-1.0-2). These gravel bars were approximately 1–2 ft above the water surface in the wetland at the time of survey and were populated with grasses and small shrubs such as rubber rabbitbrush (LANL 2016, 601432). Surveying and visual observations from the fall of 2018 indicate these features are not expanding and are still populated with graminoid species, rubber rabbitbrush, and thistle species. A very narrow trail exists on the top of the gravel bars with no vegetation; otherwise, the gravel bars are revegetating with primarily nonobligate wetland species.

The GCS wetland vegetation zone surrounding the GCS encompasses 1299 m<sup>2</sup>, an expansion of 10% from 2017. Since there is no longer a distinct boundary separating the western edge of the GCS vegetation area from the eastern edge of the established wetland of the central cattail zone or willow zone, the distinction between these zones are estimated in the field by the assumed location of the westernmost edge of the first sheet pile in the GCS. Lateral expansion of this zone has continued during 2018, with wetland obligate species continuing to revegetate the banks of the GCS area. Since 2014 there has been a 23% expansion of wetland vegetation in the GCS.

Overall, there has been a 22% increase in the total wetland vegetation area from 2014 to 2018 (Table C-3.1-2).

### **C-3.2 Wetland Vegetation Photograph Comparisons**

Representative photos from 2017 and 2018 of each transect are presented in Attachment C-1 (Photos C1-1 to C1-13) and are consistent with the results of the vegetation surveys, indicating stability of vegetation, especially in wetland obligate species, in the Sandia wetland (see Table C-3.1-1 in LANL 2018, 603022 for a comprehensive species list).

Photos C1-1 and C1-2 in Attachment C-1 show no observable change in vegetation expansion, indicating stable conditions along transects SGCS-3A and SGCS-3B. Photo C1-3 shows an overall increase in cattails along transect SGCS-4 within the mixed cattail/willow zone. Photos C1-4 through C1-10 show no observable change to the wetland vegetation, indicating stable conditions within the mixed cattail/willow zone and central cattail zone. All three GCS transect photo groups (Photos C1-11 through C1-13 in Attachment C-1) show minor cattail expansion, indicating stable conditions.

Also included in Attachment C-1 are comparison transect photos (Photos C1-14 through C1-27) from 2014 or 2015–2016 for comparison with 2018 photos to help assess the overall condition, extent, and stability of Sandia wetland vegetation. These photographs show expansion and growth of wetland vegetation within all vegetation zones in Sandia Canyon reach S-2.

Photos C1-14, C1-15, and C1-17 show no observable changes in wetland vegetation, indicating stable conditions within the mixed cattail/willow zone and western cattail zone. Photo C1-16 shows cattail growth from 2014 to 2018 along transect SCGS-4 within the mixed cattail/willow zone. Photos within the central cattail zone along transects SGCS-7, SGCS-9, SGCS-11, SGCS-12, SGCS-14, and SGCS-16 (Photos C1-18 through C1-23 in Attachment C-1) show little observable change in wetland vegetation, indicating an environment suitable for established cattails to thrive in. Photos C1-24 through C1-26 show significant vegetation growth from 2014 to 2018, indicating a favorable environment for wetland vegetation and increased stability in the GCS zone.

Photo C1-27 shows one of several satellite cattail populations discussed in the results for the western cattail zone in section C-3.1 and displayed in Figure C-3.1-1. In addition to multiple satellite populations established in 2016 that have continued to expand, a new satellite population was surveyed in 2018 on the north side of the western cattail zone, indicating an environment suitable for a stand of cattails to thrive in the upper (western) reach.

Overall, this qualitative photograph analysis indicates the vegetation in the wetland has been stable and, in some instances, expanding from 2014 to 2018, with the most notable changes occurring at the GCS wetland zone (SGCS-19, SGCS-20, and SGCS-21).

#### **C-4.0 CONCLUSIONS AND RECOMMENDATIONS**

This appendix presents the annual vegetation monitoring surveys of Sandia Canyon reach S-2. Vegetation perimeter mapping was conducted and repeat photographs were taken at established locations at all 13 vegetation transects in the fall of 2018. Moving west to east in reach S-2, the areal extent of the wetland system is initially confined to a narrow zone within a defined channel and gradually expands moving eastward across a much wider area into the central cattail zone and terminates downstream of the GCS. Between 2014 and 2018, wetland vegetation area has expanded by about 22% over the whole study area. Growth is attributed to expansion in all zones: the western and central cattail zones, the mixed cattail/willow zone, and the willow zone. The largest detected changes occurred in the western cattail zone with expansion west toward the plunge pool and the establishment of satellite cattail in the meadows adjacent. Repeat photos and perimeter mapping suggest that the wetland has remained stable between 2017 and 2018 and restoration has been successful during the last 5 yr of measurable change, especially at the Sandia wetland GCS, which continues to be efficient in stabilizing water and sediment, allowing for the generation of a healthy wetland system. Steadily increasing data trends derived from the line intercept method in 2014, 2015, and 2017 as well as vegetation perimeter mapping from 2014 to 2018 (Figure C-1.0-3) indicate a stable and growing wetland that is unlikely to regress unless a significant change is incurred by the system.



In 2019, if storm water peak discharge at gaging station E123 is greater than 100 cubic feet per second, a visual inspection of the wetland will occur to document qualitative vegetation changes. If the visual observations indicate significant vegetation changes that are not consistent with last year's observations, an aerial survey (via plane or unmanned aerial vehicle) using a hyperspectral sensor will be planned as soon as possible, preferably at the peak of photosynthetic activity in August/September. Aerial vegetation monitoring has not been performed in the past; however, a baseline vegetation survey will be performed in 2019. The hyperspectral sensor will be used to classify vegetation species and determine vegetation density, stand height, and spatial extent. In addition, the normalized difference vegetation index (NDVI), which is an indicator of photosynthetic activity using the red and near-infrared bands, will be computed as a measure of the health of the wetlands. If no large storm events occur, creating significant vegetation change, aerial hyperspectral surveys will be performed every 3 yr, with the next survey scheduled for 2022.

## **C-5.0 REFERENCES AND MAP DATA SOURCES**

### **C-5.1 References**

*The following reference list includes documents cited in this report. Parenthetical information following each reference provides the author(s), publication date, and ERID, ESHID, or EMID. This information is also included in text citations. ERIDs were assigned by the Laboratory's Associate Directorate for Environmental Management (IDs through 599999); ESHIDs were assigned by the Laboratory's Associate Directorate for Environment, Safety, and Health (IDs 600000 through 699999); and EMIDs are assigned by Newport News Nuclear BWXT-Los Alamos, LLC (N3B) (IDs 700000 and above). IDs are used to locate documents in N3B's Records Management System and in the Master Reference Set. The New Mexico Environment Department (NMED) Hazardous Waste Bureau and N3B maintain copies of the Master Reference Set. The set ensures that NMED has the references to review documents. The set is updated when new references are cited in documents.*

LANL (Los Alamos National Laboratory), April 2016. "2015 Sandia Wetland Performance Report," Los Alamos National Laboratory document LA-UR-16-22618, Los Alamos, New Mexico. (LANL 2016, 601432)

LANL (Los Alamos National Laboratory), April 2017. "2016 Sandia Wetland Performance Report," Los Alamos National Laboratory document LA-UR-17-23076, Los Alamos, New Mexico. (LANL 2017, 602341)

LANL (Los Alamos National Laboratory), April 2018. "2017 Sandia Wetland Performance Report," Los Alamos National Laboratory document LA-UR-18-23194, Los Alamos, New Mexico. (LANL 2018, 603022)

### **C-5.2 Map Data Sources**

Gaging stations; Los Alamos National Laboratory, Waste and Environmental Services Division; 1:2,500; March 19, 2011.

LANL area orthophoto; Los Alamos National Laboratory, 2014.

Geomorphic Reach Boundary, Los Alamos National Laboratory, Earth and Environmental Science, GISLab, 2009.

Geomorphology Units; Los Alamos National Laboratory, Earth and Environmental Sciences, GISLab, 2009.





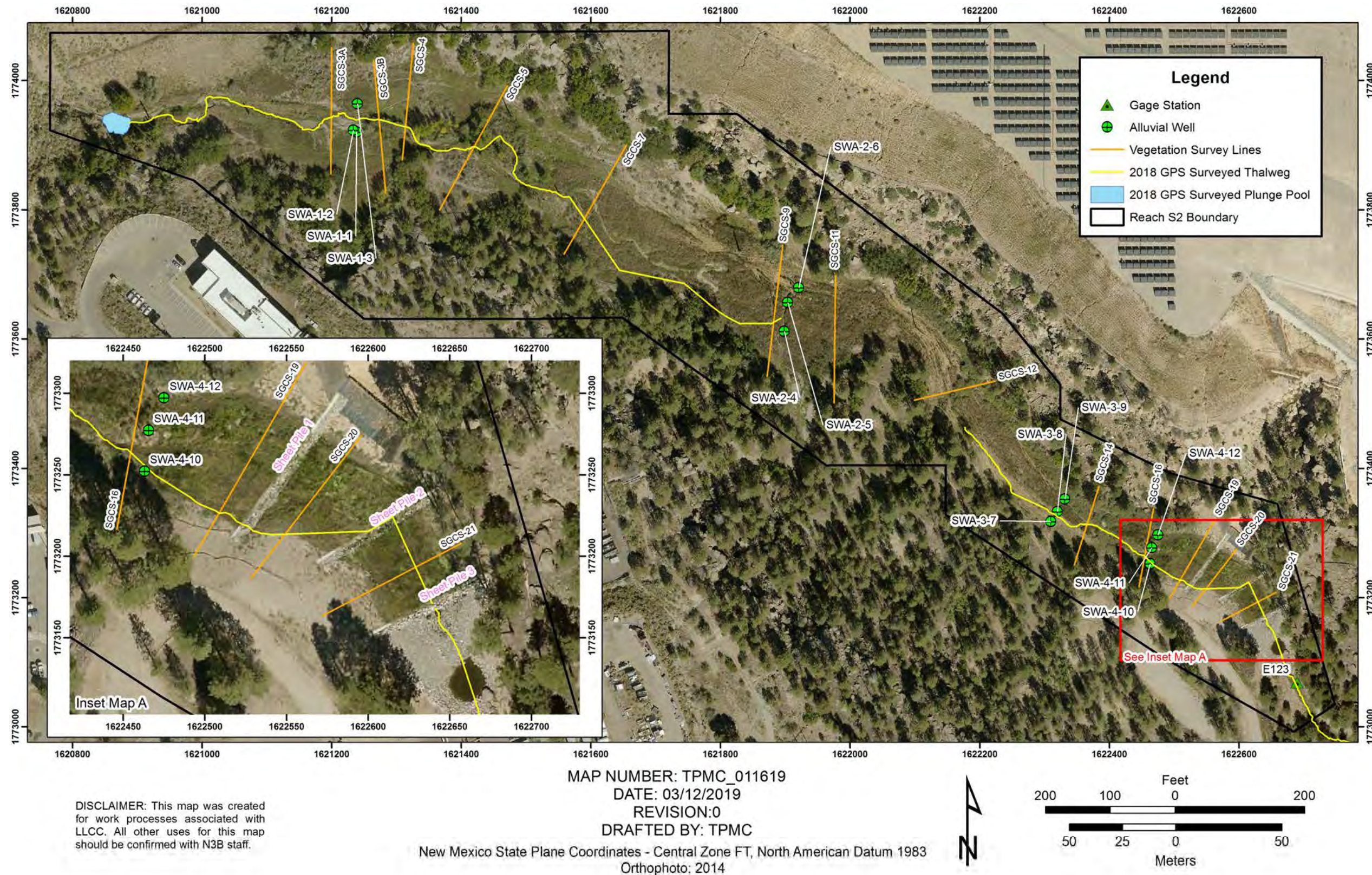


Figure C-1.0-1 Locations of transect lines, piezometers, sheet piles, and 2018 thalweg and plunge pool profile in Sandia Canyon reach S-2



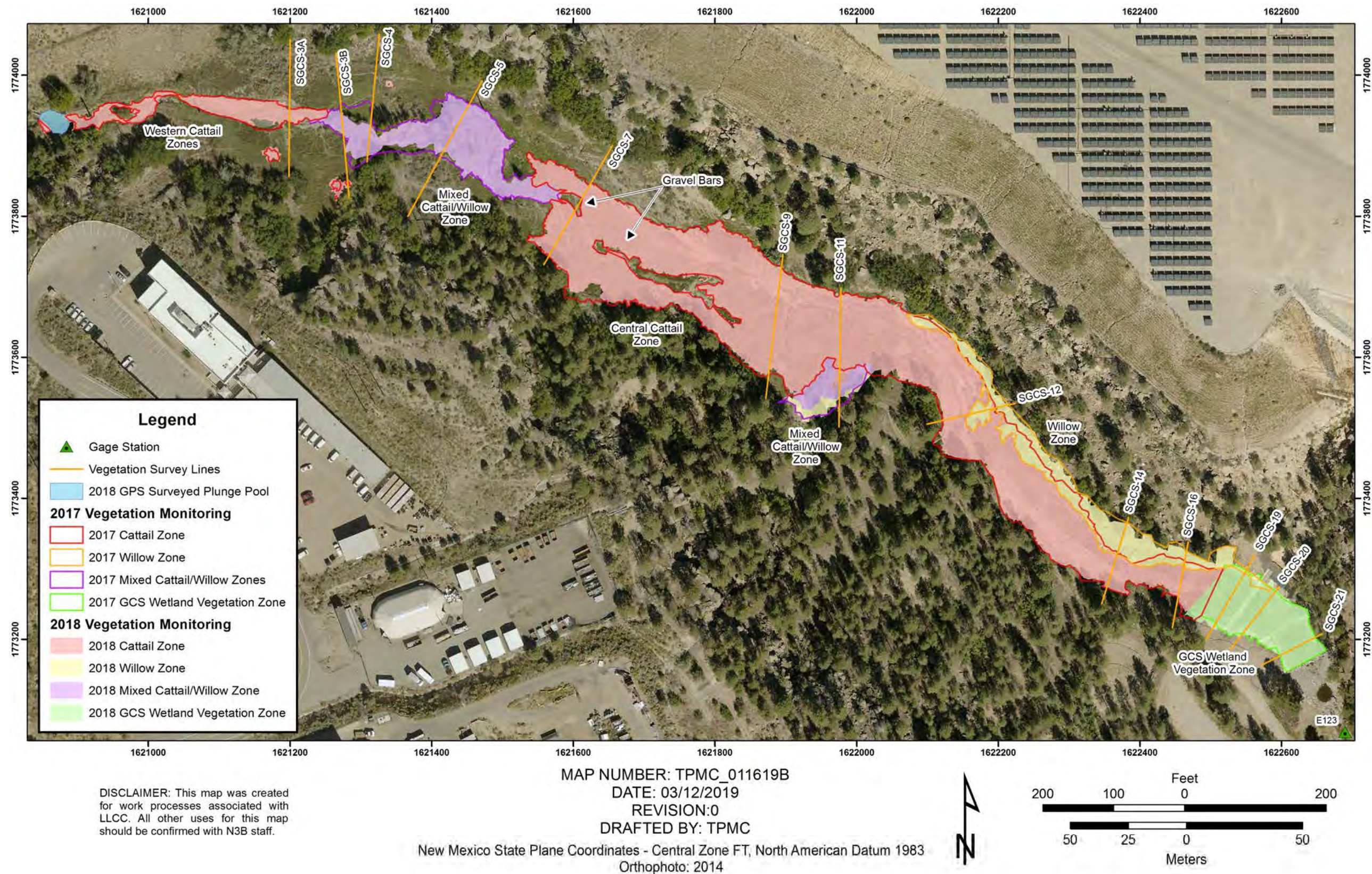


Figure C-1.0-2 2017 and 2018 vegetation perimeter mapping comparison results at Sandia Canyon reach S-2



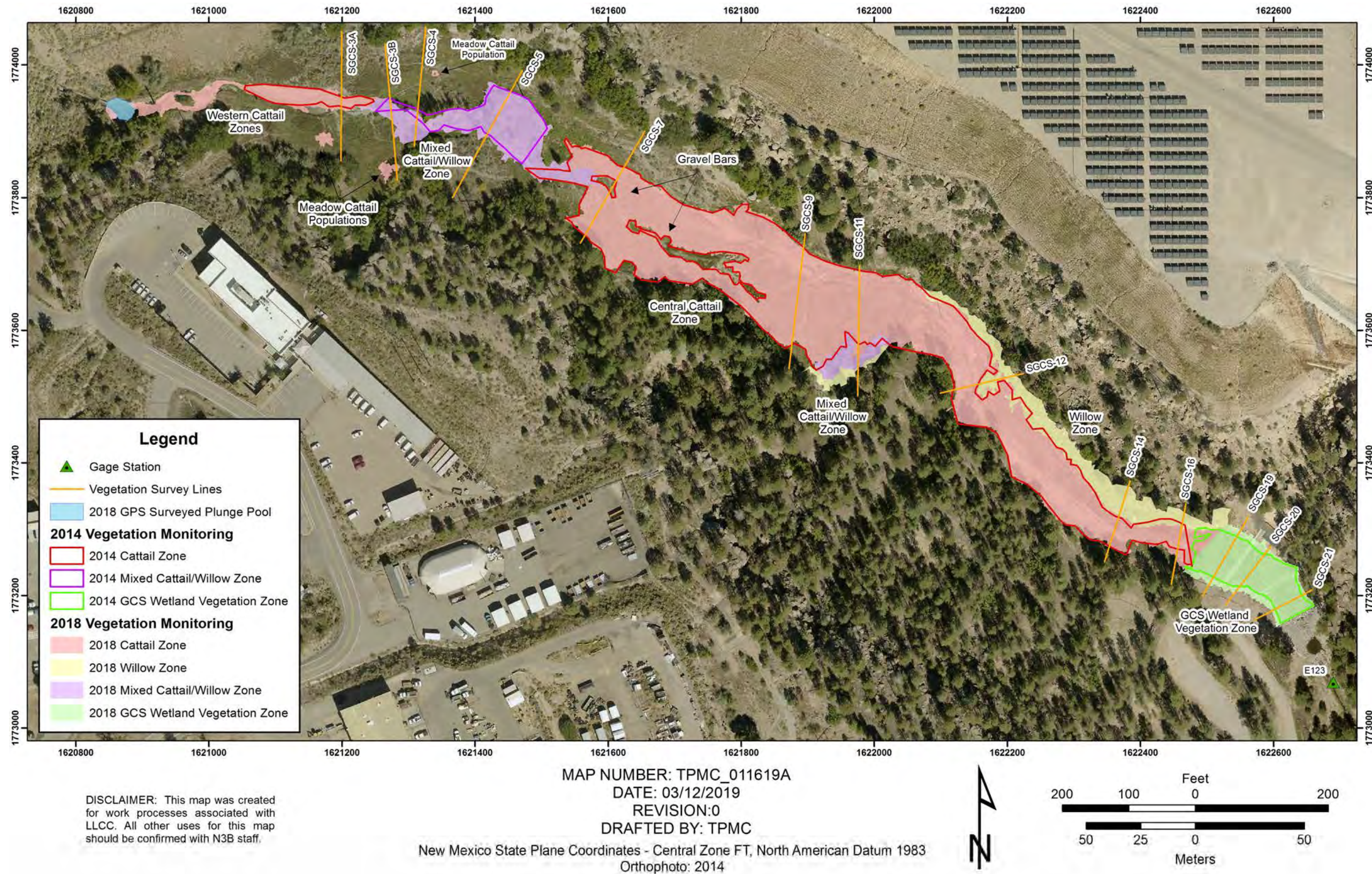


Figure C-1.0-3 2014 and 2018 vegetation perimeter mapping comparison results at Sandia Canyon reach S-2



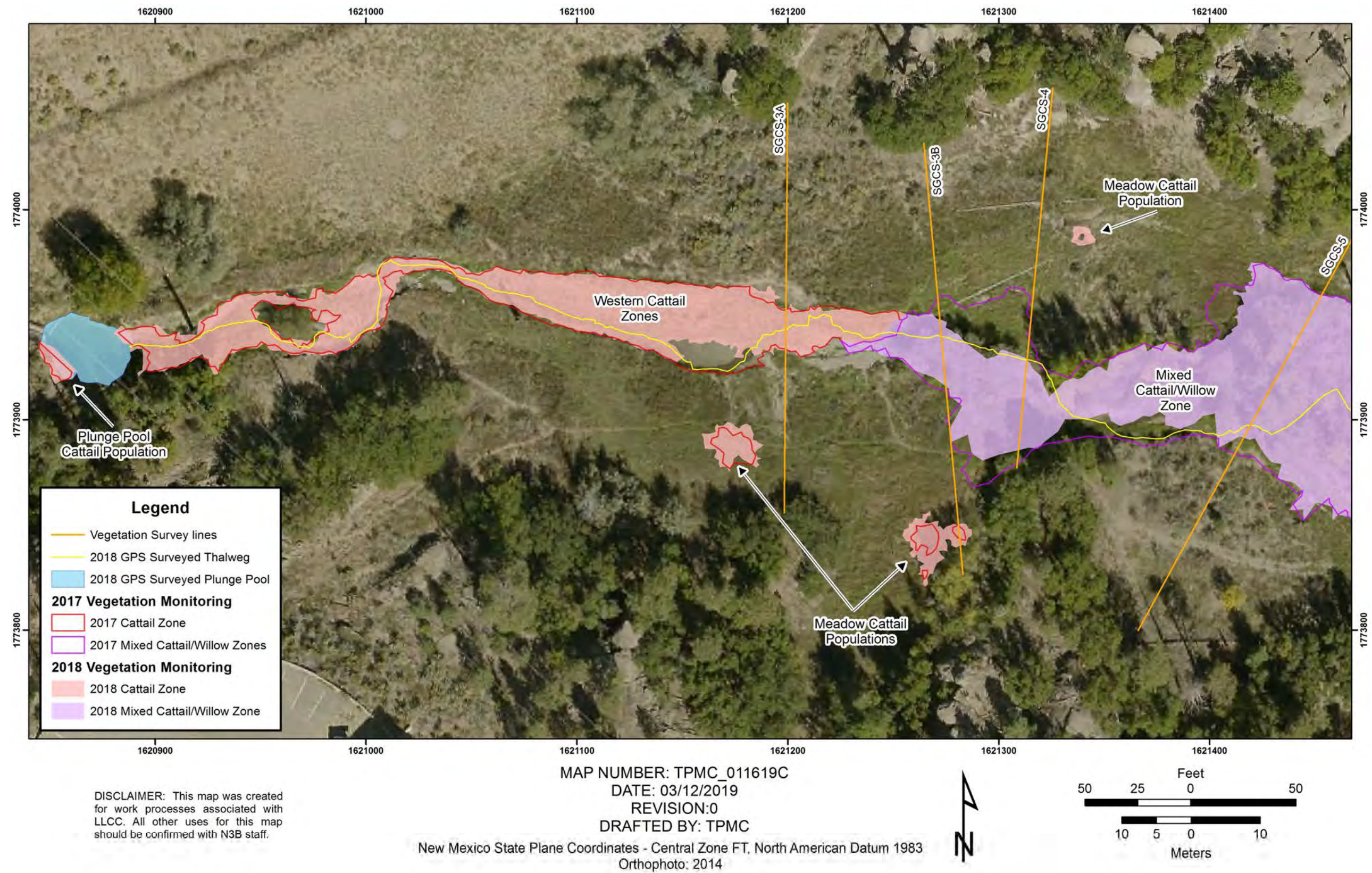


Figure C-3.1-1 Upper wetland area highlighting cattail populations



**Table C-3.1-1**  
**1-yr Wetland Vegetation Area Totals**

Zone Name	2017 Area (m <sup>2</sup> )	2018 Area (m <sup>2</sup> )	Change (m <sup>2</sup> )	% Change	Comments
West Cattail	760	802	42	6	Continued expansion of meadow cattail populations.
Mixed Cattail/Willow (central and western)	2251	1842	— <sup>a</sup>	—	Change (m <sup>2</sup> ) and percent change not calculated because of differing mapping methods in western zone and the delineation of new willow-only area along edge of central mixed cattail/willow zone.
Central Cattail	10155	10052	-103	-1	Minimal change.
GCS Vegetation	1185	1299	114	10	Continued expansion of wetland vegetation, particularly upslope and into the central cattail zone.
Willow (central and eastern)	1585	1488	-97	-6	Small loss of willow upslope at the northern wetland margin.
<b>Totals</b>					
Sum area of zones	15936	15482	0	0	Differences in 'sum areas' and 'total wetland areas' are a result of overlap between the GCS, central cattail, and mixed areas.
Total wetland area <sup>b</sup>	15356	14764	-592	-4	Small decrease in area from 2017 to 2018, in part because of mapping methods in the western mixed cattail/willow zone.

<sup>a</sup> — = Change (m<sup>2</sup>) and percent change not calculated.

<sup>b</sup> Calculated to include coverage of overlapping zones.

**Table C-3.1-2**  
**5-yr Wetland Vegetation Area Totals**

Zone Name	2014 Area (m <sup>2</sup> )	2018 Area (m <sup>2</sup> )	Change (m <sup>2</sup> )	% Change	Comments
West Cattail	350	802	452	129	Expansion of cattail populations to the west and of satellite meadow populations and at the plunge pool.
Mixed Cattail/Willow	957	1842	885	92	Growth of willow populations within the cattail-dominated areas.
Central Cattail	9728	10052	324	3	Relatively stable cattail population.
GCS Vegetation	1057	1299	242	23	Expansion of wetland vegetation in GCS in all directions.
Willow	0	1488	1488	n/a <sup>a</sup>	Delineation and expansion of willow-only populations.
<b>Totals</b>					
Sum Area of zones	12092	15482	0	0	Differences in 'sum areas' and 'total wetland areas' are a result of overlap between the GCS, central cattail, and mixed areas.
Total wetland area <sup>b</sup>	12092	14764	2672	22	Overall expansion of wetland vegetation from 2014 to 2018.

<sup>a</sup> n/a = Not applicable, cannot divide by zero.

<sup>b</sup> Calculated to include coverage of overlapping zones.





# **Attachment C-1**

---

*Comparison Photographs  
of Sandia Wetland Vegetation Monitoring*





**Photo C1-1 SGCS-3A photographs looking north; (left) August 2017 and (right) August 2018**





**Photo C1-2 SGCS-3B photographs looking south; (left) August 2017 and (right) August 2018**





Photo C1-3 SGCS-4 photographs looking north; (left) August 2017 and (right) August 2018





Photo C1-4 SGCS-5 photographs looking north; (left) August 2017 and (right) August 2018





Photo C1-5 SGCS-7 photographs looking south; (left) August 2017 and (right) August 2018





Photo C1-6 SGCS-9 photographs looking north; (left) August 2017 and (right) August 2018





Photo C1-7 SGCS-11 photographs looking north; (left) August 2017 and (right) August 2018





Photo C1-8 SGCS-12 photographs looking north; (left) August 2017 and (right) August 2018





Photo C1-9 SGCS-14 photographs looking north; (left) August 2017 and (right) August 2018





**Photo C1-10 SGCS-16 photographs looking north; (left) August 2017 and (right) August 2018**





Photo C1-11 SGCS-19 photographs looking north, upstream of sheet pile 1; (left) August 2017 and (right) August 2018





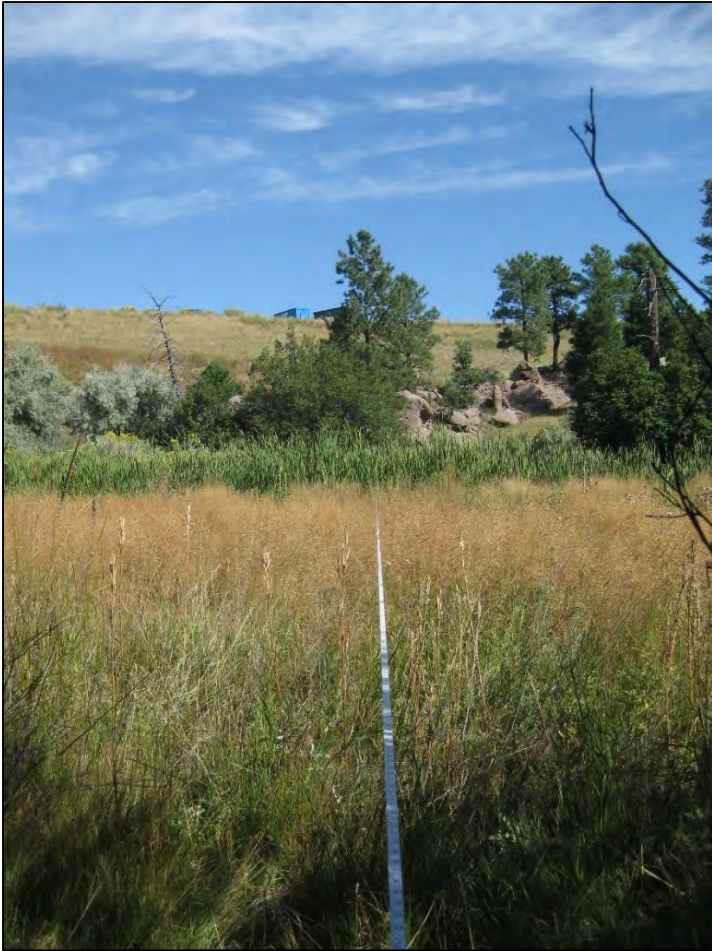
Photo C1-12 SGCS-20 photographs looking north, between sheet pile 1 and 2; (left) August 2017 and (right) August 2018





Photo C1-13 SGCS-21 photographs looking north, upstream of sheet pile 3; (left) August 2017 and (right) August 2018





**Photo C1-14 SGCS-3A photograph looking north; (left) September 2015 and (right) August 2018**





Photo C1-15 SGCS-3B photographs looking south; (left) September 2015 and (right) August 2018





Photo C1-16 SGCS-4 photographs looking north; (left) September 2014 and (right) August 2018





Photo C1-17 SGCS-5 photographs looking north; (left) September 2015 and (right) August 2018





Photo C1-18 SGCS-7 photographs looking south; (left) September 2014 and (right) August 2018





Photo C1-19 SGCS-9 photographs looking north; (left) September 2014 and (right) August 2018





Photo C1-20 SGCS-11 photographs looking north; (left) September 2014 and (right) August 2018





Photo C1-21 SGCS-12 photographs looking north; (left) September 2014 and (right) August 2018





Photo C1-22 SGCS-14 photographs looking north; (left) September 2014 and (right) August 2018





**Photo C1-23** SGCS-16 photographs looking north; (left) September 2014 and (right) August 2018





Photo C1-24 SGCS-19 photographs looking north, upstream of sheet pile 1; (left) September 2014 and (right) August 2018



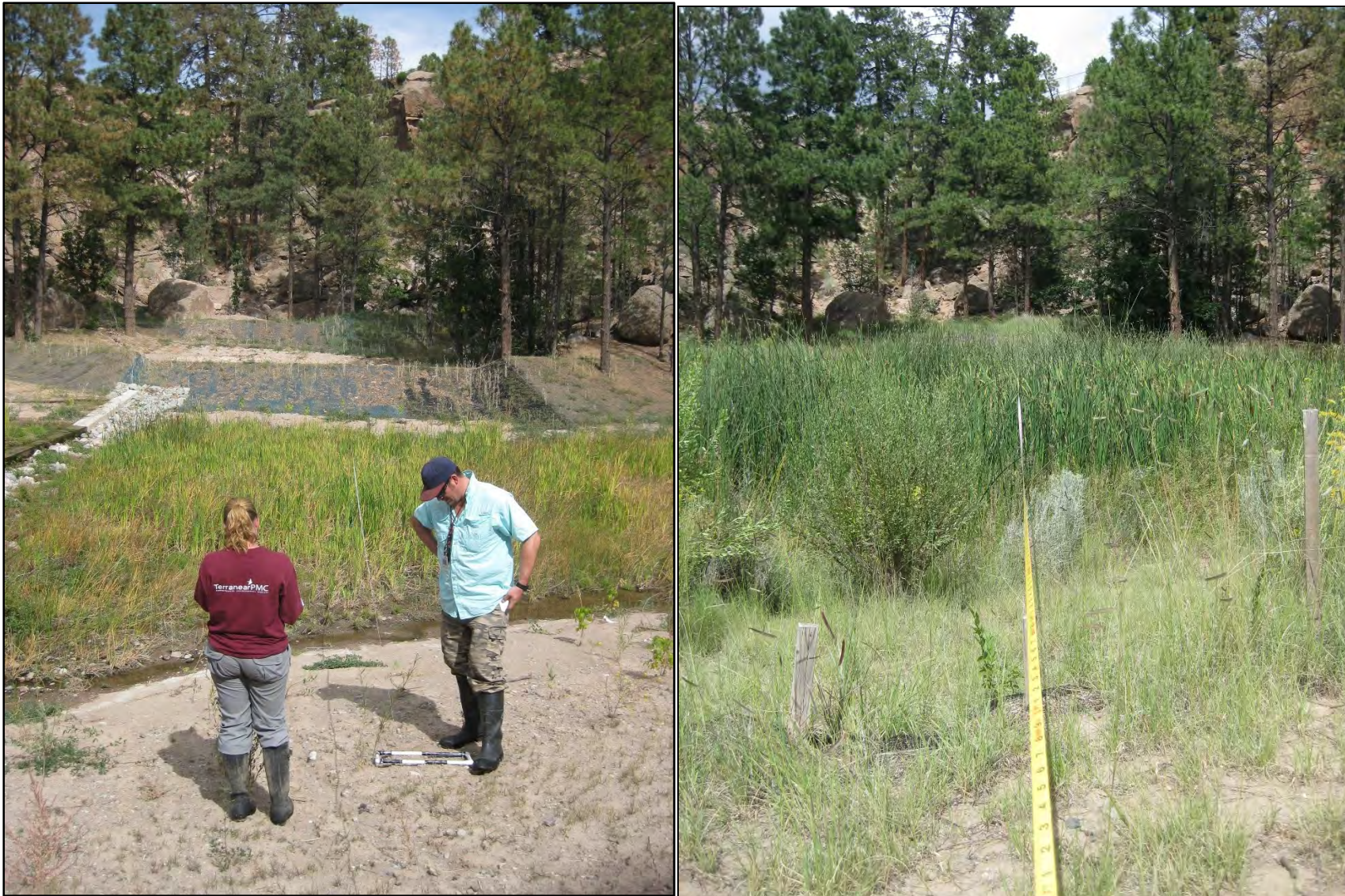


Photo C1-25 SGCS-20 photographs looking north, between sheet pile 1 and 2; (left) September 2014 and (right) August 2018





Photo C1-26 SGCS-21 photographs looking north, upstream of sheet pile 3; (left) September 2014 and (right) August 2018





**Photo C1-27** New observed cattail populations from 2016 within grass meadow along southern end of SGCS-3A and 3B, looking northeast (left); same cattail population in August 2018, looking southeast (right)





## **Attachment C-2**

---

*2018 Vegetation Survey Data  
(on CD included with this document)*



## **Appendix D**

---

*Geochemical and Hydrologic Monitoring in Sandia Canyon*





## CONTENTS

<b>D-1.0 INTRODUCTION .....</b>	<b>D-1</b>
<b>D-2.0 ANALYTICAL RESULTS FROM SURFACE WATER GAGING STATIONS E121, E122, AND E123 .....</b>	<b>D-1</b>
D-2.1 Screening Surface and Storm Water to Surface Water Quality Criteria.....	D-5
<b>D-3.0 ANALYTICAL RESULTS FROM ALLUVIAL SYSTEM .....</b>	<b>D-6</b>
D-3.1 Non-redox Sensitive Species .....	D-7
D-3.2 Redox Sensitive Species .....	D-7
D-3.3 Screening Alluvial Groundwater Results to Groundwater Standards.....	D-9
<b>D-4.0 WATER-LEVEL RESULTS FROM ALLUVIAL SYSTEM .....</b>	<b>D-10</b>
<b>D-5.0 REFERENCES .....</b>	<b>D-11</b>

### Figures

Figure D-2.0-1	Time-series plot showing chloride concentrations at gaging stations E121 and E123 and National Pollutant Discharge Elimination System– (NPDES-) permitted Outfall 001 .....	D-13
Figure D-2.0-2	Time-series plot showing nitrate plus nitrite as nitrogen concentrations at gaging stations E121 and E123 and NPDES Outfall 001.....	D-13
Figure D-2.0-3	Time-series plot showing silicon dioxide concentrations at gaging stations E121 and E123.....	D-14
Figure D-2.0-4	Time-series plot showing manganese concentrations at gaging stations E121 and E123 and NDPEs Outfall 001.....	D-14
Figure D-2.0-5	Time-series plot showing total chromium and Cr(VI) concentrations at gaging stations E121 and E123.....	D-15
Figure D-2.0-6	Time-series plots from 2010 to 2018 showing discharge at E121, E122, and E123 and total discharge from Outfalls 001, 03A027, and 03A199 .....	D-17
Figure D-2.0-7	Box-and-whisker plots of peak discharge, SSC, PCBs, filtered chromium and Cr(VI), and PAHs for base flow and storm flow at gaging stations E121, E122, and E123, pre- and post-construction (2014) of the GCS, respectively, in 2015, 2016, 2017, and 2018.....	D-18
Figure D-2.0-8	Hydrographs of storm water discharge at E121, E122, and E123 during each sample-triggering storm event in 2018 .....	D-20
Figure D-2.0-9	Storm- and base-flow discharge correlations with SSC, total PCBs, total chromium, and total PAHs from 2014 to 2018 at E121, E122, and E123 with standardized residual outliers removed; the shaded areas represent 95% confidence intervals ...	D-23
Figure D-2.0-10	Annual mass flux (top) and annual mass flux normalized by runoff volume (bottom) for sediment at gaging stations E121 (green), E122 (blue), and E123 (purple) from 2014 to 2018 .....	D-25
Figure D-2.0-11	Annual mass flux (top) and annual mass flux normalized by runoff volume (bottom) for total PCBs at gaging stations E121 (green), E122 (blue), and E123 (purple) from 2014 to 2018 .....	D-26

Figure D-2.0-12	Annual mass flux (top) and annual mass flux normalized by runoff volume (bottom) for total chromium at gaging stations E121 (green), E122 (blue), and E123 (purple) from 2014 to 2018.....	D-27
Figure D-2.0-13	Annual mass flux (top) and annual mass flux normalized by runoff volume (bottom) for total PAHs at gaging stations E121 (green), E122 (blue), and E123 (purple) from 2014 to 2018 .....	D-28
Figure D-3.0-1	Chloride concentrations in Sandia wetland surface water and alluvial system .....	D-29
Figure D-3.0-2	Sulfate concentrations in Sandia wetland surface water and alluvial system .....	D-30
Figure D-3.0-3	Sulfide concentrations in Sandia wetland surface water and alluvial system .....	D-31
Figure D-3.0-4	Iron concentrations in Sandia wetland surface water and alluvial system .....	D-32
Figure D-3.0-5	Manganese concentrations in Sandia wetland surface water and alluvial system....	D-33
Figure D-3.0-6	Ammonia as nitrogen concentrations in Sandia wetland surface water and alluvial system.....	D-34
Figure D-3.0-7	Arsenic concentrations in Sandia wetland surface water and alluvial system .....	D-35
Figure D-3.0-8	Chromium concentrations in Sandia wetland surface water and alluvial system .....	D-36
Figure D-4.0-1	Water levels recorded by sondes located in the alluvial system plotted with precipitation data from the E121.9 weather station and total daily volume of flow in surface water gaging station E121 in 2017 and 2018 .....	D-37
Figure D-4.0-2	Time series of water level and temperature in alluvial system in 2017 and 2018 .....	D-38

## Tables

Table D-2.0-1	Travel Time of Flood Bore, Peak Discharge, Increase or Decrease in Peak Discharge, and Percent Change in Peak Discharge from Upgradient to Downgradient of the Wetland for Each Sample-Triggering Storm Event in 2018 .....	D-39
Table D-2.0-2	Calculated Sediment Yield and Runoff Volume at Gaging Stations E121, E122, and E123 for Each Sample-Triggering Storm Event from 2014 to 2018 .....	D-39
Table D-2.1-1	Analytical Exceedances in Surface Water at Gaging Stations E121, E122, and E123.....	D-43
Table D-2.1-2	Summary of 2018 Base Flow and Storm Water SWQC Exceedances .....	D-46
Table D-3.3-1	Analytical Exceedances in the Alluvial System .....	D-47



## D-1.0 INTRODUCTION

The geochemical and hydrologic analytical results from performance monitoring of the Sandia wetland are presented and evaluated herein (Appendix F contains all the analytical and hydrologic data). Construction and subsequent revegetation of the Sandia grade-control structure (GCS) and the implementation of monitoring were not undertaken by Los Alamos National Laboratory (LANL or the Laboratory) with the objective of reducing concentrations of contaminants in water to specific values. Therefore, the comparison between analytical results and water-quality standards or other criteria presented in sections D-2.1 and D-3.4 is not intended to evaluate compliance with regulatory requirements.

## D-2.0 ANALYTICAL RESULTS FROM SURFACE WATER GAGING STATIONS E121, E122, AND E123

As noted in the baseline performance report (LANL 2014, 257590), similar base flow chemistry for many constituents between upgradient and downgradient locations indicates a relatively short residence time for surface water and little interaction (exchange) with alluvial groundwater. This finding is evident for chloride, nitrate plus nitrite, and silica, which are indicators of water quality in outfall discharge in the context of chemistry from Outfall 001 (Figures D-2.0-1 to D-2.0-3). Improvements in water chemistry discharged from Outfall 001 are evident for chloride and silica (as inferred from concentrations at E121) (Figures D-2.0-1 to D-2.0-3). Manganese, a sensitive redox indicator, is discussed because this base flow constituent shows some evidence for temporal trends (Figure D-2.0-4). Hexavalent chromium, a contaminant of concern along with total chromium, is also discussed (Figures D-2.0-5). Base flow and storm flow data for three key contaminants associated with wetland sediments, polychlorinated biphenyls (PCBs), chromium, and polycyclic aromatic hydrocarbons (PAHs) are discussed below.

In terms of improved water-quality indicators associated with the Sanitary Effluent Reclamation Facility (SERF) expansion, concentrations have continued to stabilize in 2018 with no strong base flow temporal concentration trends for filtered chloride and nitrate (Figures D-2.0-1 and D-2.0-2, respectively). However, the patterns observed post-SERF expansion (August 2012) are similar at both gaging stations and Outfall 001 (Figures D-2.0-1 and D-2.0-2). Nitrate has consistently lower concentrations at gaging station E123 relative to station E121 (Figure D-2.0-2). This finding is expected because nitrate is not only a water-quality indicator, it is also a plant nutrient and a redox-sensitive species that may be reduced and assimilated during surface water transport through the wetland. The peak increases in nitrate at the Outfall 001 are reflected in base flow nitrate concentrations (Figure D-2.0-2). These increases are likely related to an increase in Sanitary Waste Water System (SWWS) nitrate-containing effluent in Outfall 001 water until March 2016; however, the reason for the peak in late 2016 is unclear. Surface water base flow silicon dioxide concentrations are plotted in Figure D-2.0-3. The effect of the SERF expansion is represented by a drop in concentration (Figure D-2.0-3).

Among redox-sensitive species, dissolved manganese in base flow at gaging station E123 appears to be trending toward lower concentrations but is highly variable (Figure D-2.0-4). The cause of periodic spikes in manganese concentrations at E123 is not clear. Following completion of the GCS, manganese concentrations have remained generally lower. Manganese at E123 could represent either colloidal Mn(IV) and/or dissolved Mn(II). Manganese in alluvial groundwater will tend to be present as mobile Mn(II) and, given the slow oxidation kinetics, may not fully oxidize to less soluble Mn(IV) in the time between alluvial groundwater surfacing (at the headcut pre-GCS or at the upper impermeable wall post-GCS) and reaching gaging station E123 immediately downstream. Generally, lower manganese concentrations post-GCS are likely the result of some combination of cessation of headcutting at the terminus of the wetland, which would reduce colloidal transport of Mn(IV), and altered alluvial groundwater dynamics, which could affect Mn(II) concentrations and oxidation kinetics. Because the

wetland is still saturated (section D-4.0), it is unlikely that trends in manganese concentrations at downstream gaging station E123 reflect changes in redox conditions within the wetland. Further monitoring may explain the cause of the overall decrease through time. Dissolved concentrations of manganese are consistently higher at gaging station E123 relative to E121 because alluvial groundwater in the wetland has high manganese concentrations, probably as Mn(II) and possibly because of colloidal transport of Mn(IV). Greater mobilization of Mn(IV) colloids during construction of the GCS could account for the large spike in manganese concentration before the GCS was completed (Figure D-2.0-4).

Background concentrations of approximately 5–6 µg/L Cr(VI) occur in regional aquifer waters (LANL 2007, 095817). Because potable water is derived from the regional aquifer, it provides a starting point for expected concentrations of Cr(VI) in sanitary waste water before modifications occur at SWWS, SERF, or the cooling towers where potable water is used. Water from Outfall 03A027 analyzed for Cr(VI) in September 2015 showed a concentration of 6.41 µg/L (unfiltered), and the result falls within expected values for potable water. Cr(VI) has been detected in unfiltered samples at gaging station E121 with values up to 7.76 µg/L in May 2016. All Cr data for 2018 are as dissolved samples. At E123, most values of Cr(VI) have been below or at the detection limit, with the highest measured value of 1.33 µg/L with a detection limit at 1 µg/L. In 2018, although Cr(VI) was detected, there were no exceedances at any of the gaging stations. Hexavalent chromium shows evidence of attenuation as it is transported through the wetland; multiple detections of Cr(VI) at E121 tend to become nondetections by the time they reach gaging station E123 (Figure D-2.0-5).

Surface water at gaging stations E121, E122, and E123 is perennial; thus, the results for primary contaminants PCBs, chromium, and PAHs are separated into base flow and storm flow components. Figure D-2.0-6 shows the discharge measured at E121, E122, and E123 from 2010 to 2018 and the varying base flow at each station during this period. This figure also shows the total discharge from Outfall 001 and its influence of discharge on each gaging station, particularly E121 and E123. For both base flow and storm flow, box-and-whisker plots of peak discharge, suspended sediment concentration (SSC)/total suspended sediments (TSS), PCBs, chromium, and PAHs are presented in Figure D-2.0-7.

SSC, PCBs, chromium, and PAHs are discussed in the context of peak discharge and are used as key parameters to track the performance of the GCS. Results from gaging stations E121 and E122, which monitor most of the surface water flow into the wetland, and gaging station E123, which monitors surface water flow out of the wetland, are plotted together to show changes in surface water discharge and chemistry from upgradient to downgradient of the wetland (Figure D-2.0-7). These plots show the range of concentrations and represent a historical baseline before GCS construction (pre-GCS), during the first year of performance monitoring after GCS construction (post-GCS or 2014), and in 2015, 2016, 2017, and 2018. Multiple years of data are needed to fully delineate the performance metrics for the GCS.

In Figure D-2.0-7, storm flow discharge is expectedly greater than base flow discharge for all the gaging stations. At E121 and E123, base flow discharge is highly dependent on the outfall effluent discharge rate (Figure D-2.0-6). Therefore, the reduction in this rate from pre- to post-GCS and the seasonal fluctuations in this rate from 2015 through 2018 are reflected in the base flow discharge, more so at E121 than at E123 because of the damping effect of the wetlands on the discharge. Gaging station E122 base flow discharge is fairly stable throughout the years. One of the objectives of the GCS is to reduce the peak discharge of the storm flow, which can cause erosion and thus movement of contaminants. The storm flow peak discharge from upstream (E121 and E122) to downstream (E123) of the GCS was reduced post-GCS in 2015, 2016, 2017, and 2018. Precipitation from 2015 through 2018 was generally less intense than in 2013 and 2014, thus possibly attributing to the reduction in storm flow peak discharge. However, the wetland alone attenuates the storm flow peak discharge, as can be noted during pre-GCS conditions.

Hydrographs for the seven sample-triggering storm events recorded at E121, E122, and E123 from July 15 to September 4, 2018, are presented in Figure D-2.0-8. During these storm events, tributaries downstream of E121 and E122 can contribute significant flow. Table D-2.0-1 presents the timing of the transmission of flood bore, or peak, from E121 and E122 downstream to E123. In 2018, the average time of transmission from E121 to E123 and from E122 to E123 was approximately 83 min and 82 min, respectively. This finding indicates storm water from both upgradient stations flows through the wetland in approximately the same amount of time and quite rapidly, although not as rapidly as during 2014 (approximately 40-min average travel time between E121 and E122 to E123) when precipitation events were more intense.

In Figure D-2.0-7, the sediment content in base flow is, on average, lower than storm flow. This is typical for storm water because of the greater erosive energy associated with the increase in discharge. As expected, storm flow SSC at E121 is not significantly different pre- to post-GCS (stormflow SSC was not measured at E122 pre-GCS); however, at E123, storm flow SSC is significantly reduced after construction of the GCS and continues to remain low through 2016, possibly because of a cessation of headcutting at the terminus of the wetland. This reduction is noteworthy because contaminants in the wetland are strongly sorbed to sediments, and a reduction in SSC should be associated with a reduction in contaminant migration. In 2015, 2016, and 2017, stormflow sediment content at E121 and E122 is less than that measured during the pre- or post-GCS period (approximately 2014). This result is most likely because of the lack of more intense precipitation and erosive runoff during these years. In 2018, the stormflow SSC at E122 increased above 2014 (post-GCS) levels, but remained low relative to pre- and post-GCS levels at E121.

The box-and-whisker plots in Figure D-2.0-7 indicate that PCB concentrations in both base flow and storm flow at E123 are reduced since the GCS was constructed. While PCB concentrations in base flow and storm flow were much higher downgradient of the wetland (relative to upgradient locations E121 and E122) before the GCS was built, the concentrations are closer in magnitude upgradient and downgradient of the wetland since the GCS was constructed. The trend in base flow PCB concentrations at all of the gaging stations indicate a general decrease from 2015 through 2018. Although base flow PCB concentrations at E122 are relatively higher than they were in previous years, this location has tended to have much lower concentrations than the other two gaging stations. When combined with the results from E121, the 2018 results are not anomalous. However, there does appear to be an increasing trend in PCB concentrations in stormflow during 2017 and 2018. PCB concentrations at E121 and E122 in 2018 are similar to those in 2014 (post-GCS). While PCB concentrations at E123 are higher than they have been over the past 3 yr, they remain much lower than pre-GCS levels.

Total dissolved chromium has shown a general decreasing trend at E121 and E123 since 2015 (Figure D-2.0-7). Chromium concentrations at E122 have consistently been higher than those at E121 and E123. Dissolved Cr(VI) is much higher at the upstream gages than downstream at E123, demonstrating the reducing conditions present in the wetland. Total dissolved chromium in stormflow has remained relatively stable over the past 3 yr at all locations. Downstream, at E123, total chromium concentrations in stormflow continue to be much lower than pre-GCS construction. Stormflow samples were not analyzed for Cr(VI).

Total PAH was computed using the 18 most prominent PAHs, and nondetections were considered zero. PAHs were not analyzed in storm flow before the GCS was built. In base flow, all total PAH results were nondetections, with the exception of one sample collected at E123 in 2016 and two samples collected at E121 in 2017, and for which the total PAH concentrations were significantly lower than in storm flow. In storm flow, total PAH concentrations are similar upgradient and downgradient of the wetland. Overall, higher concentrations of PAHs were detected at E122 than at E121 and E123. This suggests that the influence of the former asphalt batch plant near the northern fork of upper Sandia Canyon is still evident



and is the most likely source of PAHs at the downstream gaging station, E123, because the low concentrations of PAHs at E121 do not indicate a source. In 2018, PAHs were not detected in any of the samples from the upstream locations, but one sample was detected downstream at E123. The source of these PAHs is unknown, but could be from runoff into the canyon from East Jemez Road.

In general, correlations exist between SSC, total PCBs, total chromium, total PAHs, and discharge, as presented in Figure D-2.0-9. Correlations show that as discharge increases, the concentrations of these constituents increase. There are exceptions to this regular correlation (e.g., E121 for SSC, E122 for total chromium, and E121 for PAH). Overall, however, these relationships show that discharge is a decent indicator of sediment and associated contaminant transport. The relationships shown in Figure D-2.0-9 were obtained after removing data points when the ISCO sampler malfunctioned and removing outliers using the standardized residual outlier method. These relationships were used to calculate the mass flux as follows. The line of best fit was used to calculate the approximate concentrations of sediment, total PCBs, total chromium, and total PAHs every 5 min using the following:

$$y_{n,i} = m_n x_i + b_n \quad \text{Equation D-1}$$

where  $y_{n,i}$  is the calculated concentration of each constituent  $n$  every 5 min or time step  $i$ ;  $n$  = SSC, total PCBs, total chromium, or total PAHs;  $x_i$  is the discharge at each time step  $i$ ; and  $m_n$  and  $b_n$  are each constituent's linear equation parameters (slope and y-intercept, respectively). The annual mass flux was then computed as the area under the 5-min concentration curve multiplied by the discharge:

$$\text{mass flux}_n = \sum_{i=1}^I \left( \frac{y_{n,i+1} + y_{n,i}}{2} \right) * (t_{i+1} - t_i) * x_i \quad \text{Equation D-2}$$

where  $t_i$  is the time of the discharge measurement at time step  $i$  and the annual mass flux was computed as the sum of the mass for calendar years 2014 through 2018.

Figures D-2.0-10 through D-2.0-13 show the estimated annual mass flux from 2014 to 2018 at each gaging station for sediment, total PCBs, total chromium, and total PAHs, respectively. Also shown in these figures is the annual mass flux normalized by annual runoff volume for each constituent. Sediment flux into the wetland is greater than the sediment flux out, which was also observed in the SSC box plots in Figure D-2.0-7. This indicates sediment is no longer being moved near the former headcut and the GCS is performing well. The normalized plots show that storm water runoff from the E121 watershed is more sediment-laden than runoff from the E122 or E123 watersheds since 2015, again indicating a reduction in sediment load through the wetland.

Total PCB and chromium flux out of the wetland is slightly lower than the PCB and chromium flux into the wetland in 2015, 2016, and 2018, suggesting a small amount of PCBs and Cr(III) is being entrained in the surface water through the wetland. In 2017, PCB flux in and out of the wetland were similar, while chromium still had a lower flux out of the wetland than in. The absence of any clear, continuing trend in PCB or chromium flux at E123 may be an indication that the wetland has stabilized after construction of the GCS. E121 has no clear trend in PCB flux over time, although there appears to be an increase in chromium flux from 2014 to 2016, following by a consistent decrease over the past 2 yr. PCB and chromium flux at E122 has remained fairly stable over time.

PAH flux out of the wetland is less than the PAH flux into the wetland, indicating that PAHs are remaining in the wetland. Note that the relationships between total PAHs and discharge, which is the foundation of the mass flux calculations, are not very strong; therefore, there is significant uncertainty associated with the flux.

In addition to using the relationship between SSC and discharge to estimate annual sediment flux, the actual sediment flux for each sampled storm event was also computed using SSC measurements (Table D-2.0-2). The relationship between sediment volume and runoff volume for storm flow tends to be a stronger relationship than sediment volume and peak discharge, and for all of upper Sandia Canyon this relationship is  $R^2 = 0.55$ :

$$\text{sediment volume} = 0.1665 * \text{runoff volume}^{1.1651} \quad \text{Equation D-3}$$

### D-2.1 Screening Surface and Storm Water to Surface Water Quality Criteria

Base flow and storm water collected and analyzed in 2018 at gaging stations E121, E122, and E123 were screened against the appropriate surface water quality criteria (SWQC) in 20.6.4.900 New Mexico Administrative Code. Chronic aquatic life criteria for hardness-dependent metals (i.e., aluminum, cadmium, copper, lead, and zinc) were calculated using concurrent hardness values for samples collected for storm water and average hardness values for base flow.

Sample results that exceed SWQC are presented in Table D-2.1-1. Base flow exceedances were observed for total PCBs and copper. Exceedances in storm water were observed for aluminum, cadmium, copper, gross alpha, lead, selenium, total PCBs, and zinc.

The Sandia wetland receives urban runoff water from developed areas within Technical Area 03 (TA-03) at the Laboratory, which affects water-quality results from E121 and E122. Developed areas in and around the Laboratory are documented sources of contaminants exceeding SWQC, including aluminum, copper, lead, zinc, and PCBs, as determined by storm water runoff monitoring (LANL 2012, 219767; LANL 2013, 239557). Therefore, exceedances of SWQC for these constituents at E121 and E122 are likely partially derived from these developed areas within TA-03. Additionally, E121 and E122 may be influenced by historical releases from solid waste management units (SWMUs) upgradient of these monitoring locations.

Gaging station E123 is located at the lower terminus of the Sandia wetland. Base flow water at E123 is composed of outfall discharges upstream of E121 and E122 and any exchange between the alluvial aquifer, sediments, and surface water flowing through the Sandia wetland. Storm flow at E123 is composed of outfall discharges upstream of E121 and E122 and storm water runoff from urban areas that drain the watersheds surrounding the Sandia wetland during precipitation events. Storm water flows through the Sandia wetland where the sediment-bound contaminant inventory may be entrained and contribute to the chemical signature of the water collected at E123. Comparing results from E121 and E122 with E123 is useful in evaluating exceedances to determine if the Sandia wetland may be a source of constituents exceeding SWQC. Table D-2.1-2 provides summary statistics for each analyte exceeding SWQC for all three gaging stations, E121, E122, and E123, in the respective media (base flow or storm water) in 2018.

Table D-2.1-2 shows that the maximum exceedance result for filtered aluminum at E123 is greater than E121, but less than E122, for storm water, but for a limited number of samples ( $n=2$ ) at that outfall. Aluminum is not a contaminant of concern associated with the Sandia wetland (LANL 2011, 203454), and is considered to be associated with the natural background geology. LANL studies of storm water runoff at background reference watersheds on the Pajarito Plateau have shown that aluminum frequently exceeds SWQC and is thought to be derived from weathered Bandelier Tuff. Bandelier Tuff is a major geologic unit that forms the mesas and canyons on the Pajarito Plateau. Bandelier Tuff geologic units range from 350 to 14,000 mg/kg of aluminum, much of which is readily leachable (Broxton et al. 1995, 050121; LANL 2013, 239557). Mineral-bound aluminum is associated with poorly crystalline volcanic silica glass of Bandelier Tuff and, as the tuff weathers, the glass particles and associated aluminum-rich sediments are

entrained and transported by storm water runoff. Aluminum exceedances observed at E123 are most likely derived from Bandelier Tuff that form the hillslopes and side drainages surrounding the Sandia wetland.

Historically, the highest values of filtered copper were most often observed in storm water runoff at E121 and E122. In 2018, the average of the SWQC exceedances of copper at E121, E122, and E123 were approximately equivalent, ranging from 5.96 µg/L at E122 to 6.28 µg/L at E123.

Copper, lead, and zinc concentrations in storm water at E123 are generally the same or less than at E121 and E122. The Sandia wetland has not proven to be a source of the copper, lead, and zinc, and generally the average SWQC exceedances observed at E123 are less than those observed at E121 and E122. Zinc, which exceeded SWQC at E121, did not exceed SWQC at E122 or E123.

PCBs, historically used in hundreds of industrial and commercial applications in developed environments in the United States, are a common constituent in storm water discharging from developed environments. However, the maximum concentrations of PCBs at E121 and E122 are less than E123 for base flow and storm water, indicating the Sandia wetland may be a source of PCBs. The Sandia wetland contains a known inventory of PCBs as a result of historic spills at SWMU 03-056(c), a former transformer storage area. SWMU 03-056(c) is located just upgradient of E121, and PCB sediments from the SWMU may still be influencing the concentrations of PCBs at E121. Figure D-2.0-7 shows box plots of PCBs concentrations in storm water at E121, E122, and E123 for 2018 and the previous 5 yr. The plots show PCB concentrations within the range of historical data since the GCS was installed at all three gaging stations.

Two samples exceeded SWQC for gross alpha at E122: one on July 17, 2018, and the other on September 4, 2018. The highest peak discharges for E122 occurred during these storm events. An additional gross alpha exceedance occurred at E123 on August 15, 2018. Bandelier Tuff contains uranium and thorium, and gross alpha radioactivity concentrations in storm water are most likely derived from these alpha emitters (LANL 2013, 239557).

### **D-3.0 ANALYTICAL RESULTS FROM ALLUVIAL SYSTEM**

Selected analytical results for water chemistry time-series data (filtered) from the alluvial sampling array are presented in Figures D-3.0-1 to D-3.0-8. Time-series plots are presented in the relative spatial distribution of the wells in the wetland (i.e., the upper plots are from the most northerly wells in each transect, ordered from west to east; the middle set of plots are from wells in the center of each transect, again ordered from west to east; and bottom plots are from the southernmost wells in each transect, in the same orientation). The alluvial sampling array is composed of four transects running north to south and spread out along the length of the wetland. Additionally, data for surface water entering the wetland at gaging station E121 and exiting the wetland at gaging station E123 are plotted at the western and easternmost parts of the wetland, respectively, serving as a comparison of input and output base flow chemistry. Differences between base flow data and alluvial groundwater data may indicate subsurface processes (e.g., reduction) and provide information about residence times in the alluvial system. Key analytes plotted include a major conservative anion (chloride); redox-sensitive species (sulfate, iron, manganese, ammonia as nitrogen, and sulfide); and key contaminants (dissolved arsenic and chromium) (Figures D-3.0-1 to D-3.0-8). Fe(II)-, As(III)-, and Cr(VI)-speciated data were collected and are plotted along with the total iron, arsenic, and chromium, respectively (Figures D-3.0-4, D-3.0-7, and D-3.0-8).



### D-3.1 Non-redox Sensitive Species

Species like chloride are not affected by the redox conditions of the wetland, providing information about changes in outfall chemistry and the connectivity between surface and alluvial groundwater. Chloride shows relatively constant concentrations at the wetland input and output surface water gaging stations. The chloride concentrations within the alluvial wells show some temporal variability with spikes in the February rounds, likely because of runoff from roads when salt is applied as a de-icing agent (Figure D-3.0-1). These spikes are most apparent in wells with more permeable sediment in the western most transect, SWA-2-4 and the wells of the eastern most transect, suggesting these locations are more strongly influenced by surface water infiltration.

### D-3.2 Redox Sensitive Species

Redox sensitive species provide information on the degree of reduction happening in the wetland sediments. Concentrations of arsenic, manganese, iron, sulfide, and ammonia as nitrogen tend to be higher in the alluvial system than in surface water, indicating reducing conditions in the alluvial system. Conversely, sulfate, an oxidized species of sulfur, tends to be lower in the wetland than in surface water, also suggesting more reducing conditions in the alluvial system. Within the surface water system, concentrations at E121 and E123 are similar for all redox sensitive species, other than Cr(VI) whose concentrations are lower at E123 (Figure D-3.0-8).

Most alluvial locations have lower sulfate concentrations than surface water input to the wetland, reflecting the strong reducing conditions in wetland sediments (Figure D-3.0-2). Locations with historically higher values of sulfate include: (1) SWA-1-2, which has coarse-grained and organic-poor sediment; (2) SWA-3-7 because of the shallow screening interval with the top of the screen at just 0.6 ft below ground surface (bgs) compared with most wells in the wetland, which are at least 3 ft bgs; and (3) SWA-4-10, SWA-4-11, and SWA-4-12, which were originally disturbed by the construction of the GCS. However, in the past few years, all locations, with exception of SWA-3-7, have observed a decrease and stabilization of sulfate concentrations, indicating increasingly reducing alluvial sediment conditions associated with the expansion of wetland vegetation and resaturation occurring at the head and terminus of the wetland. Locations SWA-2-5, SWA-2-6, and SWA-3-8 are particularly reducing based on lower sulfate concentrations relative to other locations. Location SWA-2-6 is in a very stagnant area based on observations of limited standing water with no apparent flow. Wells SWA-2-5 and SWA-3-8 are in or next to the central surface water flow path in the wetland but may be completed in tighter, more reducing sediments. The area of the easternmost transect was drier and more channelized before the GCS was constructed. Since the recovery from disturbance associated with the GCS, this transect has become more saturated and less channelized with the proliferation of vegetation, reflected in the observed decreases of sulfate, especially at SWA-4-10, indicating further stabilization of subsurface wetland conditions.

Sulfide, a reduced species of sulfur, has been detected throughout the wetland, further confirming the overall reducing nature of the system (Figure D-3.0-3). This is particularly clear when comparing sulfide concentrations in alluvial locations with those found in base flow where sulfide has not been detected. With sulfide near the bottom of the redox ladder, other species, including iron, arsenic, and chromium, are expected to be present primarily in their reduced forms, as observed in the speciated data (Figures D-3.0-4, D-3.0-7, and D-3.0-8). There was a slight increase in sulfide at SWA-4-11 and SWA-4-12 in 2017. This trend was still evident in the first two sampling quarters of 2018, but sulfide concentrations then decreased abruptly in the last two quarters. During this time, sulfide concentrations fell below the detection limit at almost all alluvial locations. The lowest values of sulfide are observed at SWA-2-5 and SWA-2-6; however, these locations seem to exemplify the most reducing conditions in the wetland through the other redox species. Sulfide may be precipitating because of the very reducing conditions such that dissolved sulfide is not present in the water samples.

Fe(II), the reduced form of iron, is the predominant form present in alluvial waters of the wetland, plotting on or just slightly below the total iron (Figure D-3.0-4). Total iron concentrations higher than Fe(II) are believed to be samples with colloidal Fe(III). The steady increase in iron concentrations that was observed at SWA-1-3, SWA-2-6, SWA-3-7, and SWA-3-9 appears to have begun to stabilize in 2018. A stabilization of iron concentrations is also observed in the easternmost downgradient transect over the last 2 yr. The historically higher values for total iron in the easternmost transect are believed to be of colloidal iron, which has decreased as a result of the recovery from disturbance caused by the installation of the GCS, as suggested by other constituents.

All the locations appear to be strongly reducing with respect to manganese at the depth of screen completion (Figure D-3.0-5). Locations SWA-1-2 and SWA-1-3 have somewhat lower manganese concentrations, consistent with their shallow completion depths in sands and gravels. Small increasing trends of manganese were observed at SWA-3-7, SWA-3-8, and SWA-3-9 in 2016 and 2017 but appear to be stabilizing in 2018 (Figure D-3.0-5). Most of the manganese is believed to be in its reduced form, with increases indicating increasing reducing conditions in alluvial sediment.

Ammonia as nitrogen concentrations are generally near or below the limit of detection in surface waters but are frequently detected in the alluvial system, confirming the high organic matter content and extended residence time of lentic waters (Figure D-3.0-6). Ammonia as nitrogen is stable under reducing and lower pH conditions in the wetland and is derived from mineralization of organic matter (e.g., dead cattail fronds). High concentrations of ammonia as nitrogen are not necessarily expected in the subsurface because of potential nutritive uptake by microbes and wetland plants; however, temporally, the decay of plant matter in fall coincides with diminished primary productivity that would put demand on available mineral nitrogen.

Arsenic can exist as As(III) or As(V). As(III) is relatively mobile and should predominate under reducing conditions. Within the range of analytical error, most of the total arsenic detected in analytical results from alluvial wells was As(III) in 2016 (when speciated data started being analyzed), confirming the reducing conditions of the wetland (Figure D-3.0-7). There was a decreasing trend in both arsenic and As(III) in 2016 that suggests a reduction in mobility of the arsenic species as the reducing environment continues to persist and new inputs of organic matter that potentially bind arsenic accumulate (Wang and Mulligan 2006, 602277). However, in 2017, total arsenic increased while As(III) either decreased or stabilized, widening the disparity between the two. While the absolute variability in arsenic concentrations is small when comparing 2017 data with earlier data, these changes may reflect a change in analytical laboratories with a higher method detection limit (MDL) for arsenic. The As(III) analyzed off-site at a different laboratory than that for total arsenic seems to follow the temporal decreasing trend in 2017. As(III) was only analyzed in the first two quarters of 2018. These data show that As(III) concentrations have remained relatively stable from the previous year and continue to be lower than total arsenic. However, the discrepancy between total arsenic and As(III) is likely to be an analytical artifact as arsenic is higher on the redox ladder than sulfide, which was observed in its reduced form in the wetland proper.

Dissolved chromium concentrations in the wetland alluvial system are quite high (the New Mexico Environment Department [NMED] groundwater standard for exceedance of chromium is 50 ppb [section D-3.4]). There is significant spatial variation in chromium distribution, but this predominantly reflects colloidal Cr(III) (Figure D-3.0-8). Given the varied environmental fate and transport of the different forms of chromium, including those in organo-metal moieties, it is difficult to make meaningful spatial comparisons of total chromium. However, locations SWA-1-2, SWA-1-3, SWA-4-10, and SWA-4-11 have higher concentrations on average, with the latter two perhaps resulting from disturbance associated with GCS construction in the easternmost transect. The reason for higher colloidal Cr(III) in the westernmost transect is not clear.

The concentrations of dissolved Cr(VI) measured in the alluvial system over the past 2 yr were nearly all at the detection limit (0.152 µg/L since May 2017) or were nondetects (Figure D-3.0-8). Before 2017, samples analyzed for Cr(VI) were not filtered, with the exception of a few unfiltered test samples in 2013. Because reporting is to the dissolved Cr(VI) standards criteria, only the filtered data are shown. The consistently low or nondetected Cr(VI) concentrations reflect the strong reducing conditions in the wetland. The highest detections of Cr(VI) concentration were at E121 and E122 with concentrations up to 11.5 µg/L in May 2015 at E122. These higher concentrations of Cr(VI) entering the wetland are believed to be from potable water derived from the regional aquifer and concentrated in the cooling towers (section D-2.0). Chromium concentrations in the alluvial system are always significantly less than values at E121 and E122, suggesting that surface water infiltration is the source of the detects in the alluvial groundwater. E123, at the terminus of the wetland, has Cr(VI) below or just at the detection limit, indicating the chromium exchange capacity and other abiotic immobilizing reductions in Cr(VI) as it moves through the wetland.

### D-3.3 Screening Alluvial Groundwater Results to Groundwater Standards

The alluvial system data from 2018 were screened to the levels required in the 2016 Compliance Order on Consent (Consent Order). Alluvial data were evaluated using the following screening process:

- Groundwater data are screened in accordance to Section IX of the Consent Order. For an individual substance, the lower of the New Mexico Water Quality Control Commission (NMWQCC) groundwater standard or U.S. Environmental Protection Agency (EPA) maximum contaminant level (MCL) is used as the screening value.
- If a NMWQCC groundwater standard or an MCL has not been established for a specific substance for which toxicological information is published, the NMED screening level for tap water is used as the groundwater screening value, using the July 2015 NMED screening levels for tap water. The NMED screening levels are for either a cancer- or noncancer-risk type. For the cancer-risk type, the screening levels are based on a  $10^{-5}$  excess cancer risk.
- If an NMED screening level for tap water has not been established for a specific substance for which toxicological information is published, the EPA regional screening level for tap water is used as the groundwater screening value, using the May 2016 EPA regional screening levels for tap water. The EPA screening levels are for either a cancer- or noncancer-risk type. For the cancer-risk type, the Consent Order specifies screening at a  $10^{-5}$  excess cancer risk. The EPA screening levels for tap water are for  $10^{-6}$  excess cancer risk, so 10 times the EPA  $10^{-6}$  screening levels is used in the screening process.

The screening standard exceedances for the alluvial system, including the screening value and screening value type, are presented in Table D-3.3-1.

During the 2018 monitoring period, all locations sampled had iron exceedances greater than the screening value of 1000 µg/L. There were also manganese exceedances greater than the screening value of 200 µg/L at all locations except SWA-1-2. These exceedances are expected because the wetland is a reducing environment, and speciated Fe(II) data indicate that most, if not all, the iron in the alluvial system within the wetland is in its reduced form (section D-3.3). Manganese has reasonably similar redox behavior as iron and is expected to be mostly in its reduced state in the alluvial aquifer.

Arsenic exceedances (>10 µg/L) were observed at two locations (SWA-2-5 and SWA-2-6) during the 2018 monitoring period. Speciated arsenic data indicate that most the aqueous arsenic in the alluvial system is As(III), the reduced and mobile form. The alluvial aquifer is strongly reducing as indicated by the presence of sulfide and absence of oxygen. Once exposed to oxygen, As (III) quickly converts to



As(V) and precipitates as or sorbs onto a solid mineral phase. As(III) was detected at all wells during each monitoring event, but always at levels less than total arsenic. This higher concentration of total arsenic is believed to be an artifact of the analysis; because of the very reducing conditions (presence of sulfide), all total arsenic is believed to be As(III) (see section D-3.2).

As discussed in section D-3.2, most of the total chromium in the alluvial aquifer is colloidal Cr(III), the nontoxic form with very low solubility. Exceedances of chromium occurred in wells SWA-1-2 and SWA-4-10 during the 2018 monitoring period. Cr(VI) was detected during this time but was never greater than the concentrations coming into the wetland from E121 and E122; concentrations that are believed to be from potable water derived from the regional aquifer and concentrated in the cooling towers (section D-2.0).

#### **D-4.0 WATER-LEVEL RESULTS FROM ALLUVIAL SYSTEM**

Water-level data was continuously recorded at the 12 Sandia wetland alluvial wells for calendar year 2018. Water-level data are presented in Figure D-4.0-1 as a continuous record from 2017 through 2018. The plots are arranged within the figures to represent the spatial distribution of the alluvial locations in the wetland with the upgradient wells at the top of the figure. Daily flows at gaging station E121 and precipitation data from the weather station at E121.9 are plotted along with the alluvial water-level data. Gage station E121 represents the incoming flow to the wetland.

The water level results for 2018 were consistent with those of previous years. All transects showed attenuated water level change because of reduced annual discharge and precipitation events in 2018. Temperatures were consistent, showing temporal changes with seasons and with less variation in wells located in the channel (SWA-2-5) and wells at a depth greater than 10 ft (SWA-1-1) (Figure D-4.0-2).

- *SWA-1-1, SWA-1-2, and SWA-1-3:* The 2018 water level data showed continued rapid responses to changes in surface water discharge as noted in previous years for this transect (top plot in Figure D-4.0-1). Water levels responded almost immediately to precipitation events (tenths of a foot to 1.5 ft, depending on the size of the event). In addition, water levels responded quickly, but to a much lesser extent, to changes in base flow (driven by effluent releases at Outfalls 001 and 03A027), confirming the aquifer material in this narrow transect is relatively transmissive and storage is minimal.
- *SWA-2-4, SWA-2-5, and SWA-2-6:* In 2018, water levels at the second transect (second plot from top in Figure D-4.0-1) also responded almost immediately to precipitation and showed much lower responses to variations in flow at gage E121. The variations are generally only a few tenths of a foot and are short-lived. The stability of water levels in this transect reflects the saturated conditions that occur in this part of the wetland. Surface flow spreads across a broad area in this well-vegetated transect. Temperatures begin to fluctuate diurnally during the winter months and may be a result of the lack of evapotranspiration from dominant vegetation. Diurnal fluctuations in the groundwater along this transect possibly indicate a connection to flowing surface waters.
- *SWA-3-7, SWA-3-8, and SWA-3-9:* In 2018, water levels at the third transect (third plot from top in Figure D-4.0-1) showed similar responses to those observed in the past. Water levels show rapid responses to both precipitation events and to outfall-driven changes in base flow. The near-instantaneous response to precipitation events and variations in base flow imply a strong connection to flowing surface waters. Water levels drop during the summer months after the monsoon season has ended and may be a result of increased evapotranspiration from vegetation along this transect. The water level increased at SWA-3-9 mid-March (and SWA-4-12) and is possibly attributed to melting of frozen surface water that accumulated during the winter. Surface flow at the northern edge of the wetland in this area was slow and ice accumulation was observed

at this location. Temperatures begin to follow a diurnal trend in the winter months once vegetation becomes dormant and evapotranspiration decreases along this transect.

- *SWA-4-10, SWA-4-11, and SWA-4-12:* In 2018, water levels in the fourth transect (bottom plot in Figure D-4.0-1) responded quickly to both precipitation events and to variations in outfall flows (as measured by gage E121). Again, drops in water level have been observed in this transect during the summers. It appears the drop in water levels occur after the monsoon season has ended and may result from increased evapotranspiration from vegetation. Water levels at SWA-4-12 show a steady increase during February and March, which may be a result of continuous melting of frozen surface water.

## D-5.0 REFERENCES

*The following reference list includes documents cited in this report. Parenthetical information following each reference provides the author(s), publication date, and ERID, ESHID, or EMID. This information is also included in text citations. ERIDs were assigned by the Laboratory's Associate Directorate for Environmental Management (IDs through 599999); ESHIDs were assigned by the Laboratory's Associate Directorate for Environment, Safety, and Health (IDs 600000 through 699999); and EMIDs are assigned by Newport News Nuclear BWXT-Los Alamos, LLC (N3B) (IDs 700000 and above). IDs are used to locate documents in N3B's Records Management System and in the Master Reference Set. The NMED Hazardous Waste Bureau and N3B maintain copies of the Master Reference Set. The set ensures that NMED has the references to review documents. The set is updated when new references are cited in documents.*

Broxton, D.E., G.H. Heiken, S.J. Chipera, and F.M. Byers, Jr., June 1995. "Stratigraphy, Petrography, and Mineralogy of Bandelier Tuff and Cerro Toledo Deposits," in *Earth Science Investigation for Environmental Restoration—Los Alamos National Laboratory, Technical Area 21*, Los Alamos National Laboratory report LA-12934-MS, Los Alamos, New Mexico, pp. 33-63. (Broxton et al. 1995, 050121)

LANL (Los Alamos National Laboratory), May 2007. "Groundwater Background Investigation Report, Revision 3," Los Alamos National Laboratory document LA-UR-07-2853, Los Alamos, New Mexico. (LANL 2007, 095817)

LANL (Los Alamos National Laboratory), May 2011. "Interim Measures Work Plan for Stabilization of the Sandia Canyon Wetland," Los Alamos National Laboratory document LA-UR-11-2186, Los Alamos, New Mexico. (LANL 2011, 203454)

LANL (Los Alamos National Laboratory), May 2012. "Polychlorinated Biphenyls in Precipitation and Stormwater within the Upper Rio Grande Watershed," Los Alamos National Laboratory document LA-UR-12-1081, Los Alamos, New Mexico. (LANL 2012, 219767)

LANL (Los Alamos National Laboratory), April 2013. "Background Metals Concentrations and Radioactivity in Storm Water on the Pajarito Plateau, Northern New Mexico," Los Alamos National Laboratory document LA-UR-13-22841, Los Alamos, New Mexico. (LANL 2013, 239557)

LANL (Los Alamos National Laboratory), June 2014. "Sandia Wetland Performance Report, Baseline Conditions 2012–2014," Los Alamos National Laboratory document LA-UR-14-24271, Los Alamos, New Mexico. (LANL 2014, 257590)

Wang, S., and C.N. Mulligan, 2006. "Effect of Natural Organic Matter on Arsenic Release from Soils and Sediments into Groundwater," *Environmental Geochemistry and Health*, Vol. 28, pp. 197-214.  
(Wang and Mulligan 2006, 602277)



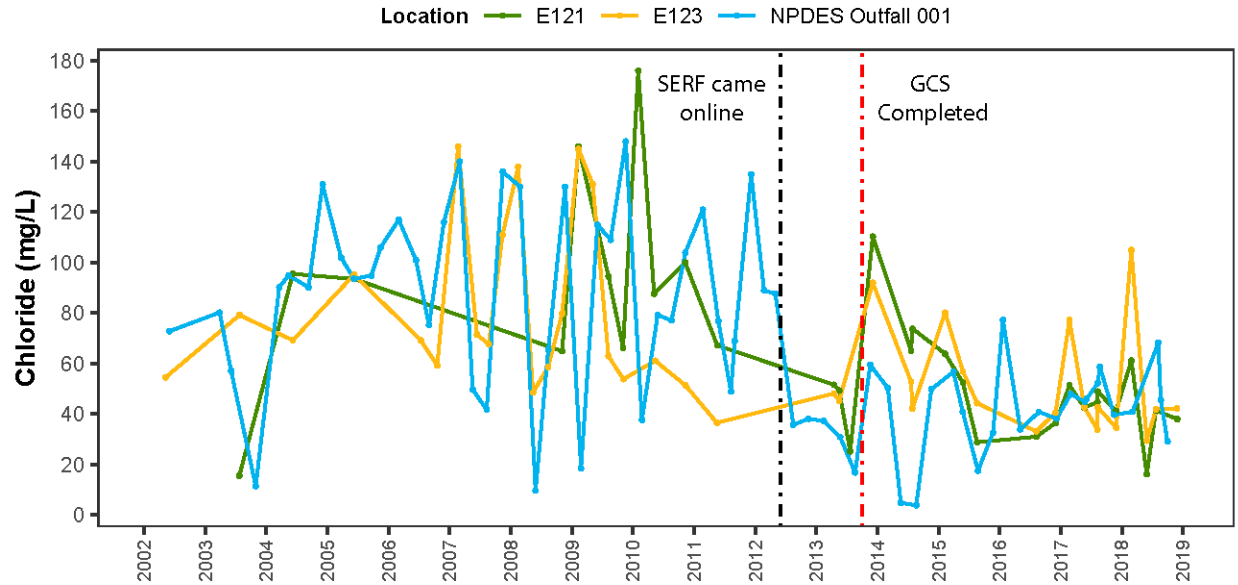


**Figure D-2.0-1 Time-series plot showing chloride concentrations at gaging stations E121 and E123 and National Pollutant Discharge Elimination System– (NPDES-) permitted Outfall 001**

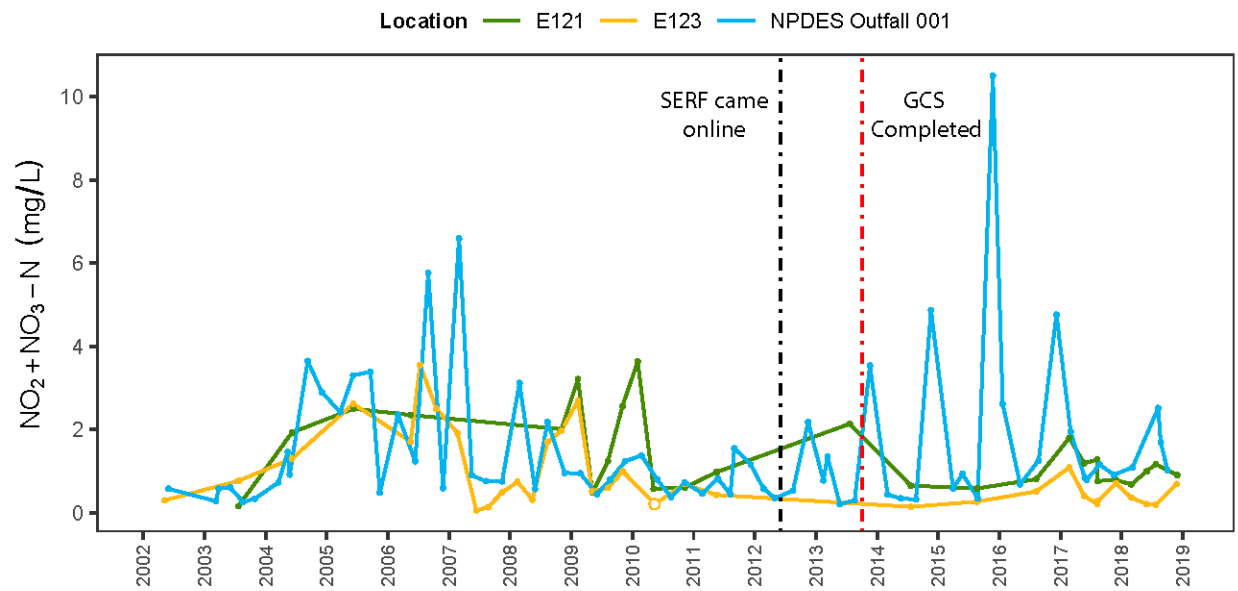


**Figure D-2.0-2 Time-series plot showing nitrate plus nitrite as nitrogen concentrations at gaging stations E121 and E123 and NPDES Outfall 001**

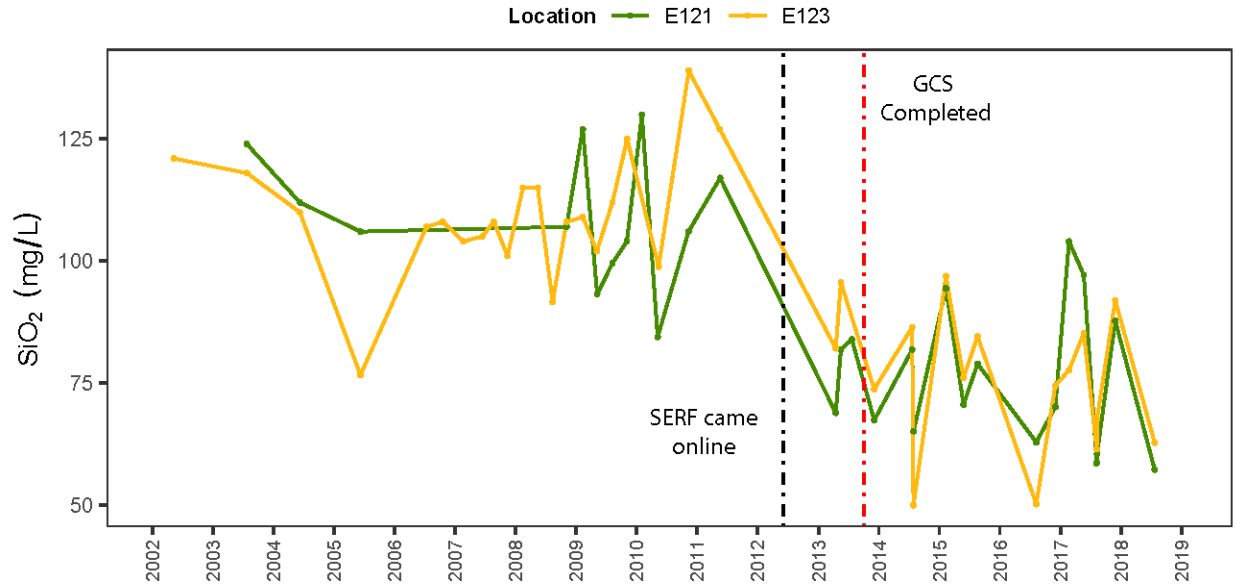


**Figure D-2.0-3** Time-series plot showing silicon dioxide concentrations at gaging stations E121 and E123

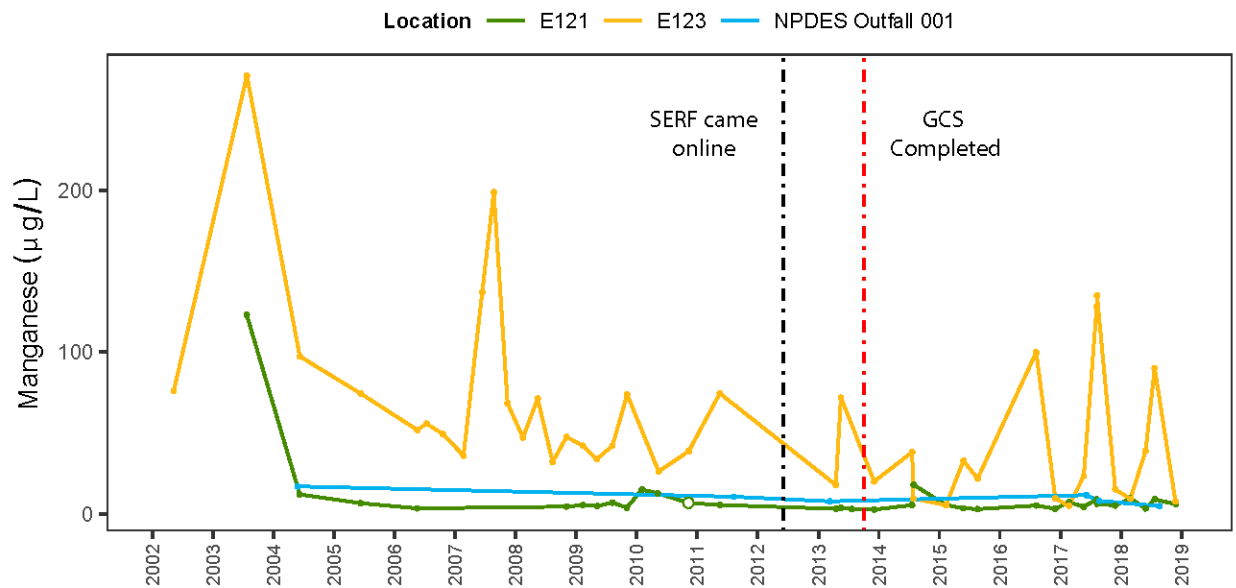
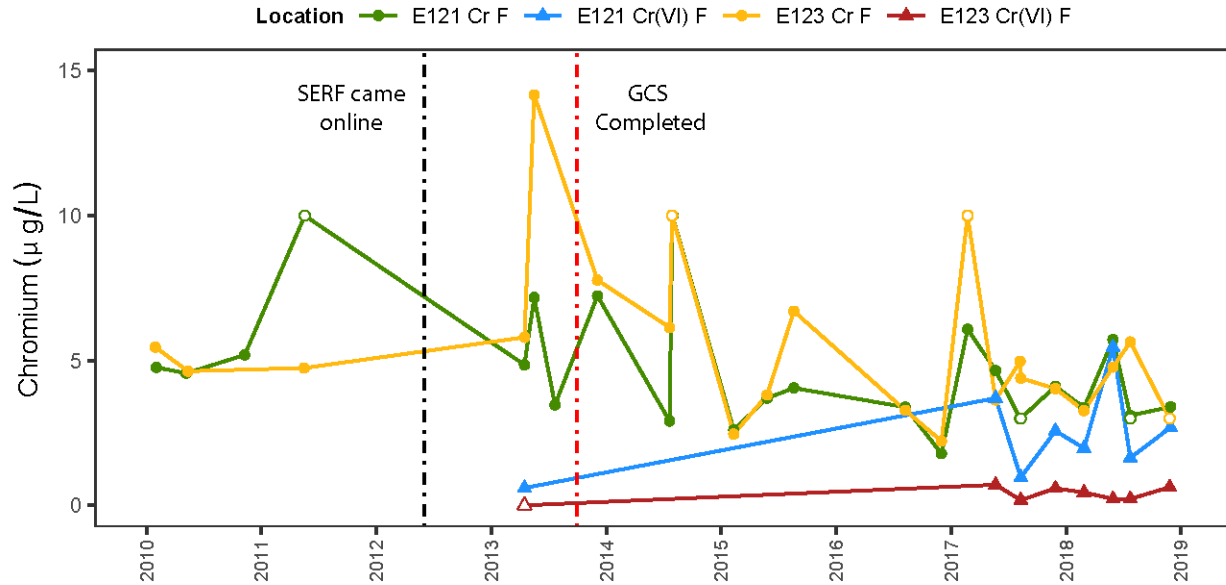


**Figure D-2.0-4** Time-series plot showing manganese concentrations at gaging stations E121 and E123 and NPDES Outfall 001



Notes: The small concentrations of Cr(VI) versus total chromium illustrate that most of the chromium within the wetland is colloidal Cr(III). Cr(VI) shows multiple detects in base flow into the wetland but is largely attenuated within the wetland with only a few detects near the detection limit at E123. MDL at gaging stations for Cr(VI) is 1  $\mu\text{g/L}$  through the February 2017 round; post the May 2017 round, the MDL at gaging stations for Cr(VI) is 0.152  $\mu\text{g/L}$ . All open symbols are nondetections.

**Figure D-2.0-5 Time-series plot showing total chromium and Cr(VI) concentrations at gaging stations E121 and E123**





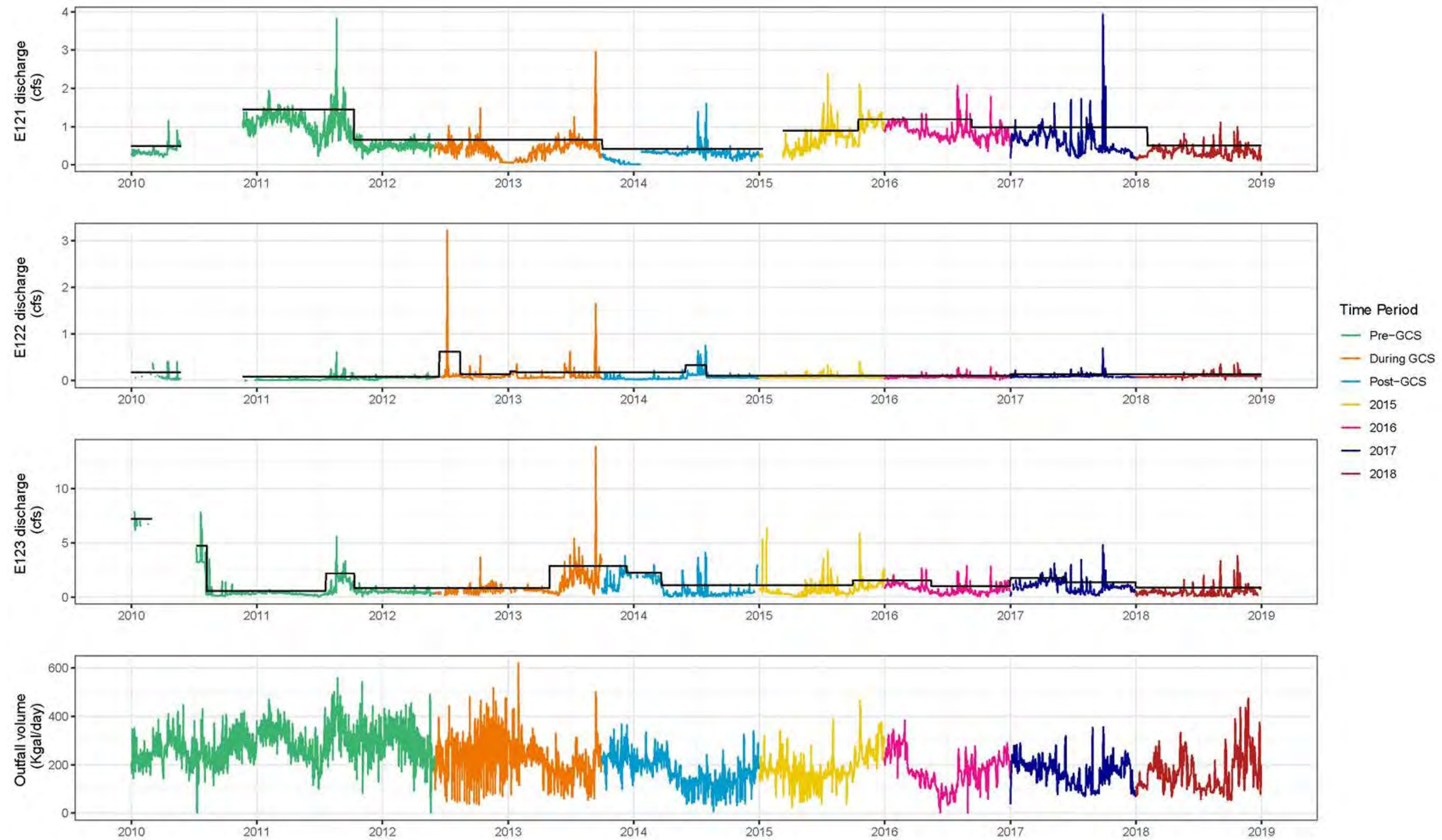


Figure D-2.0-6 Time-series plots from 2010 to 2018 showing discharge at E121, E122, and E123 and total discharge from Outfalls 001, 03A027, and 03A199. Black lines show approximate base flow, calculated as the mean daily discharge over the defined periods of stable base flow plus one standard deviation.



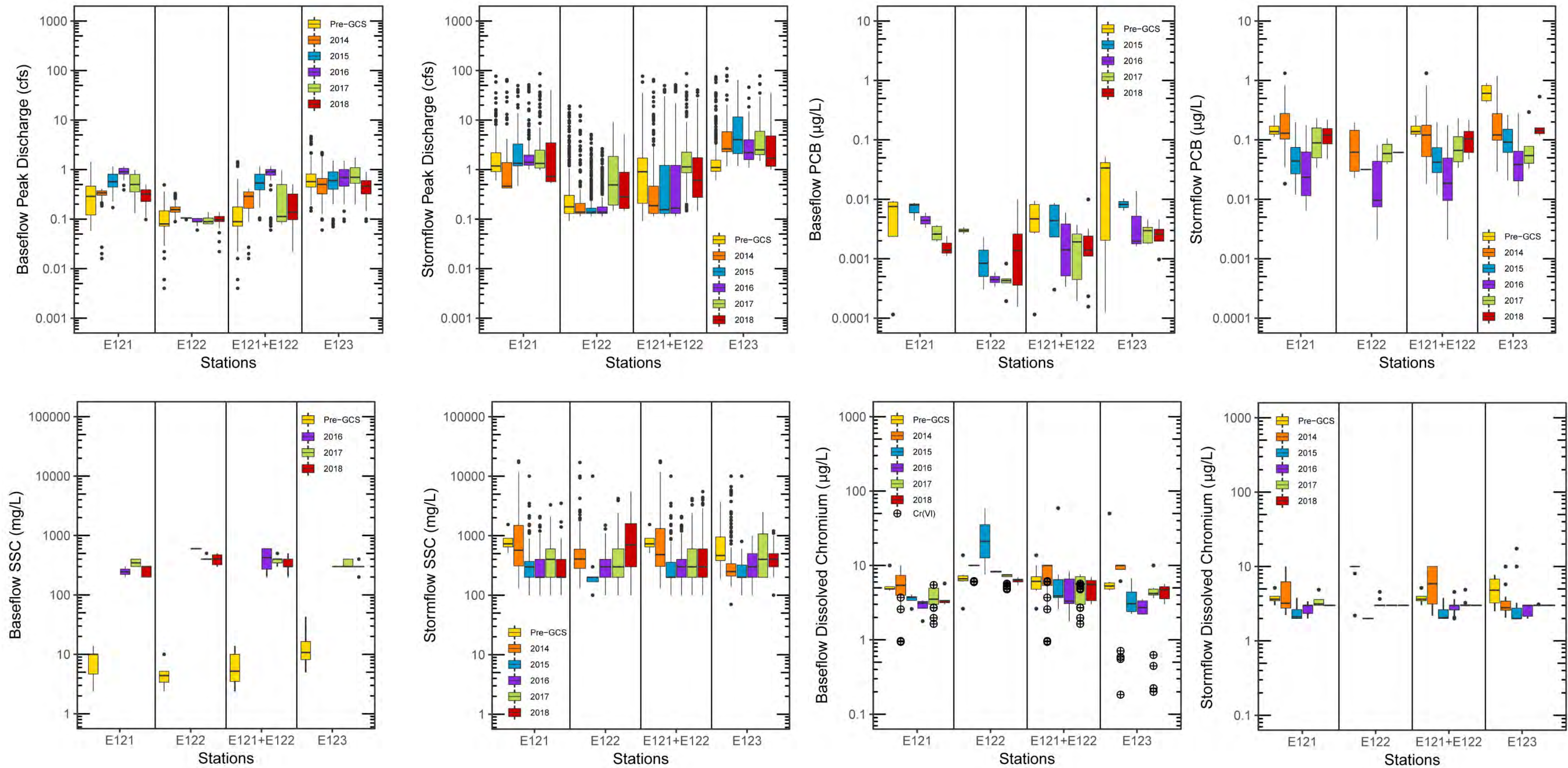
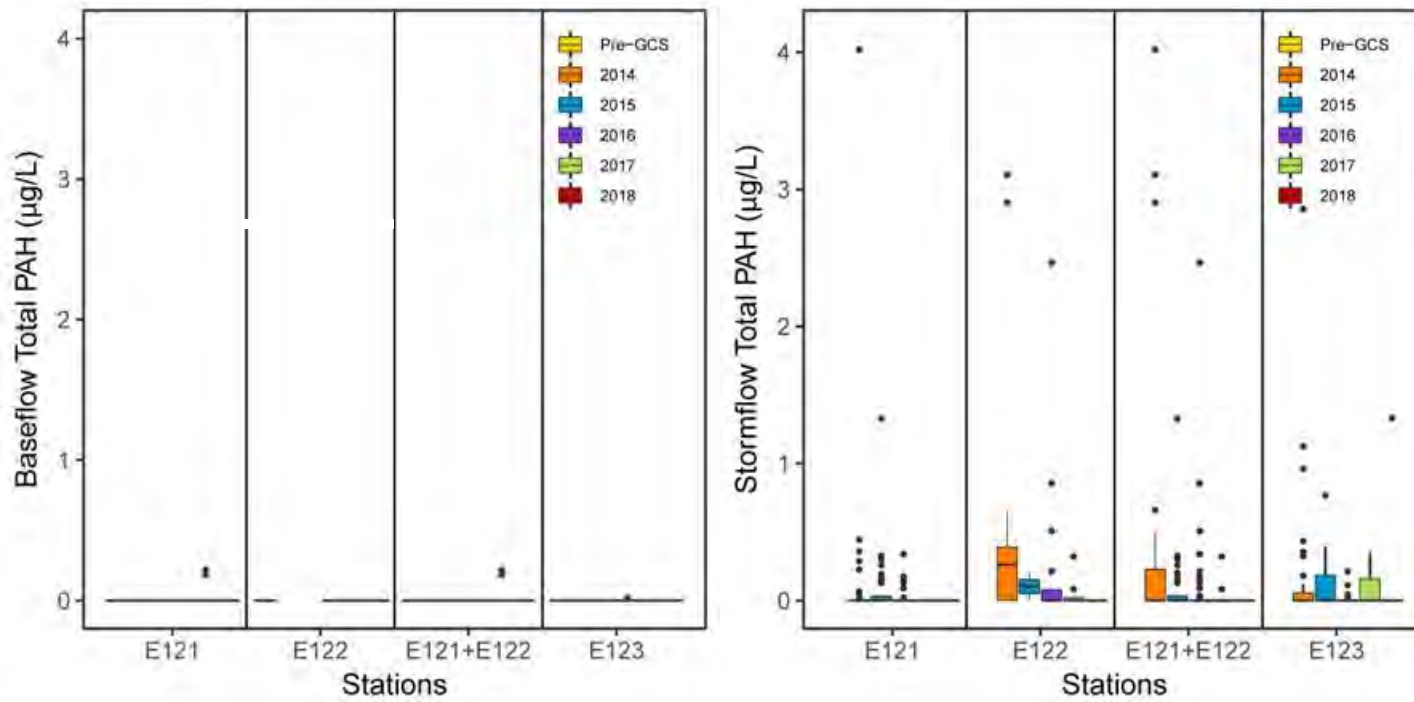


Figure D-2.0-7 Box-and-whisker plots of peak discharge, SSC, PCBs, filtered chromium and Cr(VI), and PAHs for base flow and storm flow at gaging stations E121, E122, and E123, pre- and post-construction (2014) of the GCS, respectively, in 2015, 2016, 2017, and 2018





**Figure D-2.0-7 (continued)** Box-and-whisker plots of peak discharge, SSC, PCBs, filtered chromium and Cr(VI), and PAHs for base flow and storm flow at gaging stations E121, E122, and E123, pre- and post-construction (2014) of the GCS, respectively, in 2015, 2016, 2017, and 2018

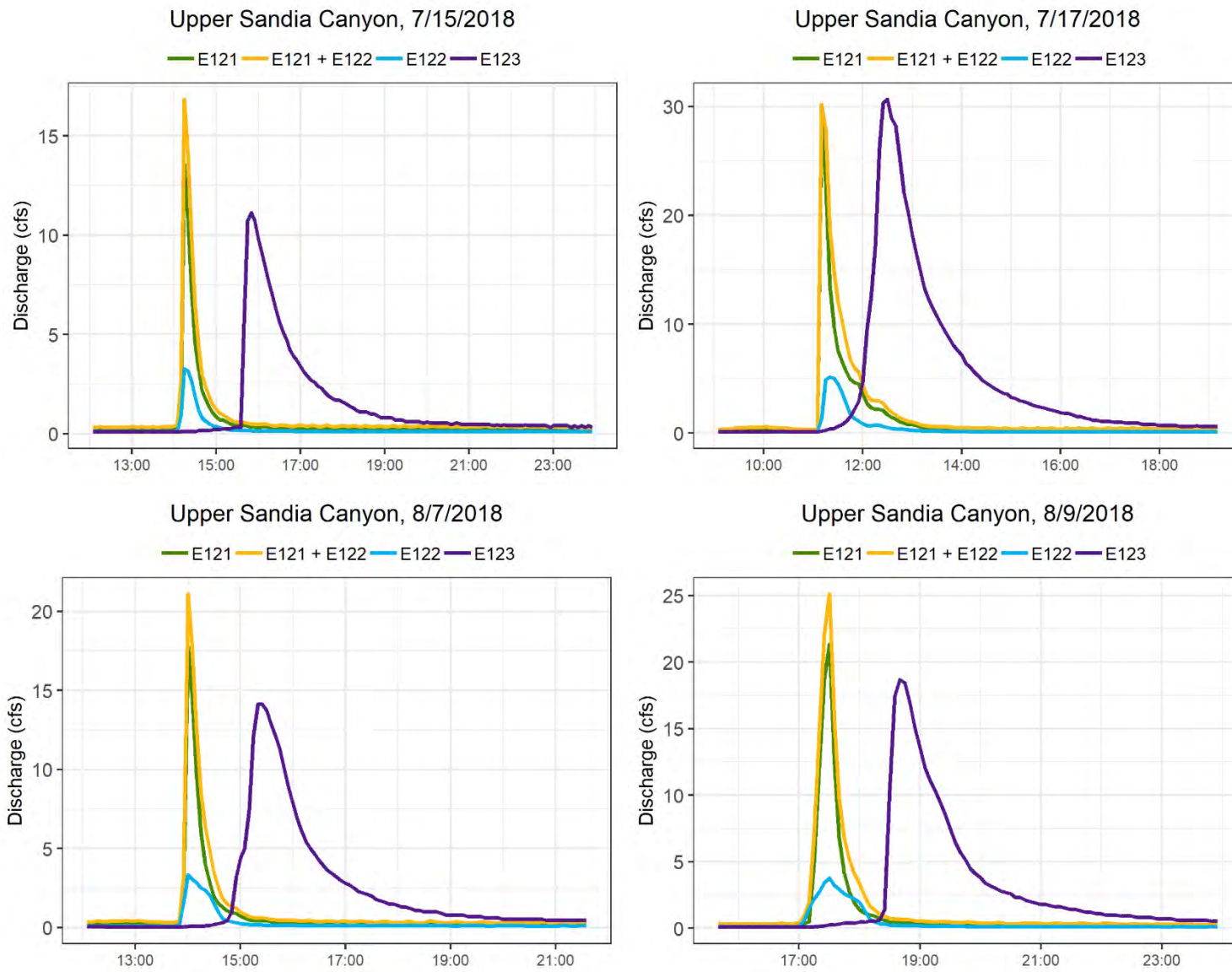


Figure D-2.0-8 Hydrographs of storm water discharge at E121, E122, and E123 during each sample-triggering storm event in 2018

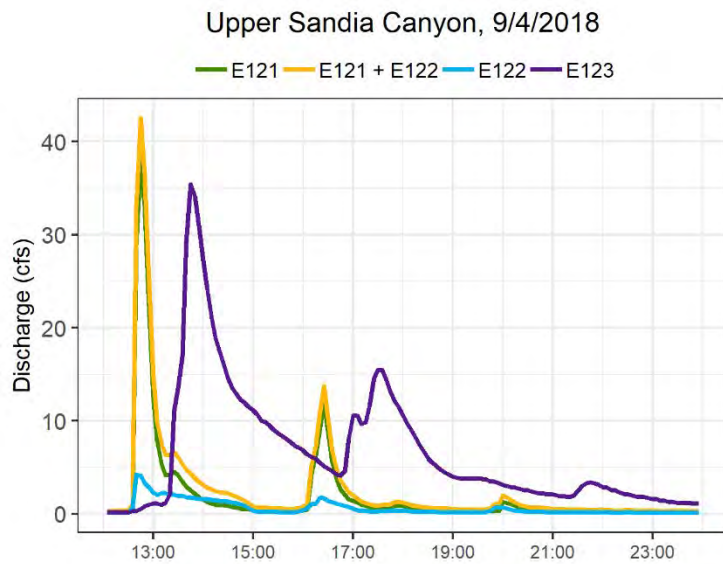
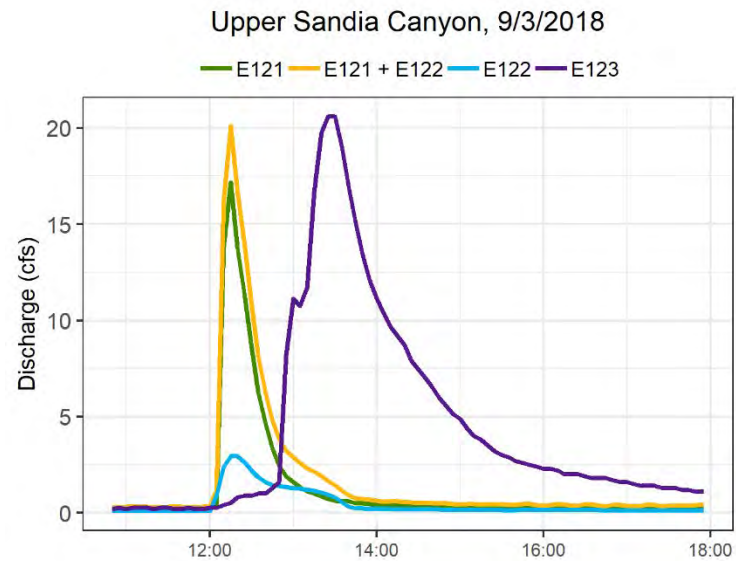
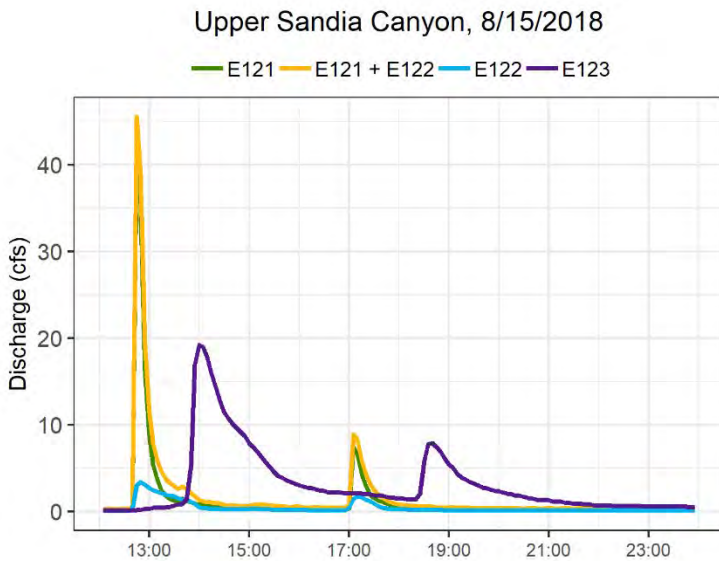
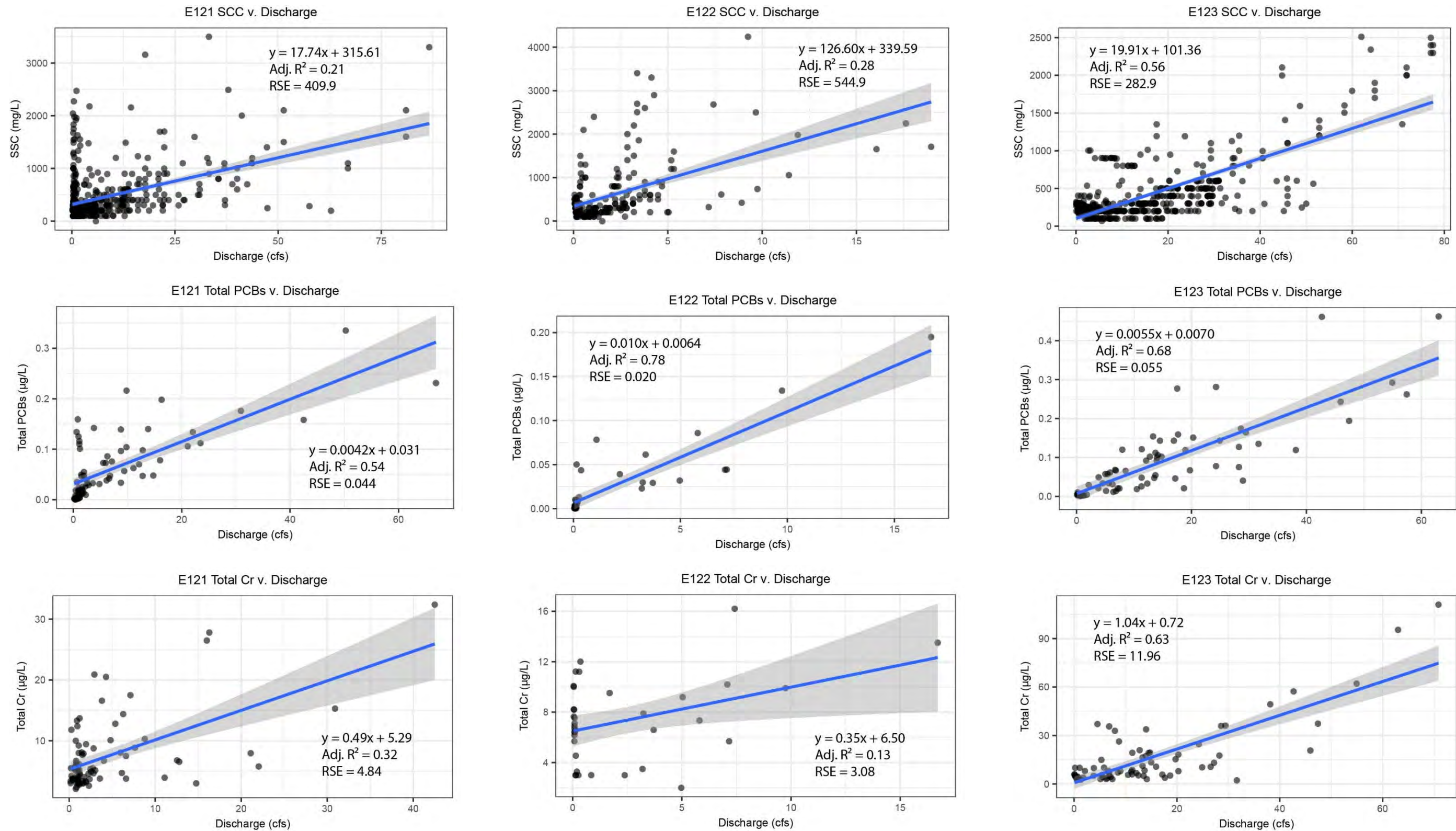


Figure D-2.0-8 (continued) Hydrographs of storm water discharge at E121, E122, and E123 during each sample-triggering storm event in 2018







**Figure D-2.0-9** Storm- and base-flow discharge correlations with SSC, total PCBs, total chromium, and total PAHs from 2014 to 2018 at E121, E122, and E123 with standardized residual outliers removed; the shaded areas represent 95% confidence intervals. The linear model equation, adjusted R², and residual standard error are provided on each plot.

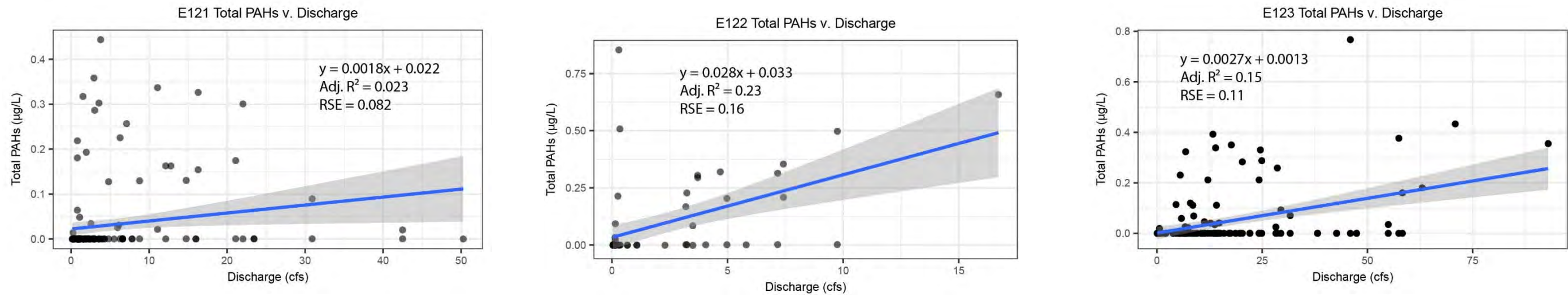
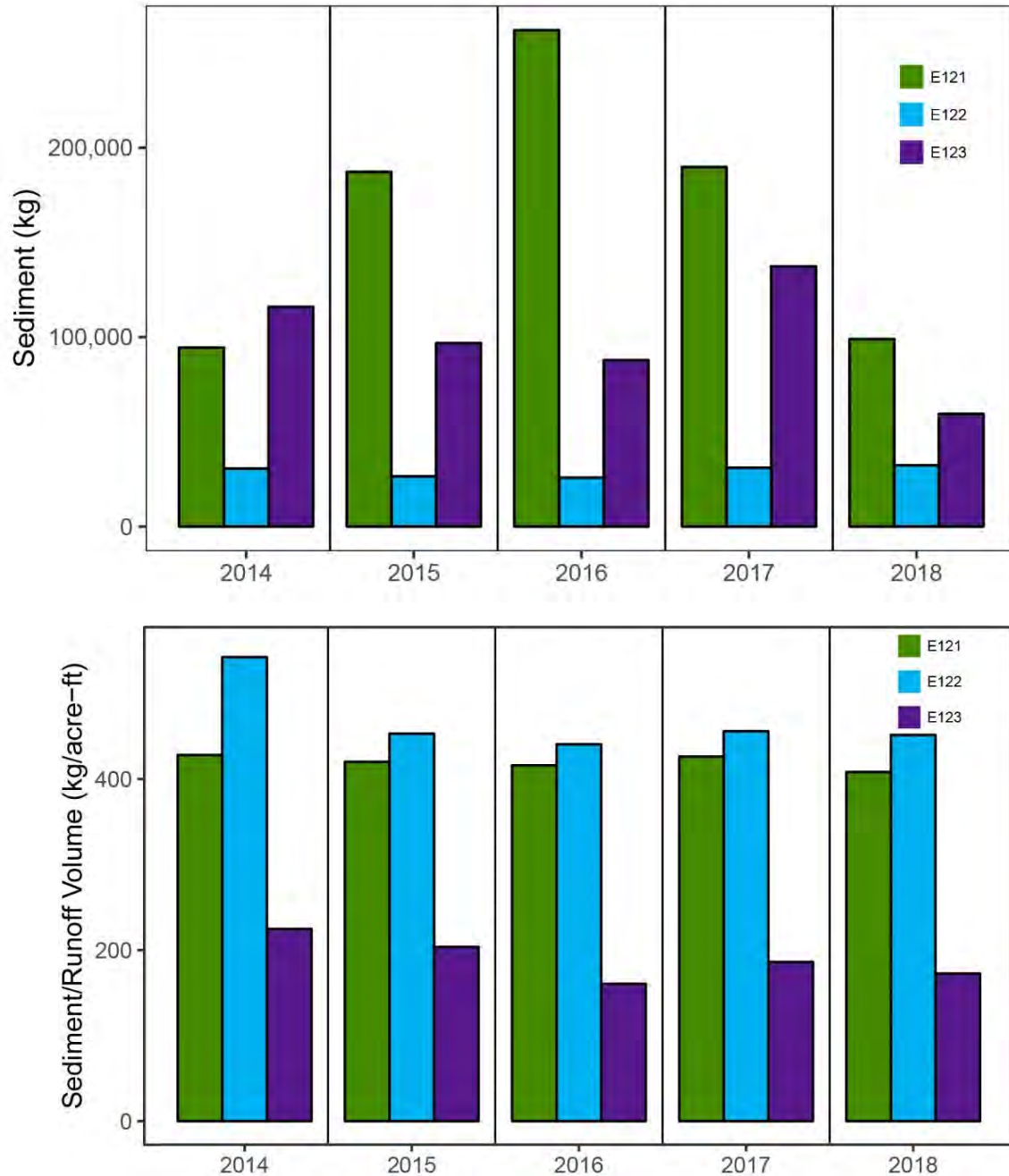
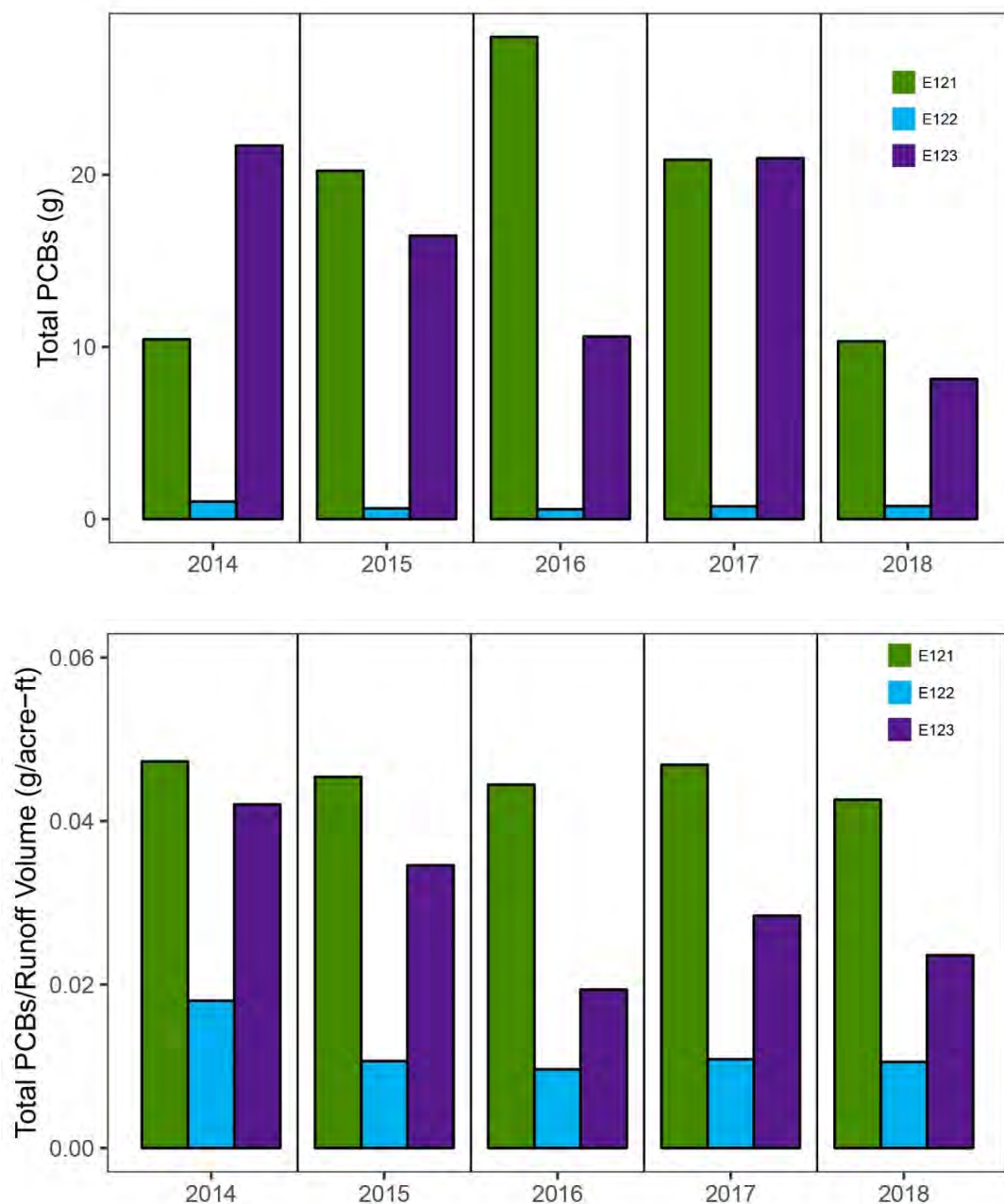


Figure D-2.0-9 (continued) Storm- and base-flow discharge correlations with SSC, total PCBs, total chromium, and total PAHs from 2014 to 2018 at E121, E122, and E123 with standardized residual outliers removed; shaded areas represent 95% confidence intervals. The linear model equation, adjusted R<sup>2</sup>, and residual standard error are provided on each plot.





**Figure D-2.0-10 Annual mass flux (top) and annual mass flux normalized by runoff volume (bottom) for sediment at gaging stations E121 (green), E122 (blue), and E123 (purple) from 2014 to 2018. Gaging stations E121 and E122 represent inputs into the wetland, and E123 represents output from the wetland.**



**Figure D-2.0-11** Annual mass flux (top) and annual mass flux normalized by runoff volume (bottom) for total PCBs at gaging stations E121 (green), E122 (blue), and E123 (purple) from 2014 to 2018. Gaging stations E121 and E122 represent inputs into the wetland, and E123 represents output from the wetland.

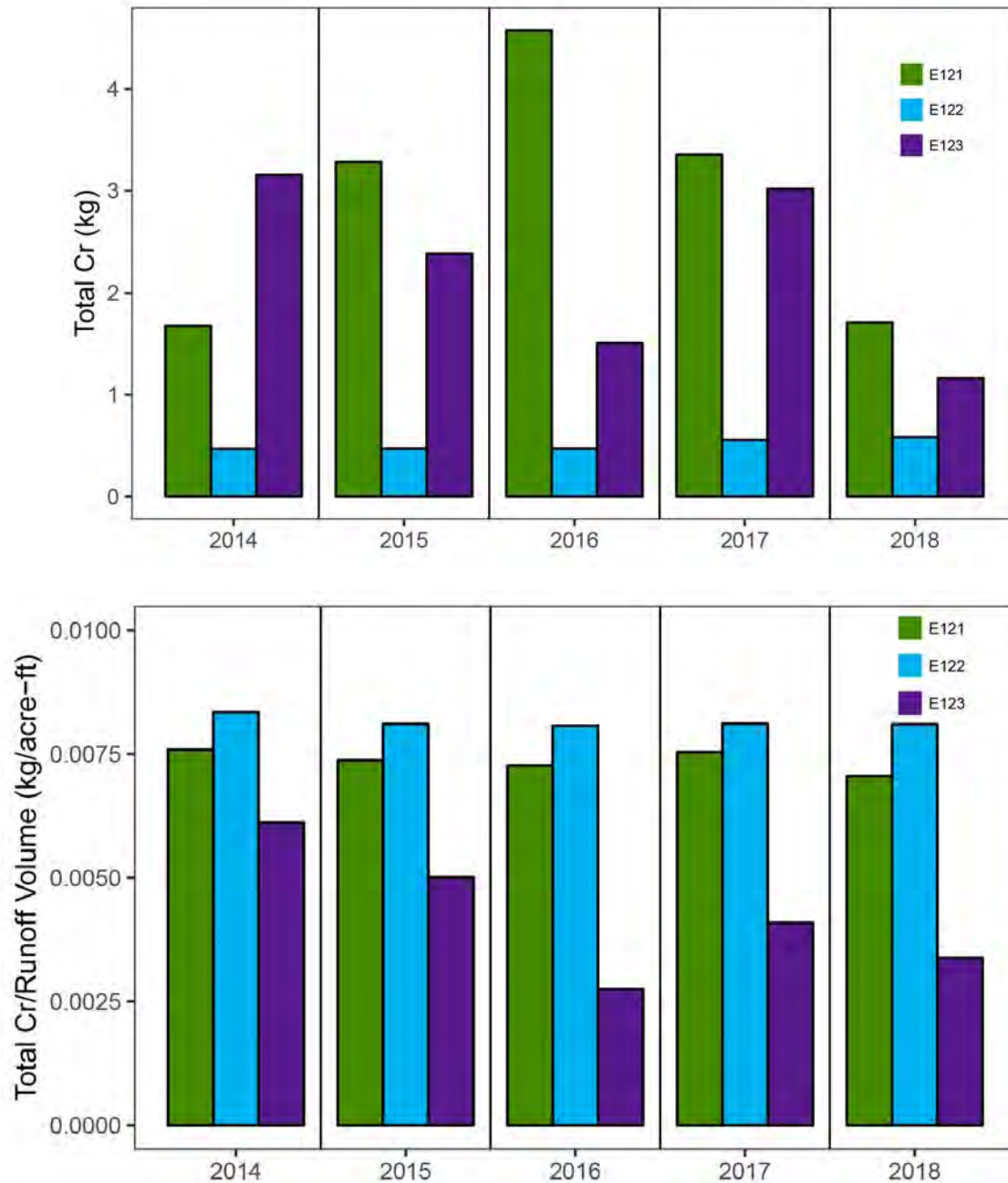


**Figure D-2.0-12** Annual mass flux (top) and annual mass flux normalized by runoff volume (bottom) for total chromium at gaging stations E121 (green), E122 (blue), and E123 (purple) from 2014 to 2018. Gaging stations E121 and E122 represent inputs into the wetland, and E123 represents output from the wetland.



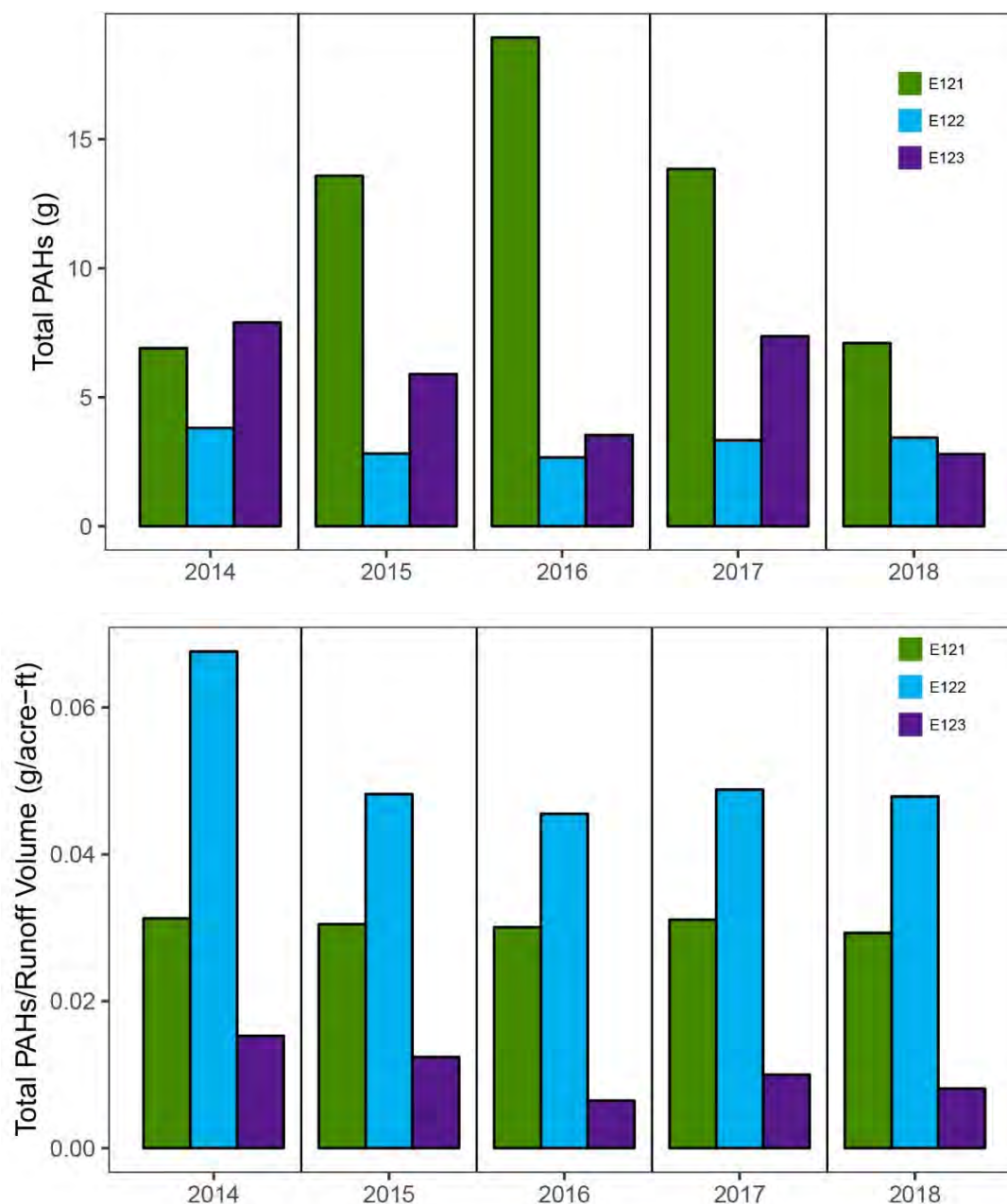
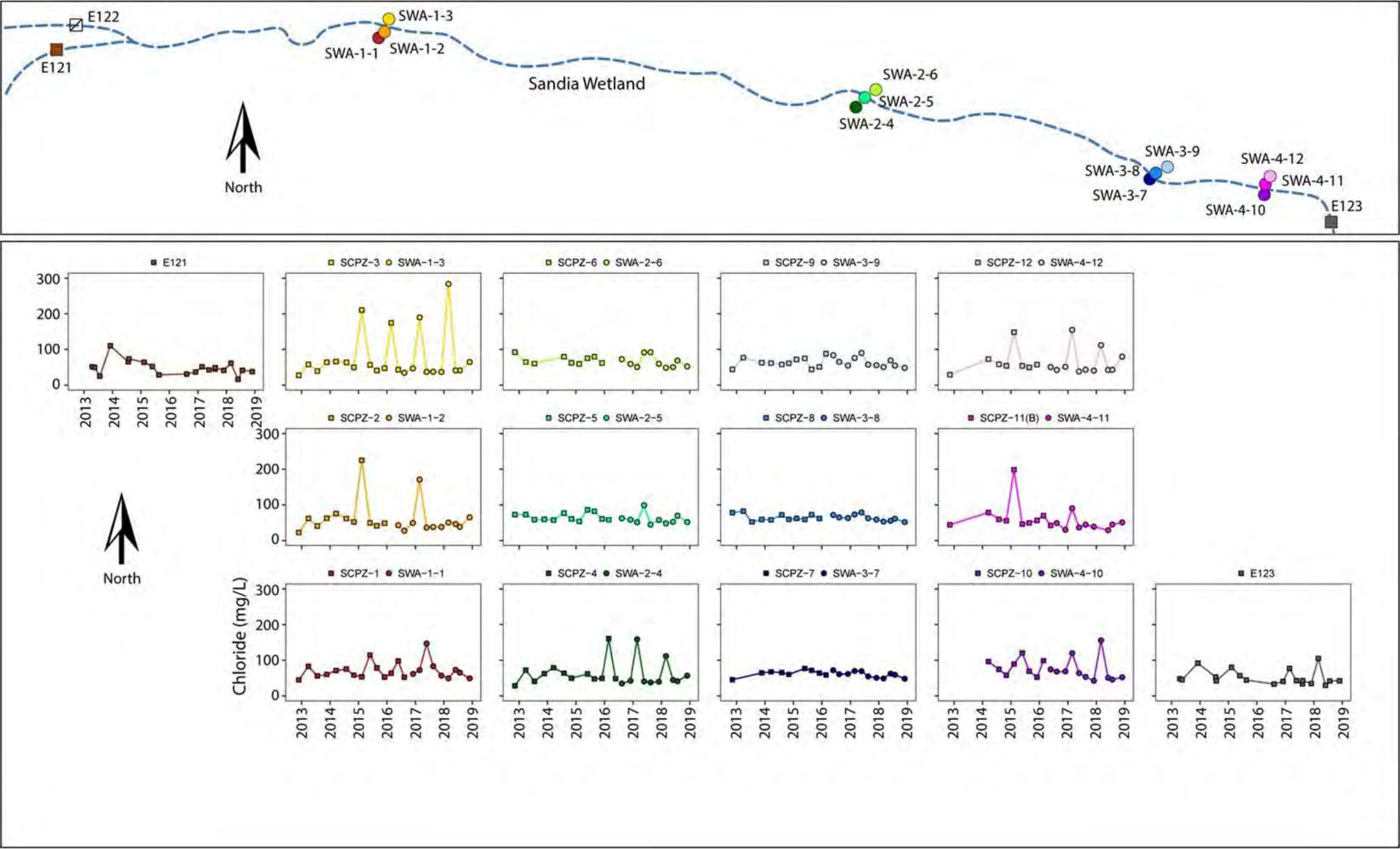
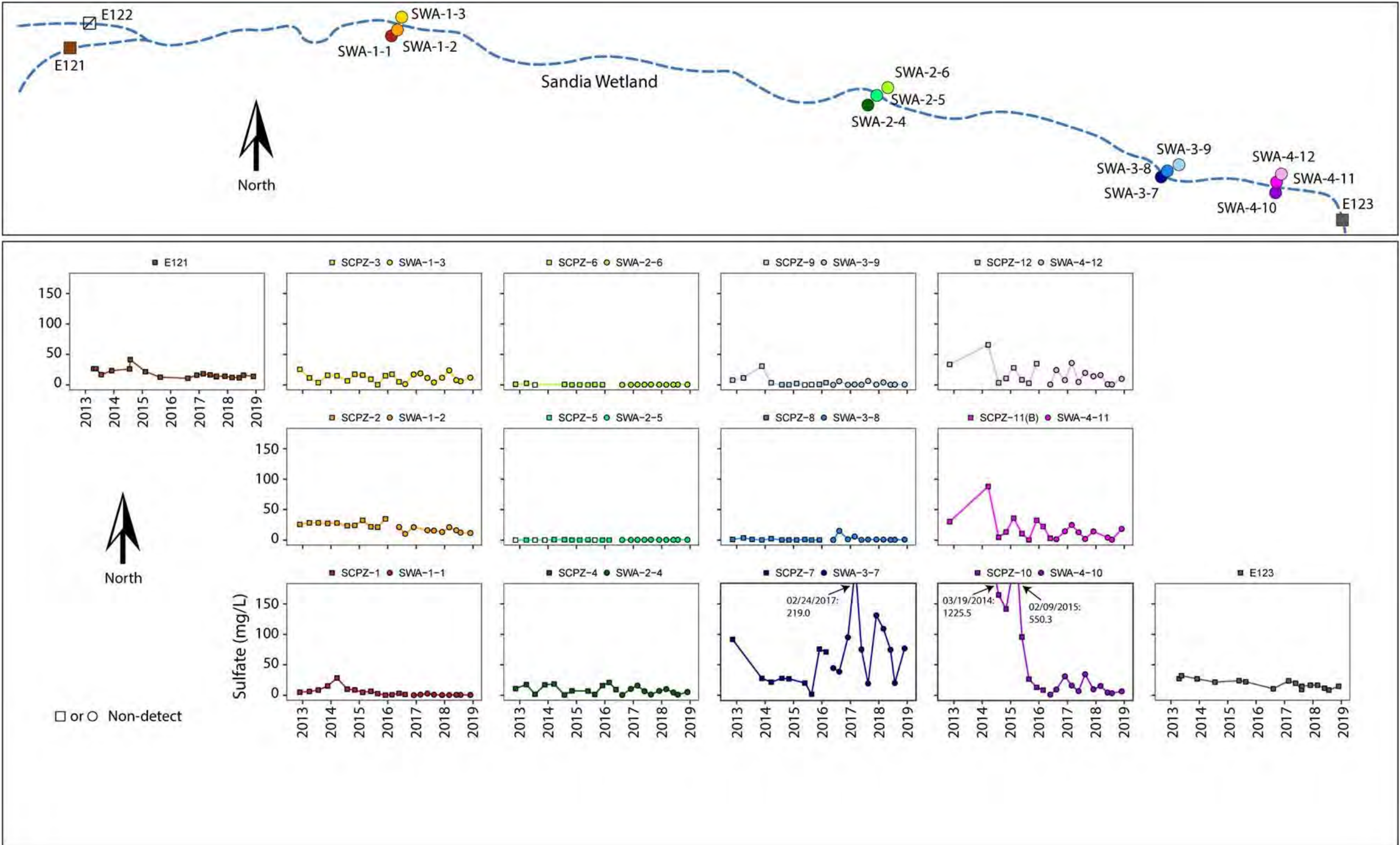


**Figure D-2.0-13** Annual mass flux (top) and annual mass flux normalized by runoff volume (bottom) for total PAHs at gaging stations E121 (green), E122 (blue), and E123 (purple) from 2014 to 2018. Gaging stations E121 and E122 represent inputs into the wetland, and E123 represents output from the wetland.



Notes: Surface water stations include E121, E122 (plot not shown), and E123. Piezometers are labeled with the prefix SCPZ (square symbols), and alluvial wells are labeled with the prefix SWA (circle symbols). The plots are arranged in four transects from west to east. Data are plotted for the full period of wetland monitoring. The map above is not to scale, but shows approximate sampling locations in relation to the approximate thalweg (blue dashed line).

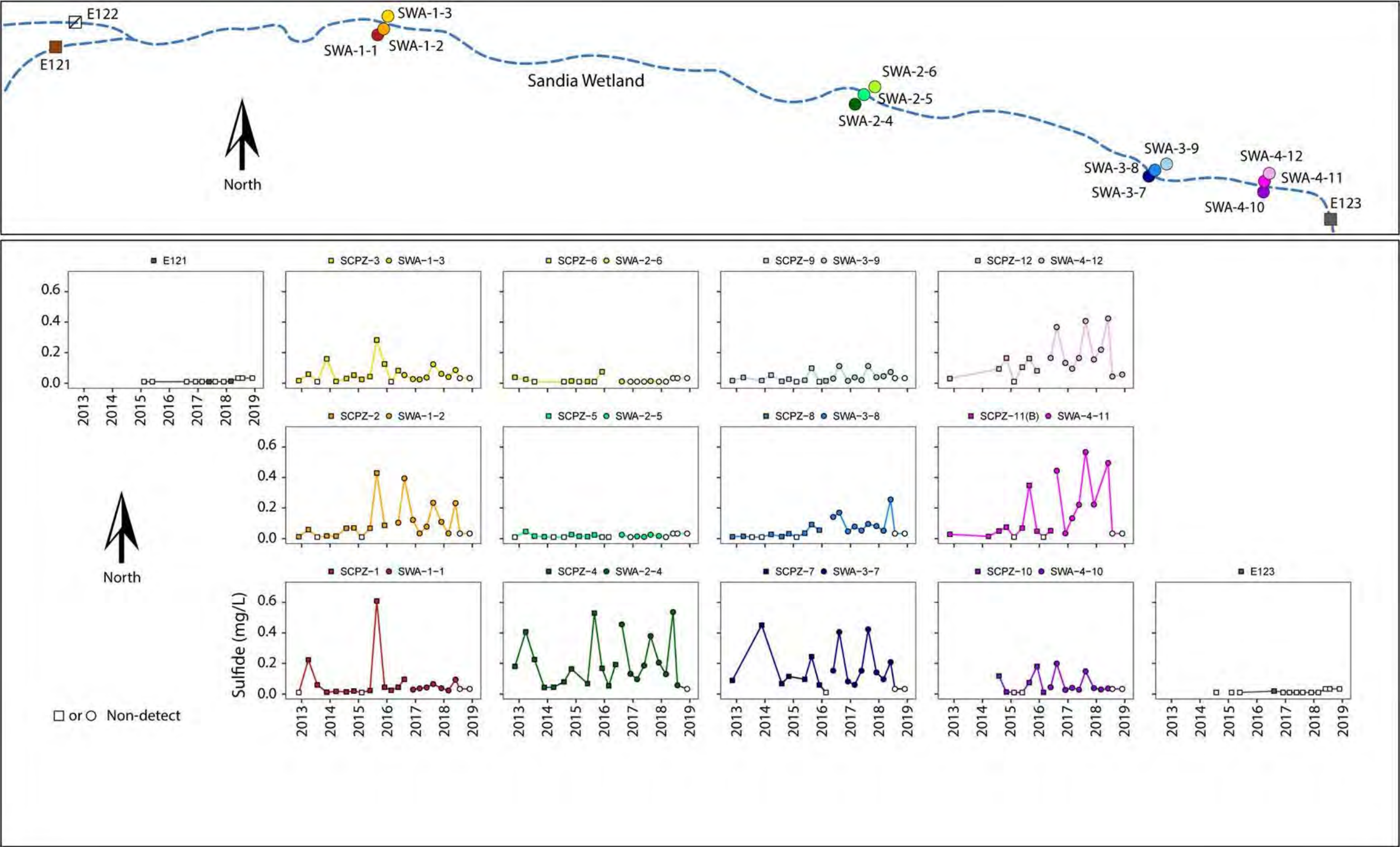
Figure D-3.0-1 Chloride concentrations in Sandia wetland surface water and alluvial system



Notes: Surface water stations include E121, E122 (plot not shown), and E123. Piezometers are labeled with the prefix SCPZ (square symbols), and alluvial wells are labeled with the prefix SWA (circle symbols). The plots are arranged in four transects from west to east. Data are plotted for the full period of wetland monitoring. Nondetects are plotted as the MDL with open symbols. The map above is not to scale but shows approximate sampling locations in relation to the approximate thalweg (blue dashed line).

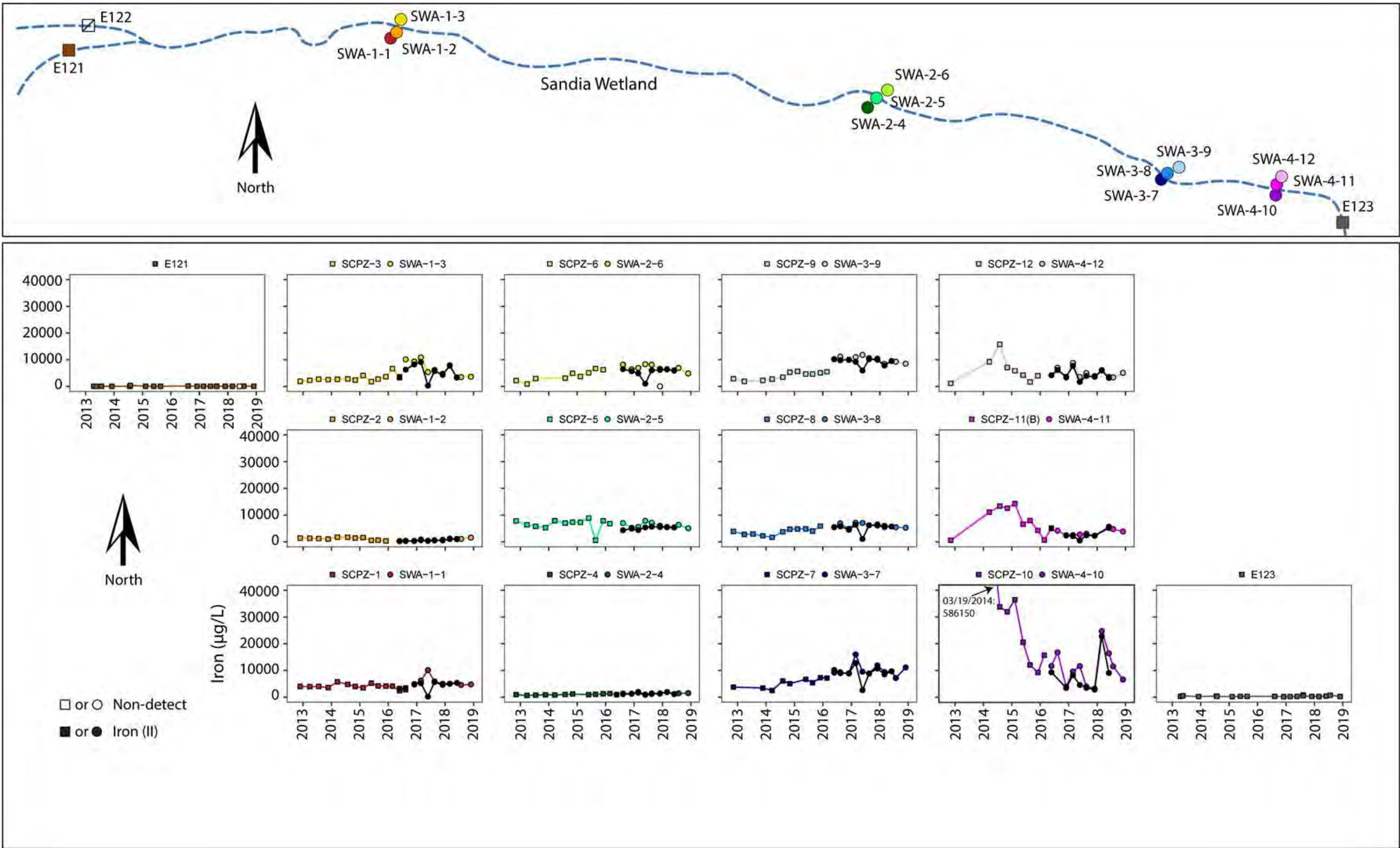
Figure D-3.0-2 Sulfate concentrations in Sandia wetland surface water and alluvial system





Notes: Surface water stations include E121, E122 (plot not shown), and E123. Piezometers are labeled with the prefix SCPZ (square symbols), and alluvial wells are labeled with the prefix SWA (circle symbols). The plots are arranged in four transects from west to east. Data are plotted for the full period of wetland monitoring. Nondetects are plotted as the MDL with open symbols. The map above is not to scale but shows approximate sampling locations in relation to the approximate thalweg (blue dashed line).

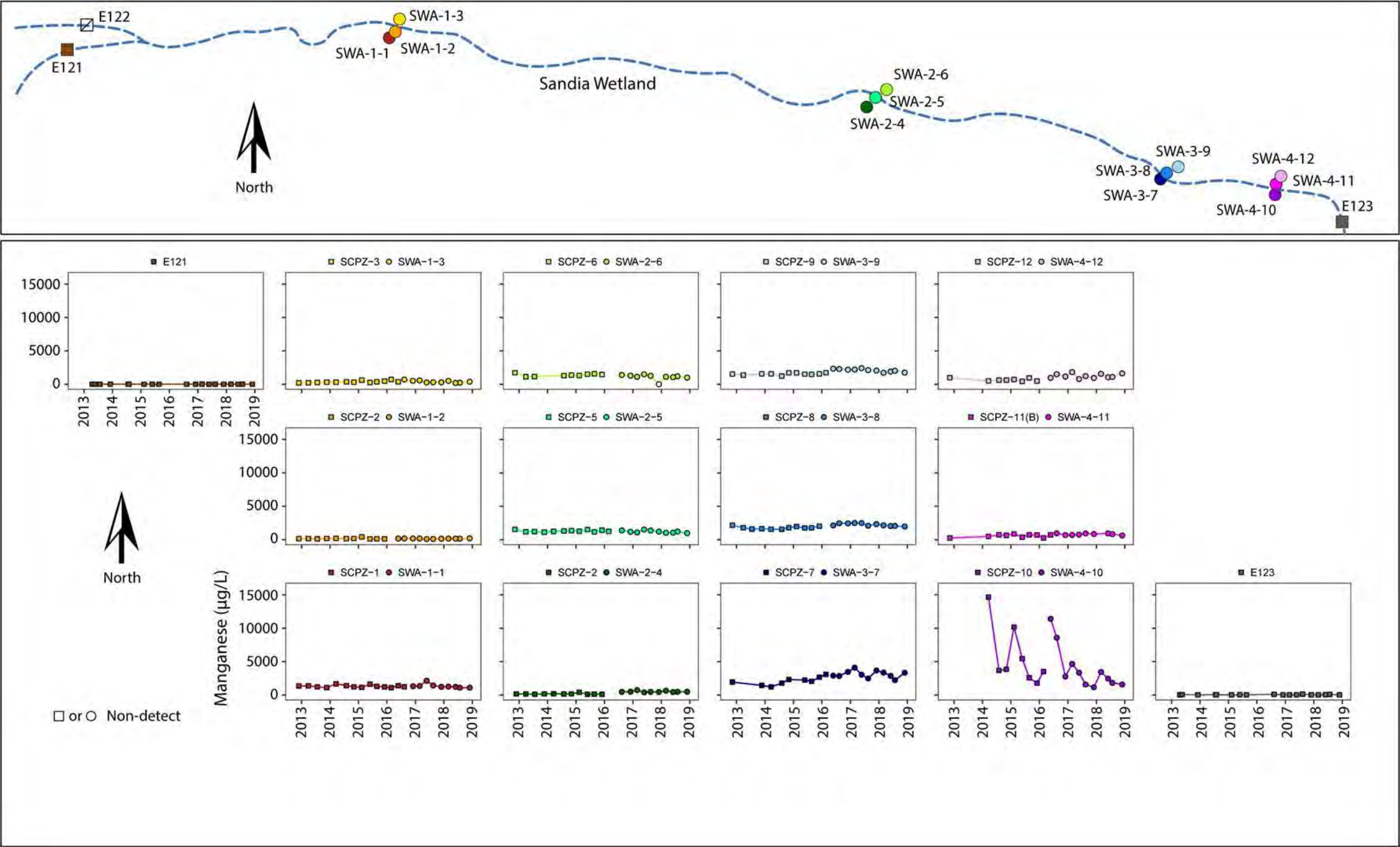
Figure D-3.0-3 Sulfide concentrations in Sandia wetland surface water and alluvial system



Notes: Surface water stations include E121, E122 (plot not shown), and E123. Piezometers are labeled with the prefix SCPZ (square symbols), and alluvial wells are labeled with the prefix SWA (circle symbols). The plots are arranged in four transects from west to east. Data are plotted for the full period of wetland monitoring. Nondetects are plotted as the MDL with open symbols. Total iron is represented with colored symbols and Fe(II) with black symbols. The map above is not to scale but shows approximate sampling locations in relation to the approximate thalweg (blue dashed line).

Figure D-3.0-4 Iron concentrations in Sandia wetland surface water and alluvial system

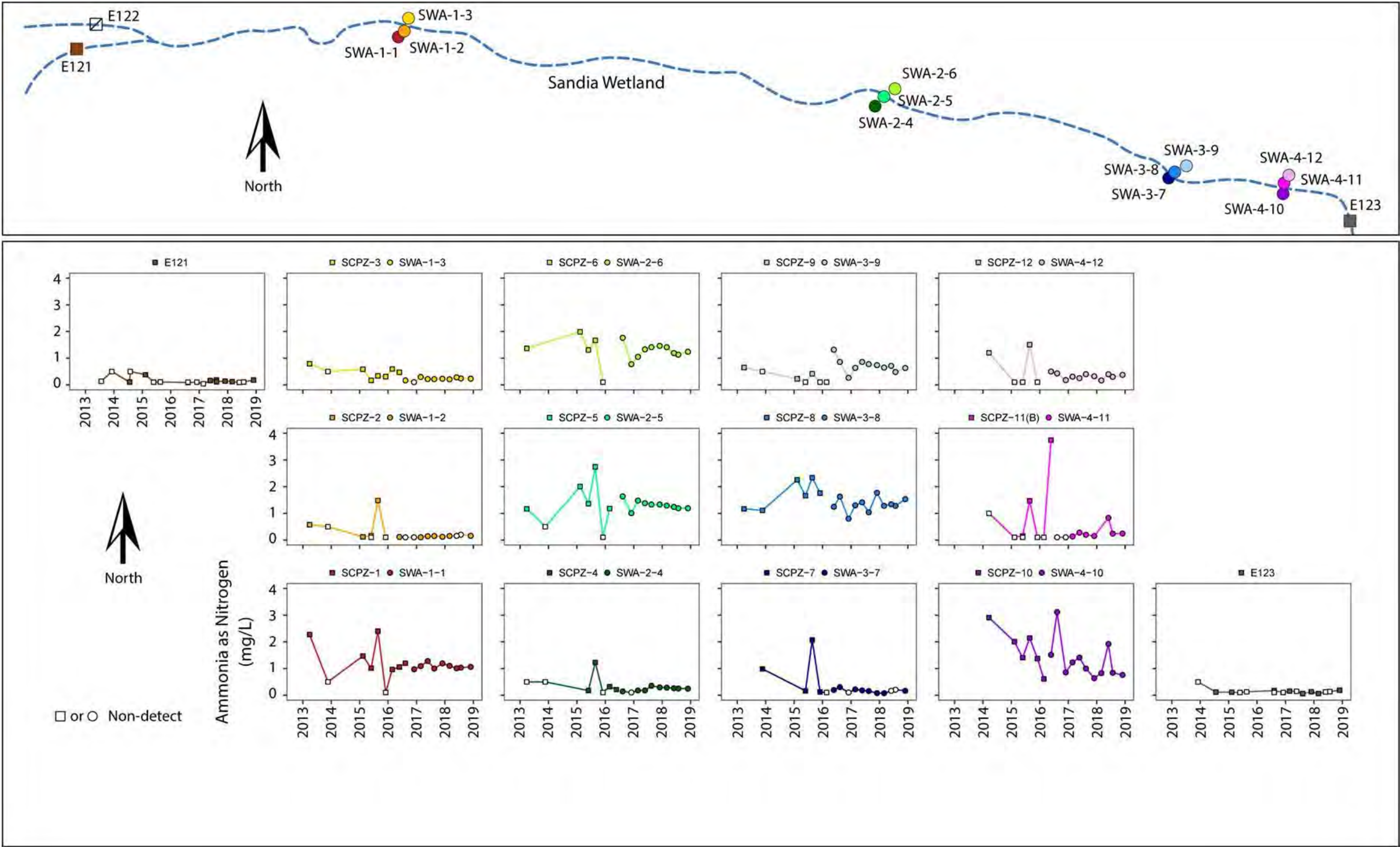




Notes: Surface water stations include E121, E122 (plot not shown), and E123. Piezometers are labeled with the prefix SCPZ (square symbols), and alluvial wells are labeled with the prefix SWA (circle symbols). The plots are arranged in four transects from west to east. Data are plotted for the full period of wetland monitoring. Nondetects are plotted as the MDL with open symbols. The map above is not to scale but shows approximate sampling locations in relation to the approximate thalweg (blue dashed line).

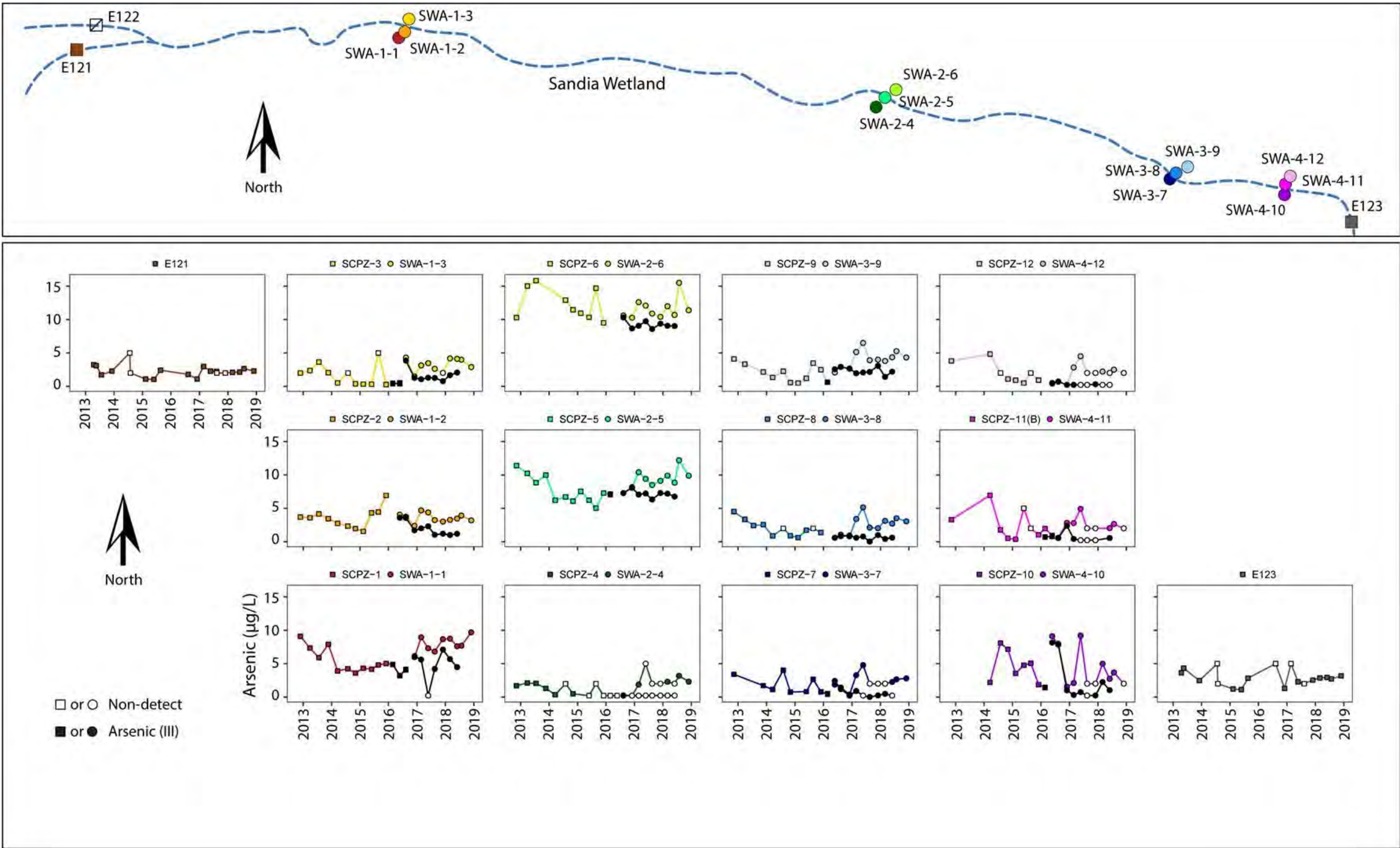
Figure D-3.0-5 Manganese concentrations in Sandia wetland surface water and alluvial system





Notes: Surface water stations include E121, E122 (plot not shown), and E123. Piezometers are labeled with the prefix SCPZ (square symbols), and alluvial wells are labeled with the prefix SWA (circle symbols). The plots are arranged in four transects from west to east. Data are plotted for the full period of wetland monitoring. Nondetects are plotted as the MDL with open symbols. The map above is not to scale but shows approximate sampling locations in relation to the approximate thalweg (blue dashed line).

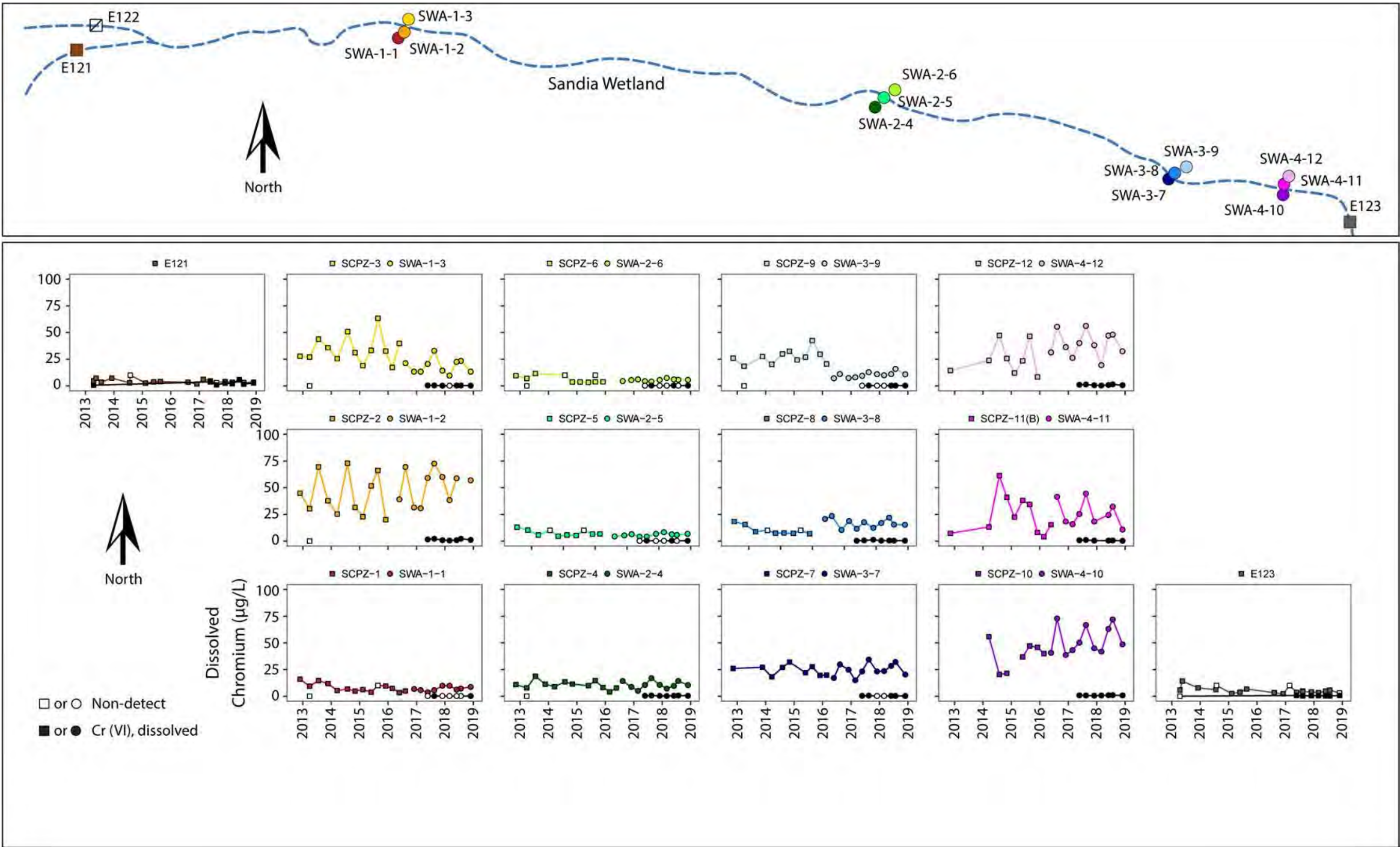
Figure D-3.0-6 Ammonia as nitrogen concentrations in Sandia wetland surface water and alluvial system



Notes: Surface water stations include E121, E122 (plot not shown), and E123. Piezometers are labeled with the prefix SCPZ (square symbols), and alluvial wells are labeled with the prefix SWA (circle symbols). The plots are arranged in four transects from west to east. Data are plotted for the full period of wetland monitoring. Nondetects are plotted as the MDL with open symbols. Total arsenic is represented with the colored symbols and As(III) with black symbols. The map above is not to scale but shows approximate sampling locations in relation to the approximate thalweg (blue dashed line).

Figure D-3.0-7 Arsenic concentrations in Sandia wetland surface water and alluvial system

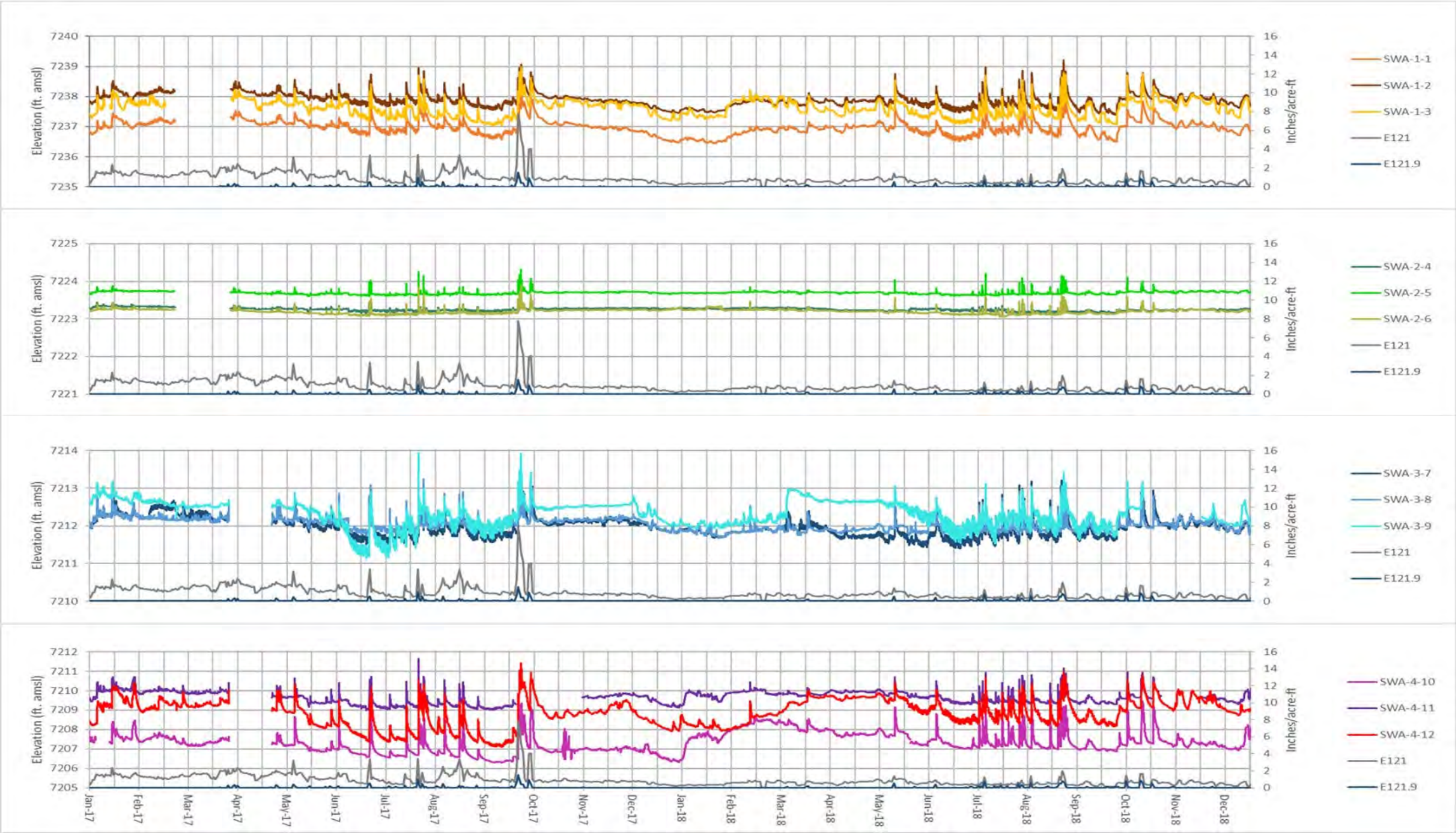




Notes: Surface water stations include E121, E122 (plot not shown), and E123. Piezometers are labeled with the prefix SCPZ (square symbols), and alluvial wells are labeled with the prefix SWA (circle symbols). The plots are arranged in four transects from west to east. Data are plotted for the full period of wetland monitoring. Nondetects are plotted as the MDL with open symbols. Total chromium is represented with the colored symbols and Cr(VI) with black symbols. The map above is not to scale but shows approximate sampling locations in relation to the approximate thalweg (blue dashed line).

Figure D-3.0-8 Chromium concentrations in Sandia wetland surface water and alluvial system





Notes: Water levels collected in the Sandia wetland were at times adjusted for reference value calculation errors and then checked against manual measurements taken in the field during sampling events. Most adjustments were made in response to inaccurate values of the wells inner/outer casing elevations and calculation errors when defining the new reference level. All changes made follow standard operating procedure ER-SOP-20231, "Groundwater-Level Data Processing, Review, and Validation."

Figure D-4.0-1 Water levels recorded by sondes located in the alluvial system plotted with precipitation data from the E121.9 weather station and total daily volume of flow in surface water gaging station E121 in 2017 and 2018



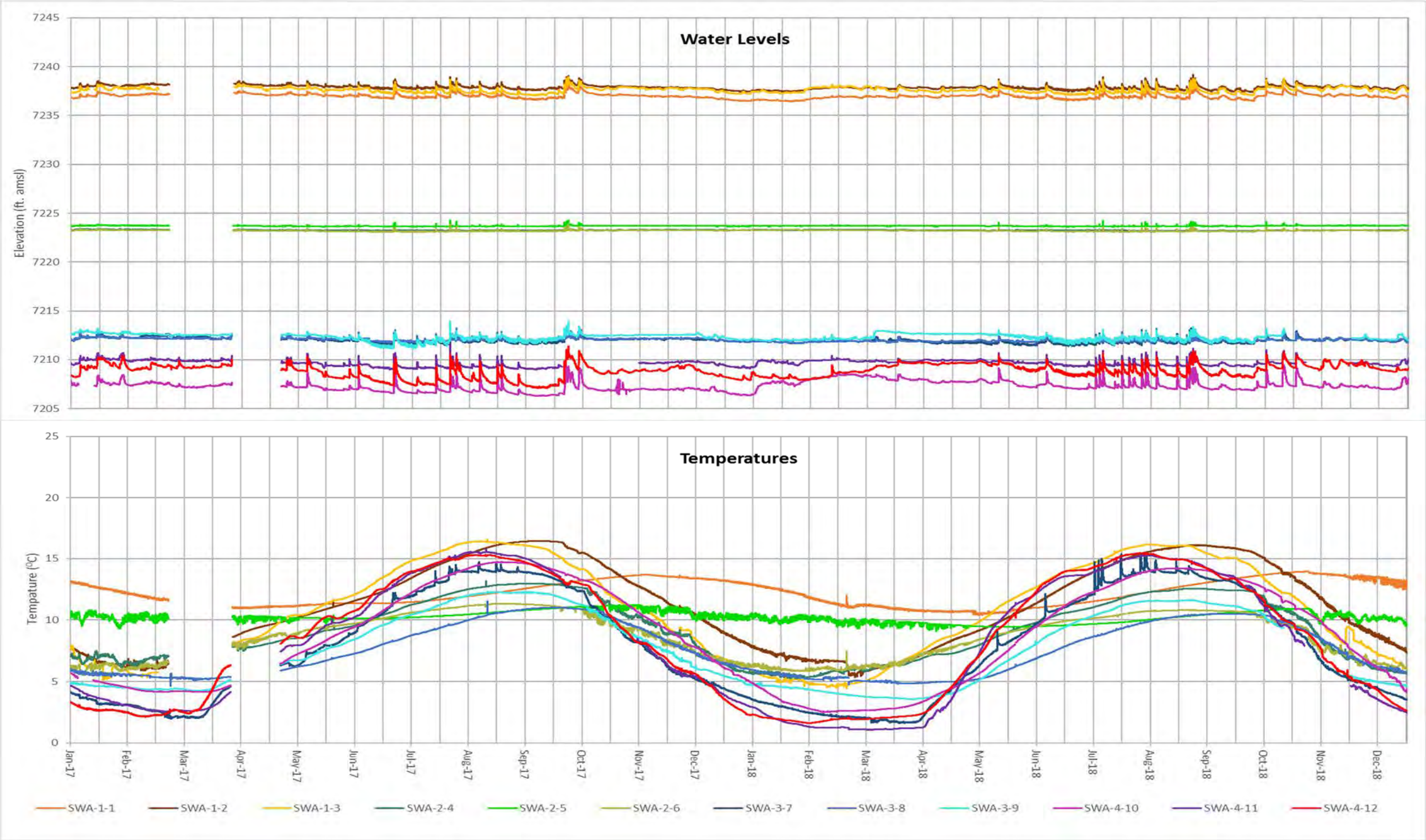


Figure D-4.0-2 Time series of water level and temperature in alluvial system in 2017 and 2018

**Table D-2.0-1**  
**Travel Time of Flood Bore, Peak Discharge, Increase or Decrease**  
**in Peak Discharge, and Percent Change in Peak Discharge from Upgradient**  
**to Downgradient of the Wetland for Each Sample-Triggering Storm Event in 2018**

Date	Travel Time from E121 to E123 (min)	Peak Discharge (cfs)		+/- <sup>a</sup>	% <sup>b</sup>	Travel Time from E122 to E123 (min)	Peak Discharge (cfs)		+/-	%
		E121	E123				E122	E123		
7/15	100	14	11	-	21	100	3.3	11	+	70
7/17	85	29	31	+	6	75	5.0	31	+	84
8/7	85	18	14	-	22	85	3.3	14	+	76
8/9	75	21	19	-	10	75	3.8	19	+	80
8/15	75	42	19	-	55	70	3.4	19	+	82
	100	7.5	7.9	+	5	95	1.7	8	+	78
9/3	85	17	21	-	19	85	2.9	21	+	86
9/4	65	38	35	-	8	70	4.3	35	+	88
<b>Min</b>	65	7.5	7.9	— <sup>c</sup>	5	70	1.7	8	—	70
<b>Mean</b>	83	23	20	—	18	81.9	3.5	20	—	81
<b>Max</b>	100	42	35	—	55	100	5.0	35	—	88

<sup>a</sup> + = Increase; - = decrease.

<sup>b</sup> % = Percent change in peak discharge.

<sup>c</sup> — = Result is not applicable.

**Table D-2.0-2**  
**Calculated Sediment Yield and Runoff Volume at Gaging Stations**  
**E121, E122, and E123 for Each Sample-Triggering Storm Event from 2014 to 2018**

Station	Date	Sediment Yield (ton)	Sediment Volume (yd <sup>3</sup> )	Runoff Volume (acre-feet)	Peak Discharge (cfs)
<b>2018</b>					
E121	7/15/2018	0.09	0.04	0.4	14
E121	7/17/2018	0.46	0.21	0.9	29
E121	8/7/2018	0.19	0.09	0.5	18
E121	8/9/2018	0.63	0.28	0.6	21
E121	8/15/2018	0.57	0.25	0.9	42
E121	9/4/2018	0.40	0.18	1.3	38
E122	7/15/2018	0.03	0.01	0.1	3.3
E122	8/9/2018	0.23	0.10	0.2	3.8
E122	9/4/2018	0.40	0.18	0.4	4.3
E123	7/17/2018	1.72	0.77	3.6	31
E123	9/3/2018	0.68	0.30	2.7	21
E123	9/4/2018	2.02	0.90	3.7	35



Table D-2.0-2 (continued)

Station	Date	Sediment Yield (ton)	Sediment Volume (yd <sup>3</sup> )	Runoff Volume (acre-feet)	Peak Discharge (cfs)
2017					
E121	6/6/2017	0.70	0.31	0.8	26
E121	6/25/2017	0.71	0.32	1.7	21
E121	7/18/2017	0.48	0.22	1.5	36
E121	7/26/2017	4.09	1.83	2.8	87
E121	7/29/2017	0.88	0.40	1.4	30
E122	7/18/2017	0.11	0.05	0.2	5
E122	7/27/2017	0.02	0.01	0.1	2
E122	7/29/2017	0.13	0.06	0.3	5
E122	8/21/2017	<0.01	<0.01	0.2	2
E123	6/25/2017	1.10	0.49	2.9	30
E123	7/26/2017	8.79	3.94	6.2	78
E123	7/29/2017	0.64	0.29	2.7	29
2016					
E121	7/1/2016	0.36	0.16	0.8	22
E121	7/15/2016	0.26	0.12	1.2	22
E121	7/31/2016	1.80	0.81	2.7	47
E121	8/3/2016	0.34	0.15	1.6	37
E121	8/27/2016	1.57	0.70	1.9	51
E121	9/6/2016	0.75	0.34	1.5	40
E121	11/4/2016	0.15	0.07	0.8	8.4
E122	10/3/2016	0.02	0.01	0.1	22
E122	10/8/2016	0.01	0.01	0.1	22
E122	11/4/2016	0.03	0.01	0.1	47
E123	7/31/2016	0.34	0.15	4.0	46
E123	8/3/2016	2.10	0.94	2.9	13
E123	8/27/2016	0.54	0.24	3.3	28
E123	9/6/2016	0.15	0.07	3.1	18
E123	11/5–11/6/2016	0.16	0.07	3.4	15

Table D-2.0-2 (continued)

Station	Date	Sediment Yield (ton)	Sediment Volume (yd <sup>3</sup> )	Runoff Volume (acre-feet)	Peak Discharge (cfs)
2015					
E121	6/1/2015	0.45	0.20	1.7	20
E121	6/26/2015	3.88	1.74	1.3	18
E121	7/3/2015	0.71	0.32	1.6	30
E121	7/15–7/16/2015	0.50	0.22	1.3	39
E121	7/20–7/21/2015	1.62	0.73	4.0	50
E121	7/29–7/30/2015	0.38	0.17	2.2	14
E121	7/31/2015	0.27	0.12	1.1	9.2
E121	8/17/2015	0.45	0.20	1.6	36
E121	10/23–10/24/2015	0.38	0.17	2.0	28
E122	10/23–10/24/2015	0.07	0.03	0.4	5.1
E123	7/3/2015	1.26	0.56	3.9	35
E123	7/20–7/21/2015	2.58	1.16	10.6	64
E123	7/29–7/30/2015	0.84	0.37	5.8	29
E123	8/8/2015	0.15	0.07	1.8	16
E123	8/17/2015	1.06	0.47	3.2	38
E123	10/20/2015	0.25	0.11	1.9	16
E123	10/23/2015	1.19	0.53	4.6	48
2014					
E121	7/7/2014	0.84	0.38	2.3	63
E121	7/14–7/15/2014	0.19	0.09	0.7	4.8
E121	7/15–7/16/2014	1.64	0.73	0.6	10
E121	7/19/2014	3.22	1.44	0.6	11
E121	7/27–7/28/2014	0.57	0.26	0.9	29
E121	7/31/2014	15.4	6.91	2.9	66
E122	7/8/2014	0.60	0.27	1.0	10
E122	7/27–7/28/2014	0.05	0.02	0.6	6.2
E122	7/29/2014	0.73	0.33	1.2	12
E122	7/31/2014	1.55	0.69	1.0	19
E123	5/23/2014	1.62	0.73	2.7	18
E123	7/7/2014	4.12	1.84	6.4	80
E123	7/8/2014	18.2	8.14	7.0	76
E123	7/15–7/16/2014	2.01	0.90	3.1	20
E123	7/19/2014	0.39	0.17	1.7	18
E123	7/29/2014	7.36	3.30	7.5	62
E123	7/31/2014	28.6	12.8	7.2	109





**Table D-2.1-1**  
**Analytical Exceedances in Surface Water at Gaging Stations E121, E122, and E123**

Location	Location Alias	Date	Sample Time	Analyte	Field Prep Code <sup>a</sup>	Sample Type <sup>b</sup>	Sample Usage Code <sup>c</sup>	Result	MDL <sup>d</sup>	PQL <sup>e</sup>	Unit	Screening Level	Screening Level Type <sup>f</sup>	Hardness
Sandia right fork at Pwr Plant	E121	2/27/2018	9:56:00	Total PCB	UF	WS	INV	0.00111	na <sup>g</sup>	na	µg/L	0.00064	NM Human Health OO	na
Sandia right fork at Pwr Plant	E121	5/30/2018	10:10:00	Total PCB	UF	WS	INV	0.00139	na	na	µg/L	0.00064	NM Human Health OO	na
Sandia right fork at Pwr Plant	E121	7/17/2018	11:31:00	Aluminum	F	WT	INV	243	19.3	50	µg/L	116.1987	NM Aqu Chronic	16.5
Sandia right fork at Pwr Plant	E121	7/17/2018	11:31:00	Copper	F	WT	INV	5.35	0.3	1	µg/L	2.460843	NM Aqu Acute	16.5
Sandia right fork at Pwr Plant	E121	7/17/2018	11:31:00	Copper	F	WT	INV	5.35	0.3	1	µg/L	1.920623	NM Aqu Chronic	16.5
Sandia right fork at Pwr Plant	E121	7/17/2018	11:23:00	Total PCB	UF	WT	INV	0.216	na	na	µg/L	0.014	NM Aqu Chronic	na
Sandia right fork at Pwr Plant	E121	7/17/2018	11:23:00	Total PCB	UF	WT	INV	0.216	na	na	µg/L	0.00064	NM Human Health OO	na
Sandia right fork at Pwr Plant	E121	7/17/2018	11:23:00	Total PCB	UF	WT	INV	0.216	na	na	µg/L	0.014	NM Wildlife Habitat	na
Sandia right fork at Pwr Plant	E121	7/24/2018	11:37:00	Copper	F	WS	INV	5.16	3	10	µg/L	4.83633	NM Aqu Acute	33.8
Sandia right fork at Pwr Plant	E121	7/24/2018	11:37:00	Copper	F	WS	INV	5.16	3	10	µg/L	3.544552	NM Aqu Chronic	33.8
Sandia right fork at Pwr Plant	E121	7/24/2018	11:37:00	Total PCB	UF	WS	INV	0.00241	na	na	µg/L	0.00064	NM Human Health OO	na
Sandia right fork at Pwr Plant	E121	8/7/2018	14:19:00	Aluminum	F	WT	INV	254	19.3	50	µg/L	164.3849	NM Aqu Acute	10.9
Sandia right fork at Pwr Plant	E121	8/7/2018	14:19:00	Aluminum	F	WT	INV	254	19.3	50	µg/L	65.85864	NM Aqu Chronic	10.9
Sandia right fork at Pwr Plant	E121	8/7/2018	14:19:00	Copper	F	WT	INV	6.02	0.3	1	µg/L	1.665075	NM Aqu Acute	10.9
Sandia right fork at Pwr Plant	E121	8/7/2018	14:19:00	Copper	F	WT	INV	6.02	0.3	1	µg/L	1.347668	NM Aqu Chronic	10.9
Sandia right fork at Pwr Plant	E121	8/7/2018	14:19:00	Lead	F	WT	INV	0.502	0.5	2	µg/L	0.210939	NM Aqu Chronic	10.9
Sandia right fork at Pwr Plant	E121	8/7/2018	14:11:00	Total PCB	UF	WT	INV	0.104	na	na	µg/L	0.014	NM Aqu Chronic	na
Sandia right fork at Pwr Plant	E121	8/7/2018	14:11:00	Total PCB	UF	WT	INV	0.104	na	na	µg/L	0.00064	NM Human Health OO	na
Sandia right fork at Pwr Plant	E121	8/7/2018	14:11:00	Total PCB	UF	WT	INV	0.104	na	na	µg/L	0.014	NM Wildlife Habitat	na
Sandia right fork at Pwr Plant	E121	8/7/2018	14:19:00	Zinc	F	WT	INV	32	3.3	10	µg/L	21.31893	NM Aqu Acute	10.9
Sandia right fork at Pwr Plant	E121	8/7/2018	14:19:00	Zinc	F	WT	INV	32	3.3	10	µg/L	16.14712	NM Aqu Chronic	10.9
Sandia right fork at Pwr Plant	E121	8/9/2018	17:50:00	Aluminum	F	WT	INV	303	19.3	50	µg/L	191.8122	NM Aqu Acute	12.2
Sandia right fork at Pwr Plant	E121	8/9/2018	17:50:00	Aluminum	F	WT	INV	303	19.3	50	µg/L	76.84701	NM Aqu Chronic	12.2
Sandia right fork at Pwr Plant	E121	8/9/2018	17:50:00	Copper	F	WT	INV	4.23	0.3	1	µg/L	1.851565	NM Aqu Acute	12.2
Sandia right fork at Pwr Plant	E121	8/9/2018	17:50:00	Copper	F	WT	INV	4.23	0.3	1	µg/L	1.483872	NM Aqu Chronic	12.2
Sandia right fork at Pwr Plant	E121	8/9/2018	17:42:00	Total PCB	UF	WT	INV	0.0475	na	na	µg/L	0.014	NM Aqu Chronic	na
Sandia right fork at Pwr Plant	E121	8/9/2018	17:42:00	Total PCB	UF	WT	INV	0.0475	na	na	µg/L	0.00064	NM Human Health OO	na
Sandia right fork at Pwr Plant	E121	8/9/2018	17:42:00	Total PCB	UF	WT	INV	0.0475	na	na	µg/L	0.014	NM Wildlife Habitat	na
Sandia right fork at Pwr Plant	E121	8/9/2018	17:50:00	Zinc	F	WT	INV	27.2	3.3	10	µg/L	23.61921	NM Aqu Acute	12.2
Sandia right fork at Pwr Plant	E121	8/9/2018	17:50:00	Zinc	F	WT	INV	27.2	3.3	10	µg/L	17.88937	NM Aqu Chronic	12.2
Sandia right fork at Pwr Plant	E121	8/15/2018	13:06:00	Aluminum	F	WT	INV	381	19.3	50	µg/L	256.8711	NM Aqu Acute	15.1
Sandia right fork at Pwr Plant	E121	8/15/2018	13:06:00	Aluminum	F	WT	INV	381	19.3	50	µg/L	102.912	NM Aqu Chronic	15.1
Sandia right fork at Pwr Plant	E121	8/15/2018	13:06:00	Copper	F	WT	INV	6.04	0.3	1	µg/L	2.263616	NM Aqu Acute	15.1
Sandia right fork at Pwr Plant	E121	8/15/2018	13:06:00	Copper	F	WT	INV	6.04	0.3	1	µg/L	1.780483	NM Aqu Chronic	15.1
Sandia right fork at Pwr Plant	E121	8/15/2018	12:58:00	Total PCB	UF	WT	INV	0.139	na	na	µg/L	0.014	NM Aqu Chronic	na
Sandia right fork at Pwr Plant	E121	8/15/2018	12:58:00	Total PCB	UF	WT	INV	0.139	na	na	µg/L	0.00064	NM Human Health OO	na
Sandia right fork at Pwr Plant	E121	8/15/2018	12:58:00	Total PCB	UF	WT	INV	0.139	na	na	µg/L	0.014	NM Wildlife Habitat	na
Sandia right fork at Pwr Plant	E121	8/15/2018	13:06:00	Zinc	F	WT	INV	35.5	3.3	10	µg/L	28.6742	NM Aqu Acute	15.1

Table D-2.1-1 (continued)

Location	Location Alias	Date	Sample Time	Analyte	Field Prep Code <sup>a</sup>	Sample Type <sup>b</sup>	Sample Usage Code <sup>c</sup>	Result	MDL <sup>d</sup>	PQL <sup>e</sup>	Unit	Screening Level	Screening Level Type <sup>f</sup>	Hardness
Sandia right fork at Pwr Plant	E121	8/15/2018	13:06:00	Zinc	F	WT	INV	35.5	3.3	10	µg/L	21.71807	NM Aqu Chronic	15.1
Sandia right fork at Pwr Plant	E121	9/4/2018	13:02:00	Aluminum	F	WT	INV	314	19.3	50	µg/L	123.9618	NM Aqu Acute	8.87
Sandia right fork at Pwr Plant	E121	9/4/2018	13:02:00	Aluminum	F	WT	INV	314	19.3	50	µg/L	49.66364	NM Aqu Chronic	8.87
Sandia right fork at Pwr Plant	E121	9/4/2018	13:02:00	Cadmium	F	WT	INV	1.63	0.3	1	µg/L	0.208436	NM Aqu Acute	8.87
Sandia right fork at Pwr Plant	E121	9/4/2018	13:02:00	Cadmium	F	WT	INV	1.63	0.3	1	µg/L	0.078976	NM Aqu Chronic	8.87
Sandia right fork at Pwr Plant	E121	9/4/2018	13:02:00	Copper	F	WT	INV	2.87	0.3	1	µg/L	1.371211	NM Aqu Acute	8.87
Sandia right fork at Pwr Plant	E121	9/4/2018	13:02:00	Copper	F	WT	INV	2.87	0.3	1	µg/L	1.130063	NM Aqu Chronic	8.87
Sandia right fork at Pwr Plant	E121	11/29/2018	8:35:00	Copper	F	WS	INV	10.7	3	10	µg/L	8.226824	NM Aqu Acute	59.4
Sandia right fork at Pwr Plant	E121	11/29/2018	8:35:00	Copper	F	WS	INV	10.7	3	10	µg/L	5.738555	NM Aqu Chronic	59.4
Sandia left fork at Asph Plant	E122	7/17/2018	11:23:00	Aluminum	F	WT	INV	416	19.3	50	µg/L	314.3742	NM Aqu Acute	17.5
Sandia left fork at Asph Plant	E122	7/17/2018	11:23:00	Aluminum	F	WT	INV	416	19.3	50	µg/L	125.9499	NM Aqu Chronic	17.5
Sandia left fork at Asph Plant	E122	7/17/2018	11:23:00	Copper	F	WT	INV	5.96	0.3	1	µg/L	2.601124	NM Aqu Acute	17.5
Sandia left fork at Asph Plant	E122	7/17/2018	11:23:00	Copper	F	WT	INV	5.96	0.3	1	µg/L	2.019659	NM Aqu Chronic	17.5
Sandia left fork at Asph Plant	E122	7/17/2018	11:27:00	Gross alpha	UF	WT	INV	26	2.56	1.75	pCi/L	15	NM Livestock Watering	na
Sandia left fork at Asph Plant	E122	7/17/2018	11:23:00	Lead	F	WT	INV	0.602	0.5	2	µg/L	0.361524	NM Aqu Chronic	17.5
Sandia left fork at Asph Plant	E122	9/4/2018	12:55:00	Aluminum	F	WT	INV	2500	19.3	50	µg/L	515.1806	NM Aqu Acute	25.1
Sandia left fork at Asph Plant	E122	9/4/2018	12:55:00	Aluminum	F	WT	INV	2500	19.3	50	µg/L	206.4003	NM Aqu Chronic	25.1
Sandia left fork at Asph Plant	E122	9/4/2018	12:55:00	Copper	F	WT	INV	4.81	0.3	1	µg/L	3.653787	NM Aqu Acute	25.1
Sandia left fork at Asph Plant	E122	9/4/2018	12:55:00	Copper	F	WT	INV	4.81	0.3	1	µg/L	2.748674	NM Aqu Chronic	25.1
Sandia left fork at Asph Plant	E122	9/4/2018	13:01:00	Gross alpha	UF	WT	INV	25.3	2.99	2.04	pCi/L	15	NM Livestock Watering	na
Sandia left fork at Asph Plant	E122	9/4/2018	12:55:00	Lead	F	WT	INV	3.88	0.5	2	µg/L	0.543406	NM Aqu Chronic	25.1
Sandia left fork at Asph Plant	E122	9/4/2018	12:55:00	Selenium	UF	WT	INV	8.23	2	5	µg/L	5	NM Aqu Chronic	na
Sandia left fork at Asph Plant	E122	9/4/2018	12:55:00	Selenium	UF	WT	INV	8.23	2	5	µg/L	5	NM Wildlife Habitat	na
Sandia left fork at Asph Plant	E122	9/4/2018	12:49:00	Total PCB	UF	WT	INV	0.0613	na	na	µg/L	0.014	NM Aqu Chronic	na
Sandia left fork at Asph Plant	E122	9/4/2018	12:49:00	Total PCB	UF	WT	INV	0.0613	na	na	µg/L	0.00064	NM Human Health OO	na
Sandia left fork at Asph Plant	E122	9/4/2018	12:49:00	Total PCB	UF	WT	INV	0.0613	na	na	µg/L	0.014	NM Wildlife Habitat	na
Sandia below Wetlands	E123	2/27/2018	11:50:00	Total PCB	UF	WS	INV	0.0027	na	na	µg/L	0.00064	NM Human Health OO	na
Sandia below Wetlands	E123	5/30/2018	8:49:00	Total PCB	UF	WS	INV	0.00246	na	na	µg/L	0.00064	NM Human Health OO	na
Sandia below Wetlands	E123	7/17/2018	12:47:00	Aluminum	F	WT	INV	518	19.3	50	µg/L	473.4884	NM Aqu Acute	23.6
Sandia below Wetlands	E123	7/17/2018	12:47:00	Aluminum	F	WT	INV	518	19.3	50	µg/L	189.6969	NM Aqu Chronic	23.6
Sandia below Wetlands	E123	7/17/2018	12:47:00	Copper	F	WT	INV	6.28	0.3	1	µg/L	3.447691	NM Aqu Acute	23.6
Sandia below Wetlands	E123	7/17/2018	12:47:00	Copper	F	WT	INV	6.28	0.3	1	µg/L	2.607686	NM Aqu Chronic	23.6
Sandia below Wetlands	E123	7/17/2018	12:47:00	Lead	F	WT	INV	0.592	0.5	2	µg/L	0.506954	NM Aqu Chronic	23.6
Sandia below Wetlands	E123	7/17/2018	12:41:00	Total PCB	UF	WT	INV	0.127	na	na	µg/L	0.014	NM Aqu Chronic	na
Sandia below Wetlands	E123	7/17/2018	12:41:00	Total PCB	UF	WT	INV	0.127	na	na	µg/L	0.00064	NM Human Health OO	na
Sandia below Wetlands	E123	7/17/2018	12:41:00	Total PCB	UF	WT	INV	0.127	na	na	µg/L	0.014	NM Wildlife Habitat	na
Sandia below Wetlands	E123	7/24/2018	10:11:00	Total PCB	UF	WS	INV	0.00457	na	na	µg/L	0.00064	NM Human Health OO	na
Sandia below Wetlands	E123	8/9/2018	18:55:00	Aluminum	F	WT	INV	802	19.3	50	µg/L	372.2968	NM Aqu Acute	19.8
Sandia below Wetlands	E123	8/9/2018	18:55:00	Aluminum	F	WT	INV	802	19.3	50	µg/L	149.1558	NM Aqu Chronic	19.8
Sandia below Wetlands	E123	8/9/2018	18:55:00	Copper	F	WT	INV	4.63	0.3	1	µg/L	2.922056	NM Aqu Acute	19.8
Sandia below Wetlands	E123	8/9/2018	18:55:00	Copper	F	WT	INV	4.63	0.3	1	µg/L	2.244411	NM Aqu Chronic	19.8

Table D-2.1-1 (continued)

Location	Location Alias	Date	Sample Time	Analyte	Field Prep Code <sup>a</sup>	Sample Type <sup>b</sup>	Sample Usage Code <sup>c</sup>	Result	MDL <sup>d</sup>	PQL <sup>e</sup>	Unit	Screening Level	Screening Level Type <sup>f</sup>	Hardness
Sandia below Wetlands	E123	8/9/2018	18:55:00	Lead	F	WT	INV	0.908	0.5	2	µg/L	0.415778	NM Aqu Chronic	19.8
Sandia below Wetlands	E123	8/9/2018	18:49:00	Total PCB	UF	WT	INV	0.143	na	na	µg/L	0.014	NM Aqu Chronic	na
Sandia below Wetlands	E123	8/9/2018	18:49:00	Total PCB	UF	WT	INV	0.143	na	na	µg/L	0.00064	NM Human Health OO	na
Sandia below Wetlands	E123	8/9/2018	18:49:00	Total PCB	UF	WT	INV	0.143	na	na	µg/L	0.014	NM Wildlife Habitat	na
Sandia below Wetlands	E123	8/15/2018	14:15:00	Aluminum	F	WT	INV	633	19.3	50	µg/L	377.4565	NM Aqu Acute	20
Sandia below Wetlands	E123	8/15/2018	14:15:00	Aluminum	F	WT	INV	633	19.3	50	µg/L	151.223	NM Aqu Chronic	20
Sandia below Wetlands	E123	8/15/2018	14:15:00	Copper	F	WT	INV	5.28	0.3	1	µg/L	2.949858	NM Aqu Acute	20
Sandia below Wetlands	E123	8/15/2018	14:15:00	Copper	F	WT	INV	5.28	0.3	1	µg/L	2.263769	NM Aqu Chronic	20
Sandia below Wetlands	E123	8/15/2018	14:21:00	Gross alpha	UF	WT	INV	16.2	3.65	1.55	pCi/L	15	NM Livestock Watering	na
Sandia below Wetlands	E123	8/15/2018	14:15:00	Lead	F	WT	INV	0.825	0.5	2	µg/L	0.420531	NM Aqu Chronic	20
Sandia below Wetlands	E123	8/15/2018	14:09:00	Total PCB	UF	WT	INV	0.159	na	na	µg/L	0.014	NM Aqu Chronic	na
Sandia below Wetlands	E123	8/15/2018	14:09:00	Total PCB	UF	WT	INV	0.159	na	na	µg/L	0.00064	NM Human Health OO	na
Sandia below Wetlands	E123	8/15/2018	14:09:00	Total PCB	UF	WT	INV	0.159	na	na	µg/L	0.014	NM Wildlife Habitat	na
Sandia below Wetlands	E123	9/3/2018	13:50:00	Aluminum	F	WT	INV	860	19.3	50	µg/L	282.8376	NM Aqu Acute	16.2
Sandia below Wetlands	E123	9/3/2018	13:50:00	Aluminum	F	WT	INV	860	19.3	50	µg/L	113.3152	NM Aqu Chronic	16.2
Sandia below Wetlands	E123	9/3/2018	13:50:00	Copper	F	WT	INV	3.87	0.3	1	µg/L	2.418665	NM Aqu Acute	16.2
Sandia below Wetlands	E123	9/3/2018	13:50:00	Copper	F	WT	INV	3.87	0.3	1	µg/L	1.890743	NM Aqu Chronic	16.2
Sandia below Wetlands	E123	9/3/2018	13:50:00	Lead	F	WT	INV	0.791	0.5	2	µg/L	0.331216	NM Aqu Chronic	16.2
Sandia below Wetlands	E123	9/3/2018	13:36:00	Total PCB	UF	WT	INV	0.119	na	na	µg/L	0.014	NM Aqu Chronic	na
Sandia below Wetlands	E123	9/3/2018	13:36:00	Total PCB	UF	WT	INV	0.119	na	na	µg/L	0.00064	NM Human Health OO	na
Sandia below Wetlands	E123	9/3/2018	13:36:00	Total PCB	UF	WT	INV	0.119	na	na	µg/L	0.014	NM Wildlife Habitat	na
Sandia below Wetlands	E123	9/4/2018	14:02:00	Aluminum	F	WT	INV	793	19.3	50	µg/L	290.0351	NM Aqu Acute	16.5
Sandia below Wetlands	E123	9/4/2018	14:02:00	Aluminum	F	WT	INV	793	19.3	50	µg/L	116.1987	NM Aqu Chronic	16.5
Sandia below Wetlands	E123	9/4/2018	14:02:00	Copper	F	WT	INV	3.62	0.3	1	µg/L	2.460843	NM Aqu Acute	16.5
Sandia below Wetlands	E123	9/4/2018	14:02:00	Copper	F	WT	INV	3.62	0.3	1	µg/L	1.920623	NM Aqu Chronic	16.5
Sandia below Wetlands	E123	9/4/2018	14:02:00	Lead	F	WT	INV	0.807	0.5	2	µg/L	0.338186	NM Aqu Chronic	16.5
Sandia below Wetlands	E123	9/4/2018	13:56:00	Total PCB	UF	WT	INV	0.534	na	na	µg/L	0.014	NM Aqu Chronic	na
Sandia below Wetlands	E123	9/4/2018	13:56:00	Total PCB	UF	WT	INV	0.534	na	na	µg/L	0.00064	NM Human Health OO	na
Sandia below Wetlands	E123	9/4/2018	13:56:00	Total PCB	UF	WT	INV	0.534	na	na	µg/L	0.014	NM Wildlife Habitat	na
Sandia below Wetlands	E123	11/26/2018	10:45:00	Total PCB	UF	WS	INV	0.000971	na	na	µg/L	0.00064	NM Human Health OO	na

Note: Shaded rows indicate base flow, unshaded rows indicate storm flow.

<sup>a</sup> F = Filtered using 0.45-µm pore size; UF = nonfiltered.

<sup>b</sup> W and WS = Base flow water; WT = storm water.

<sup>c</sup> INV = Investigative sample.

<sup>d</sup> MDL = Method detection limit.

<sup>e</sup> PQL = Practical quantitation limit.

<sup>f</sup> NM Human Health OO = New Mexico Human Health Organism Only.  
NM Aqu Chronic = New Mexico NMWQCC Aquatic Life Standards Chronic.  
NM Aqu Acute = New Mexico NMWQCC Aquatic Life Standards Acute.  
NM Wildlife Habitat = New Mexico Wildlife Habitat.  
NM Livestock Watering = New Mexico Livestock Watering Standard.

<sup>g</sup> na = Not available.



**Table D-2.1-2**  
**Summary of 2018 Base Flow and Storm Water SWQC Exceedances**

Location	Media Type	Filtration	Analyte	Total Samples	Number of Samples Exceeding SWQC	Average of Sample Results Exceeding SWQC	Maximum Sample Results Exceeding SWQC	Units	Screening Level Type
E121	Storm water	F <sup>a</sup>	Aluminum	5	5	299	381	µg/L	NM Aqu Chronic
E122	Storm water	F	Aluminum	2	2	1458	2500	µg/L	NM Aqu Chronic
E123	Storm water	F	Aluminum	5	5	721.2	860	µg/L	NM Aqu Chronic
E121	Storm water	F	Cadmium	1	1	1.63	1.63	µg/L	NM Aqu Chronic
E121	Base flow	F	Copper	3	2	7.75	10.7	µg/L	NM Aqu Chronic
E121	Storm water	F	Copper	5	5	4.902	6.04	µg/L	NM Aqu Chronic
E122	Storm water	F	Copper	2	2	5.385	5.96	µg/L	NM Aqu Chronic
E123	Storm water	F	Copper	5	5	4.736	6.28	µg/L	NM Aqu Chronic
E122	Storm water	UF <sup>b</sup>	Gross alpha	2	2	25.65	26	pCi/L	NM Livestock Watering
E123	Storm water	UF	Gross alpha	5	1	16.2	16.2	pCi/L	NM Livestock Watering
E121	Storm water	F	Lead	1	1	0.502	0.502	µg/L	NM Aqu Chronic
E122	Storm water	F	Lead	2	2	2.241	3.88	µg/L	NM Aqu Chronic
E123	Storm water	F	Lead	5	5	0.7846	0.908	µg/L	NM Aqu Chronic
E122	Storm water	UF	Selenium	1	1	8.23	8.23	µg/L	NM Aqu Chronic
E121	Base flow	UF	Total PCB	5	3	0.00163667	0.00241	µg/L	NM Human Health OO
E121	Storm water	UF	Total PCB	4	4	0.126625	0.216	µg/L	NM Human Health OO
E122	Storm water	UF	Total PCB	1	1	0.0613	0.0613	µg/L	NM Human Health OO
E123	Base flow	UF	Total PCB	4	4	0.00267525	0.00457	µg/L	NM Human Health OO
E123	Storm water	UF	Total PCB	5	5	0.2164	0.534	µg/L	NM Human Health OO
E121	Storm water	F	Zinc	4	3	31.5666667	35.5	µg/L	NM Aqu Chronic

<sup>a</sup> F = Filtration using 0.45-µm pore size.

<sup>b</sup> UF = Non-filtered.

**Table D-3.3-1**  
**Analytical Exceedances in the Alluvial System**

Location	Date	Analyte	Field Prep Code <sup>a</sup>	Result	Unit	MDL <sup>b</sup>	Screening Value	Screening Value Type <sup>c</sup>
SWA-1-1	2/28/2018	Iron	F	4990	µg/L	30	1000	NM GW STD
SWA-1-1	2/28/2018	Iron	F	5040	µg/L	52.1	1000	NM GW STD
SWA-1-1	5/30/2018	Iron	F	5360	µg/L	52.1	1000	NM GW STD
SWA-1-1	5/30/2018	Iron	F	5150	µg/L	30	1000	NM GW STD
SWA-1-1	7/24/2018	Iron	F	4550	µg/L	30	1000	NM GW STD
SWA-1-1	11/27/2018	Iron	F	4750	µg/L	30	1000	NM GW STD
SWA-1-1	2/28/2018	Manganese	F	1250	µg/L	2	200	NM GW STD
SWA-1-1	5/30/2018	Manganese	F	1220	µg/L	2	200	NM GW STD
SWA-1-1	7/24/2018	Manganese	F	1090	µg/L	2	200	NM GW STD
SWA-1-1	11/27/2018	Manganese	F	1090	µg/L	2	200	NM GW STD
SWA-1-2	5/30/2018	Chromium	F	58.8	µg/L	3	50	NM GW STD
SWA-1-2	5/30/2018	Chromium	F	55.7	µg/L	3	50	NM GW STD
SWA-1-2	7/24/2018	Chromium	F	105	µg/L	3	50	NM GW STD
SWA-1-2	11/27/2018	Chromium	F	56.9	µg/L	3	50	NM GW STD
SWA-1-2	2/28/2018	Iron	F	1030	µg/L	30	1000	NM GW STD
SWA-1-2	2/28/2018	Iron	F	1220	µg/L	52.1	1000	NM GW STD
SWA-1-2	5/30/2018	Iron	F	1100	µg/L	52.1	1000	NM GW STD
SWA-1-2	5/30/2018	Iron	F	1100	µg/L	52.1	1000	NM GW STD
SWA-1-2	7/24/2018	Iron	F	1090	µg/L	30	1000	NM GW STD
SWA-1-2	11/27/2018	Iron	F	1570	µg/L	30	1000	NM GW STD
SWA-1-3	2/28/2018	Chloride	F	284	mg/L	2.68	250	NM GW STD
SWA-1-3	2/28/2018	Iron	F	7270	µg/L	30	1000	NM GW STD
SWA-1-3	2/28/2018	Iron	F	7920	µg/L	52.1	1000	NM GW STD
SWA-1-3	5/30/2018	Iron	F	3220	µg/L	30	1000	NM GW STD
SWA-1-3	5/30/2018	Iron	F	3360	µg/L	52.1	1000	NM GW STD
SWA-1-3	7/24/2018	Iron	F	3470	µg/L	30	1000	NM GW STD
SWA-1-3	11/27/2018	Iron	F	3640	µg/L	30	1000	NM GW STD
SWA-1-3	11/27/2018	Iron	F	3650	µg/L	30	1000	NM GW STD
SWA-1-3	2/28/2018	Manganese	F	506	µg/L	2	200	NM GW STD
SWA-1-3	7/24/2018	Manganese	F	231	µg/L	2	200	NM GW STD
SWA-1-3	11/27/2018	Manganese	F	375	µg/L	2	200	NM GW STD
SWA-1-3	11/27/2018	Manganese	F	378	µg/L	2	200	NM GW STD
SWA-2-4	2/28/2018	Iron	F	1590	µg/L	30	1000	NM GW STD
SWA-2-4	2/28/2018	Iron	F	1920	µg/L	52.1	1000	NM GW STD
SWA-2-4	2/28/2018	Iron	F	1940	µg/L	52.1	1000	NM GW STD
SWA-2-4	2/28/2018	Iron	F	1830	µg/L	30	1000	NM GW STD
SWA-2-4	5/30/2018	Iron	F	1190	µg/L	52.1	1000	NM GW STD

Table D-3.3-1 (continued)

Location	Date	Analyte	Field Prep Code <sup>a</sup>	Result	Unit	MDL <sup>b</sup>	Screening Value	Screening Value Type <sup>c</sup>
SWA-2-4	5/30/2018	Iron	F	1160	µg/L	30	1000	NM GW STD
SWA-2-4	7/26/2018	Iron	F	1400	µg/L	30	1000	NM GW STD
SWA-2-4	11/27/2018	Iron	F	1480	µg/L	30	1000	NM GW STD
SWA-2-4	2/28/2018	Manganese	F	647	µg/L	2	200	NM GW STD
SWA-2-4	2/28/2018	Manganese	F	756	µg/L	2	200	NM GW STD
SWA-2-4	5/30/2018	Manganese	F	441	µg/L	2	200	NM GW STD
SWA-2-4	7/26/2018	Manganese	F	479	µg/L	2	200	NM GW STD
SWA-2-4	11/27/2018	Manganese	F	479	µg/L	2	200	NM GW STD
SWA-2-5	7/26/2018	Arsenic	AXL	12.2	µg/L	2	10	EPA MCL
SWA-2-5	2/28/2018	Iron	F	5520	µg/L	52.1	1000	NM GW STD
SWA-2-5	2/28/2018	Iron	F	5140	µg/L	30	1000	NM GW STD
SWA-2-5	5/30/2018	Iron	F	5230	µg/L	30	1000	NM GW STD
SWA-2-5	5/30/2018	Iron	F	5380	µg/L	52.1	1000	NM GW STD
SWA-2-5	7/26/2018	Iron	F	6360	µg/L	30	1000	NM GW STD
SWA-2-5	11/27/2018	Iron	F	5080	µg/L	30	1000	NM GW STD
SWA-2-5	2/28/2018	Manganese	F	1020	µg/L	2	200	NM GW STD
SWA-2-5	5/30/2018	Manganese	F	1030	µg/L	2	200	NM GW STD
SWA-2-5	7/26/2018	Manganese	F	1210	µg/L	2	200	NM GW STD
SWA-2-5	11/27/2018	Manganese	F	980	µg/L	2	200	NM GW STD
SWA-2-6	2/28/2018	Arsenic	AXL	12	µg/L	2	10	EPA MCL
SWA-2-6	5/30/2018	Arsenic	AXL	10.7	µg/L	2	10	EPA MCL
SWA-2-6	7/26/2018	Arsenic	AXL	15.5	µg/L	2	10	EPA MCL
SWA-2-6	11/27/2018	Arsenic	AXL	11.4	µg/L	2	10	EPA MCL
SWA-2-6	2/28/2018	Iron	F	6450	µg/L	52.1	1000	NM GW STD
SWA-2-6	2/28/2018	Iron	F	6340	µg/L	30	1000	NM GW STD
SWA-2-6	5/30/2018	Iron	F	6020	µg/L	52.1	1000	NM GW STD
SWA-2-6	5/30/2018	Iron	F	6000	µg/L	30	1000	NM GW STD
SWA-2-6	7/26/2018	Iron	F	6910	µg/L	30	1000	NM GW STD
SWA-2-6	11/27/2018	Iron	F	4860	µg/L	30	1000	NM GW STD
SWA-2-6	2/28/2018	Manganese	F	1120	µg/L	2	200	NM GW STD
SWA-2-6	5/30/2018	Manganese	F	1060	µg/L	2	200	NM GW STD
SWA-2-6	7/26/2018	Manganese	F	1200	µg/L	2	200	NM GW STD
SWA-2-6	11/27/2018	Manganese	F	994	µg/L	2	200	NM GW STD
SWA-3-7	3/1/2018	Iron	F	9010	µg/L	30	1000	NM GW STD
SWA-3-7	3/1/2018	Iron	F	9380	µg/L	52.1	1000	NM GW STD
SWA-3-7	5/31/2018	Iron	F	9680	µg/L	30	1000	NM GW STD
SWA-3-7	5/31/2018	Iron	F	9670	µg/L	52.1	1000	NM GW STD
SWA-3-7	7/25/2018	Iron	F	7150	µg/L	30	1000	NM GW STD



Table D-3.3-1 (continued)

Location	Date	Analyte	Field Prep Code <sup>a</sup>	Result	Unit	MDL <sup>b</sup>	Screening Value	Screening Value Type <sup>c</sup>
SWA-3-7	11/28/2018	Iron	F	11100	µg/L	30	1000	NM GW STD
SWA-3-7	3/1/2018	Manganese	F	3350	µg/L	2	200	NM GW STD
SWA-3-7	5/31/2018	Manganese	F	2870	µg/L	2	200	NM GW STD
SWA-3-7	7/25/2018	Manganese	F	2210	µg/L	2	200	NM GW STD
SWA-3-7	11/28/2018	Manganese	F	3330	µg/L	2	200	NM GW STD
SWA-3-8	3/1/2018	Iron	F	5950	µg/L	52.1	1000	NM GW STD
SWA-3-8	3/1/2018	Iron	F	5900	µg/L	30	1000	NM GW STD
SWA-3-8	5/31/2018	Iron	F	5720	µg/L	30	1000	NM GW STD
SWA-3-8	5/31/2018	Iron	F	5700	µg/L	52.1	1000	NM GW STD
SWA-3-8	7/25/2018	Iron	F	5440	µg/L	30	1000	NM GW STD
SWA-3-8	7/25/2018	Iron	F	5510	µg/L	30	1000	NM GW STD
SWA-3-8	11/28/2018	Iron	F	5270	µg/L	30	1000	NM GW STD
SWA-3-8	3/1/2018	Manganese	F	2140	µg/L	2	200	NM GW STD
SWA-3-8	5/31/2018	Manganese	F	2030	µg/L	2	200	NM GW STD
SWA-3-8	7/25/2018	Manganese	F	2060	µg/L	2	200	NM GW STD
SWA-3-8	7/25/2018	Manganese	F	2050	µg/L	2	200	NM GW STD
SWA-3-8	11/28/2018	Manganese	F	1970	µg/L	2	200	NM GW STD
SWA-3-9	3/1/2018	Iron	F	8210	µg/L	30	1000	NM GW STD
SWA-3-9	3/1/2018	Iron	F	8440	µg/L	52.1	1000	NM GW STD
SWA-3-9	5/31/2018	Iron	F	9520	µg/L	52.1	1000	NM GW STD
SWA-3-9	5/31/2018	Iron	F	9140	µg/L	30	1000	NM GW STD
SWA-3-9	7/25/2018	Iron	F	9280	µg/L	30	1000	NM GW STD
SWA-3-9	11/28/2018	Iron	F	8520	µg/L	30	1000	NM GW STD
SWA-3-9	3/1/2018	Manganese	F	1720	µg/L	2	200	NM GW STD
SWA-3-9	5/31/2018	Manganese	F	1900	µg/L	2	200	NM GW STD
SWA-3-9	7/25/2018	Manganese	F	2020	µg/L	2	200	NM GW STD
SWA-3-9	11/28/2018	Manganese	F	1750	µg/L	2	200	NM GW STD
SWA-4-10	5/31/2018	Chromium	F	63.1	µg/L	3	50	NM GW STD
SWA-4-10	7/25/2018	Chromium	F	72	µg/L	3	50	NM GW STD
SWA-4-10	3/1/2018	Iron	F	24700	µg/L	30	1000	NM GW STD
SWA-4-10	3/1/2018	Iron	F	24400	µg/L	521	1000	NM GW STD
SWA-4-10	5/31/2018	Iron	F	9400	µg/L	52.1	1000	NM GW STD
SWA-4-10	5/31/2018	Iron	F	16400	µg/L	30	1000	NM GW STD
SWA-4-10	7/25/2018	Iron	F	11500	µg/L	30	1000	NM GW STD
SWA-4-10	11/28/2018	Iron	F	6600	µg/L	30	1000	NM GW STD
SWA-4-10	3/1/2018	Manganese	F	3430	µg/L	2	200	NM GW STD
SWA-4-10	5/31/2018	Manganese	F	2440	µg/L	2	200	NM GW STD
SWA-4-10	7/25/2018	Manganese	F	1810	µg/L	2	200	NM GW STD

Table D-3.3-1 (continued)

Location	Date	Analyte	Field Prep Code <sup>a</sup>	Result	Unit	MDL <sup>b</sup>	Screening Value	Screening Value Type <sup>c</sup>
SWA-4-10	11/28/2018	Manganese	F	1570	µg/L	2	200	NM GW STD
SWA-4-11	5/31/2018	Iron	F	5620	µg/L	30	1000	NM GW STD
SWA-4-11	5/31/2018	Iron	F	5280	µg/L	52.1	1000	NM GW STD
SWA-4-11	7/25/2018	Iron	F	4730	µg/L	30	1000	NM GW STD
SWA-4-11	11/28/2018	Iron	F	3850	µg/L	30	1000	NM GW STD
SWA-4-11	5/31/2018	Manganese	F	934	µg/L	2	200	NM GW STD
SWA-4-11	7/25/2018	Manganese	F	818	µg/L	2	200	NM GW STD
SWA-4-11	11/28/2018	Manganese	F	617	µg/L	2	200	NM GW STD
SWA-4-12	3/1/2018	Iron	F	6090	µg/L	52.1	1000	NM GW STD
SWA-4-12	3/1/2018	Iron	F	5920	µg/L	30	1000	NM GW STD
SWA-4-12	5/31/2018	Iron	F	3260	µg/L	52.1	1000	NM GW STD
SWA-4-12	5/31/2018	Iron	F	3550	µg/L	30	1000	NM GW STD
SWA-4-12	7/25/2018	Iron	F	3390	µg/L	30	1000	NM GW STD
SWA-4-12	11/28/2018	Iron	F	5060	µg/L	30	1000	NM GW STD
SWA-4-12	3/1/2018	Manganese	F	1560	µg/L	2	200	NM GW STD
SWA-4-12	5/31/2018	Manganese	F	1040	µg/L	2	200	NM GW STD
SWA-4-12	7/25/2018	Manganese	F	1090	µg/L	2	200	NM GW STD
SWA-4-12	11/28/2018	Manganese	F	1630	µg/L	2	200	NM GW STD

Note: All values with 5.21 as the MDL had a dilution factor of 10, but this has been accounted for in the results.

<sup>a</sup> F = Filtered using 0.45-µm pore size.

<sup>b</sup> MDL = Method detection limit.

<sup>c</sup> EPA regional screening levels for tap water.

## **Appendix E**

---

*2018 Watershed Mitigations Inspections*





## **E-1.0 INTRODUCTION**

Watershed storm water controls and grade-control structures (GCSs) are inspected annually and after significant flow events (greater than 50 cfs at locations with gaging stations). These inspections are completed to ensure watershed mitigations are functioning properly and to determine if maintenance is required. Examples of items evaluated during inspections include:

- debris/sediment accumulation that could impede operation
- water levels behind retention structures
- physical damage of structure, or failure of structural components
- undermining, piping, flanking, settling, movement, or breaching of structure
- vegetation establishment and vegetation that may negatively impact structural components
- rodent damage
- vandalism
- erosion

The photographs in this appendix show the 2018 May inspection of watershed mitigations in Sandia Canyon. Each group of photographs is associated with a specific feature (e.g., standpipe, weir, upstream, downstream, vegetated cover) that could develop issues. Photographs of features were taken to mirror previous inspection photos as closely as possible.

In 2018, Sandia GCS downstream gage did not record significant flow events. One regular inspection was conducted in May of 2018. The typical October inspection was not conducted in 2018. However, a post-monsoon walk-down of the Sandia wetlands was organized in conjunction with the New Mexico Environment Department and occurred in October 2018. At the site visit, undercutting erosion to a side drainage log check dam was observed. Further documentation and monitoring of the noted erosion will occur in 2019.

The photographs in the appendix illustrate the health of the wetland in and around the GCS, revegetation of adjacent slopes, and the best management practices in place to help maintain the integrity of the GCS and its associated wetland vegetation.

Additional data on the position of the channel thalweg in the area of the GCS can be found in Appendix B. Quantitative data from vegetation perimeter mapping in and around the GCS can be found in Appendix C.

## **E-2.0 CONTROLS INSTALLED IN 2018**

In January 2018, maintenance was performed on two log check dams installed in September 2017 on a side drainage of the GCS. The log check dams were modified by adding a percolation prevention cut-off wall made of riprap, crushed stone, and geotextile fabric placed subsurface and downstream of the spillways. The log check dam scour protection was replaced with gabion mattresses filled with riprap and crushed stone and buried under native channel material. The displaced logs making up the flow spreader were replaced and anchored with riprap. Riprap was also added to any areas where channelization was occurring to promote sheet flow and prevent further channelization. These new control structures were added to the annual GCS inspection in May 2018, and will be inspected on all subsequent inspections.

## E-2.1 Maintenance on Side-Drainage Controls Upstream of GCS



**Figure E-2.1-1** January 2018: View of repaired log check dams with additional riprap erosion protection (looking downstream)



### E-3.0 SANDIA CANYON GCS INSPECTION PHOTOGRAPHS

#### E-3.1 GCS South Bank—Upper Structure



**Figure E-3.1-1** May 2018: South bank of vegetation looking upstream. Vegetation continuing to establish on south bank. No erosion is present.

### E-3.2 GCS North Bank—Upper Structure



**Figure E-3.2-1** May 2018: North bank looking north. Established vegetation with no sign of erosion. Vegetation showing good stability and density.



### E-3.3 GCS Wetland—Upper Structure



**Figure E-3.3-1** May 2018: Upper wetland looking upstream. There is some evidence of wetland channelization. Continue to monitor to preferential flow paths within wetland with slight channelization.



**E-3.4 GCS Wetland—Middle Structure**



**Figure E-3.4-1 May 2018: Middle wetland looking upstream**



**E-3.5 GCS South Bank—Lower Structure**



**Figure E-3.5-1** May 2018: Lower wetland looking downstream. There is slight vegetation establishment in riprap. The structure is working as designed with no evidence of channelization.

### E-3.6 GCS Cascade Structure



**Figure E-3.6-1** May 2018: Cascade structure (looking downstream) working as designed. There is no evidence of rock displacement. There is no evidence of erosion in/near cascade pool.



### E-3.7 GCS Upper Run-on Defense Cell Barriers



**Figure E-3.7-1** May 2018: Upper defense cell sediment migration has recently occurred. There is approximately 1 ft of capacity from the bottom of the pond to the spillway.



### **E-3.8 GCS Lower Run-on Defense Cell Barriers**



**Figure E-3.8-1 May 2018: Lower defense cell. Need to monitor erosion occurring at the west end of the spillway. Investigate need for possible maintenance to address erosion occurring under the turf-reinforcement mat on spillway rundowns.**





**Figure E-3.8-2 May 2018: Lower defense cell barrier with approximately 3.5 ft of capacity available from bottom of pond to spillway**



### E-3.9 Upper Log Check Dam



Figure E 3.9-1 May 2018: Upper log check dam



**E-3.10 Lower Log Check Dam**



**Figure E 3.10-1 May 2018: Lower log check dam**



### E-3.11 Energy Dissipater



Figure E 3.11-1 May 2018: Log flow spreader



## **Appendix F**

---

*Analytical Data and 5-Min Stage,  
Discharge, and Precipitation Data  
(on CD included with this document)*

